Some Aspects of the Wilson Loop / Amplitude Duality at Strong and Weak Coupling

Dissertation
zur Erlangung des akademischen Grades
doctorum rerum naturalium (Dr. rer. nat.)
im Fach Physik

eingereicht an der
Mathematisch Naturwissenschaftlichen Fakultät I
der Humboldt-Universität zu Berlin

von:
Herrn Dipl.-Phys. Sebastian Johannes Wuttke

Präsident der Humboldt-Universität zu Berlin
Prof. Dr. Jan-Hendrik Olbertz

Dekan der Mathematisch Naturwissenschaftlichen Fakultät I
Prof. Stefan Hecht, PhD

Gutachter:

1. Prof. Jan Plefka
2. Dr. Harald Dorn
3. Dr. Paul Heslop

Tag der mündlichen Prüfung: 19.11.2014

to Konstantin

Contents

Acknowledgements

I would like to take this opportunity to thank the people who have supported me during the work on this thesis. Foremost, I wish to express my sincere gratitude to my advisor Dr. Harald Dorn. During the last years he was always available for discussion and patient with questions of mine. The quality of his supervision was far beyond what I could expect from a advisor.

I also want to thank Prof. Jan Plefka for providing the possibility to do my PhD studies in his group, which provided a friendly and productive atmosphere.

Besides my advisor, I would like to thank the rest of my thesis committee: Prof. Jan Plefka, Dr. Paul Heslop, Prof. Matthias Staudacher and Prof. Ulli Wolff.

I thank my collaborators Dr. Harald Dorn, Dr. George Jorjadze, Dr. Chrysostomos Kalousios and Luka Megrelidze for a productive and very enjoyable collaboration.

Furthermore, I want to mention our graduate school GK 1504 here, as they provided financial and professional support during my studies.

I am grateful to Tina Pietsch for reading through the manuscript.

Last, but not least, I want to thank my parents and my wife for their continuous love and support in every stage of my life and kind words when I needed them.

1 Overview

This work is concerned with the study of light-like polygonal Wilson loops in planar $\mathcal{N} = 4$ super Yang-Mills theory in the context of AdS/CFT correspondence [1]. The AdS/CFT correspondence is one of the most interesting developments in modern physics and states a duality between certain conformal field theories to certain string theories on backgrounds containing an AdS factor. Although several examples of these dualities are studied, we will focus on the most popular duality between planar $\mathcal{N} = 4$ super Yang-Mills theory and type IIb super string theory on $\mathrm{AdS}_5 \times \mathrm{S}^5$ background. This correspondence is extremely interesting as it relates the perturbative regime of string theory to the strongly coupled (non-perturbative) part of gauge theory. So there is the possibility to use perturbation theory on the string theory side to calculate scattering amplitudes at strong coupling, for example. The possibility to extract gluon scattering amplitudes at strong coupling from the calculation of a minimal surface in $\mathrm{AdS}_5 \times \mathrm{S}^5$ has been propagated in [4, 6]. In the first part of this work we examine a certain class of minimal surfaces in $\mathrm{AdS}_3 \times \mathrm{S}^3 \subset \mathrm{AdS}_5 \times \mathrm{S}^5$ as they are potentially interesting for this kind of correspondence.

A further important feature of $\mathcal{N} = 4$ super Yang Mills theory is the correspondence between gluon scattering amplitudes and closed light-like polygonal Wilson loops. This correspondence also implies a dual set of symmetries, which are called dual conformal symmetries. Up to a remainder function which depends on conformal invariants only, Wilson loops and gluon scattering amplitudes obey the so-called BDS Ansatz [12, 13]. The all-loop structure of the Wilson loop is given via

$$\log \mathcal{W} \;=\; \sum_{l=1}^{\infty} a^l \big(f^{(l)}(\epsilon)\; w_n(l\epsilon) \;+\; C_n^{(l)} \big) \;+\; \mathcal{R}_n \;+\; \mathcal{O}(\epsilon)\;,$$

where the $C^{(l)}$ are numbers, $f^{(l)}(\epsilon) = f_0^{(l)} + \epsilon f_1^{(l)} + \epsilon^2 f_2^{(l)}$, and $w_n(\epsilon)$ is the one loop contribution

$$w_n(\epsilon) \;=\; -\frac{1}{2} \sum_{k=1}^{n} \frac{1}{\epsilon^2} \left(-\mu^2 s_{k-1,k+1} + i\varepsilon\right)^{\epsilon} \;+\; F_n(\mu^2, \epsilon, s)\;.$$

By n we indicate the number of cusps of the Wilson loop. For $n = 4, 5$ the structure is completely fixed via the anomalous conformal Ward identities. Starting with six legs (cusps) the structure involves a so-called remainder function $\mathcal{R}_n$ which depends on conformal invariants only. At strong coupling this remainder function can be mapped to the solutions of TBA equations for

some Y-system [9, 10, 11]. At weak coupling the only explicit general results are known for hexagon remainder at two loops [22, 23] and recently three loops [24]. In [39] the differential of the n-gon remainder function is analysed and yields analytic expressions for some parts while only giving the symbol for other parts. Explicit results are also known for the octagon that is embedded in a two dimensional Minkowski space [25]. The second part of this work is devoted to analysis of self-crossing Wilson loops in general with applications to the self- crossing hexagon and octagon. We use a renormalisation group technique developed in [26] to obtain the leading divergences of the self-crossing remainder function and present results beyond the scope of our work in [27, 28].

Übersicht

Die vorliegende Arbeit behandelt lichtartige plolygonale Wilsonschleifen in planarer $\mathcal{N} = 4$ super Yang Mills Theorie im Zusammenhang mit der AdS/CFT Korrespondenz [1]. AdS/CFT Korrespondenzen sind eine der spannensten Entwicklungen in der modernen theoretischen Physik und beschreiben eine Dualität zwischen bestimmten konformen Feldtheorien und Stringtheorien auf einem Hintergrund, der einen AdS (Anti de Sitter Raum) Faktor enthält. Es sind einige solcher Korrespondenzen bekannt bzw. vermutet . Die meiststudierte ist jedoch die Korrespondenz zwischen $\mathcal{N} = 4$ sYM Theorie und Typ IIb Stringtheorie auf einem $\mathrm{AdS}_5 \times \mathrm{S}^5$ Hintergrund. Diese Korrespondenz ist dahingehend interessant, dass der Fall starker Kopplung in der Eichtheorie mit dem perturbativen Fall bei schwacher Kopplung auf der Stringtheorieseite verknüpft ist. Das eröffnet die Möglichkeit mittels Störungstheorie auf der Stringseite zum Beispiel Streuamplituden bei starker Kopplung zu berechnen. Die Möglichkeit der Berechnung von Streuamplituden bei starker Kopplung wurde in [4, 6] propagiert und beinhaltet die Berechnung bestimmter Minimalflächen in $\mathrm{AdS}_5 \times \mathrm{S}^5$. Im ersten Teil der Arbeit untersuchen und klassifizieren wir die Klasse der flachen Minimalflächen in $\mathrm{AdS}_3 \times \mathrm{S}^3 \subset \mathrm{AdS}_5 \times \mathrm{S}^5$, die in diesem Zusammenhang interessant sind.

Eine weitere wichtige Eigenschaft von $\mathcal{N} = 4$ sYM ist die Korrespondenz zwischen Gluonenstreuamplituden und geschlossenen lichtartigen polygonalen Wilsonschleifen. Aus dieser Korrespondenz folgt ein dualer Satz von Symmetrien, welche dual konforme Symmetrien genannt werden. Wilsonschleifen und Gluonenstreuamplituden werden bis auf eine Remainderfunktion, welche nur von konformen Invarianten abhängt, durch den sogenannten BDS Ansatz beschrieben [12, 13]. Die durch den BDS Ansatz festgelegte Struktur in allen Ordnungen der Kopplung lautet

$$\log \mathcal{W} \;=\; \sum_{l=1}^{\infty} a^l \big(f^{(l)}(\epsilon)\; w_n(l\epsilon) \;+\; C_n^{(l)} \big) \;+\; \mathcal{R}_n \;+\; \mathcal{O}(\epsilon)\;,$$

wobei die $C^{(l)}$ reine Zahlen sind, $f^{(l)}(\epsilon) = f_0^{(l)} + \epsilon f_1^{(l)} + \epsilon^2 f_2^{(l)}$ und $w_n(\epsilon)$ der Einschleifen- Beitrag

$$w_n(\epsilon) \;=\; -\frac{1}{2} \sum_{k=1}^{n} \frac{1}{\epsilon^2} \left(-\mu^2 s_{k-1,k+1} + i\varepsilon\right)^{\epsilon} \;+\; F_n(\mu^2, \epsilon, s)$$

ist. Mit n wird die Anzahl der Kanten des polygonalen Wilsonschleifen bezeichnet. Für $n = 4, 5$ ist die Struktur durch die anomalen konformen Wardidentitäten komplett fixiert. Ab sechs Kanten wird die sogennante Remainderfunktion $\mathcal{R}_n$ wichtig, welche nur von konformen Invarianten abhängt. Bei

starker Kopplung kann diese Remainderfunktion mit den Lösungen der TBA Gleichungen für ein Y-System in Verbindung gebracht werden [9, 10, 11]. Bei schwacher Kopplung sind explizite Resultate nur für das Hexagon auf zwei-Schleifen Ebene [22, 23] und kürzlich auch auf drei-Schleifen Ebene [24] bekannt. In [39] wird das Differential der Remainderfunktion für ein n-gon untersucht und analytische Resultate für Teile der Remainderfunktion, sowie Symbole der anderen Teile angegeben. Explizite Resultate sind ebenfalls für das Oktagon, welches in einen zweidimensionalen Minkowskiraum eingebettet werden kann bekannt [25]. Der zweite Teil der Arbeit widmet sich selbstkreuzenden Wilsonschleifen mit Anwendung beim Hexagon und Oktagon. Dabei nutzen wir die Renormierungsgruppengleichung für selbstkreuzende Wilsonschleifen. Diese Techik wurde in [26] vorgeschlagen. Die hier vorgstellte Arbeit geht über die Grenzen unserer Publikationen [27, 28] hinaus.

2 Introduction

Symmetry is one of the most important ingredients for the construction of physical theories. Poincaré symmetry, i.e. the invariance of the theory under Lorentz transformations and translations, is the most fundamental symmetry that a physical theory should implement. These symmetries often simplify calculations. In this sense physical theories that obey more symmetry are "easier". One extension of Poincaré symmetry is conformal symmetry, which is the invariance under transformations that preserve angles. Many theories are conformally invariant on a classical level (such as QCD), but the symmetry is usually broken by quantum corrections. However, in some super-symmetric theories conformal symmetry is also present at quantum level. The "most" symmetric generalization of pure gauge theory in four dimensions is $\mathcal{N} = 4$ super Yang-Mills theory, which may be a toy-model but which allows amazing techniques that also have impact on more realistic theories, such as QCD. A short introduction on conformal symmetry can be found in appendix 8.1.

First conjectured at strong coupling and later also verified at weak coupling there is a correspondence between light-like polygonal Wilson loops and MHV gluon scattering amplitudes. Both quantities are governed by (dual) anomalous conformal Ward identities and obey the BDS Ansatz [12, 13], corrected by a remainder function. These Ward Identities uniquely fix the structure of the amplitudes up to 5 external legs. However, if the number of external legs is larger than 5, an additional remainder function remains unfixed.

In the following subsections we will construct the $\mathcal{N} = 4$ sYM Lagrangian in four dimensions using a dimensional reduction of the $\mathcal{N} = 1$ sYM Lagrangian in ten dimensions. We will introduce the polygonal Wilson loop and comment on important properties of the cusp anomalous dimension. Furthermore, we present the structure of the anomalous conformal Ward identities for light-like Wilson loops, which fix the structure of the finite part of the Wilson loop up to a function that depends on conformal invariants only an which is called remainder function. We will end this section with some comments on gluon scattering amplitudes and formulate the duality to light-like Wilson loops.

This thesis is divided into two main aspects of our research. Part I deals with the classification of a certain subclass of minimal surfaces in $\mathrm{AdS}_3 \times \mathrm{S}^3$ which is a natural generalization of the surface that was presented in [4, 6] which is related to the strong coupling limit of the four gluon amplitude. Part I will also contain a more specialised introduction. Part II is concerned with the calculation of the most divergent parts of the remainder function of

Wilson loops in the limit of self-crossing. Likewise, a specialised introduction is also included in Part II .

2.0.1 $\mathcal{N} = 4$ sYM

One of the most important AdS/CFT correspondences is the duality between planar $\mathcal{N} = 4$ sYM theory to type IIb string theory. $\mathcal{N} = 4$ sYM is the most symmetric gauge theory in four dimensions. It contains a SU(N) gauge field A^μ, six real scalar fields ϕ_m , $m \in \{1, \ldots, 6\}$ and four complex fermions λ^A_α , $A \in \{1, 2, 3, 4\}$. The Lagrangian can be constructed from the ten dimensional $\mathcal{N} = 1$ Lagrangian [29]. The ten dimensional $\mathcal{N} = 1$ action we start with is

$$S = \int \mathrm{d}^{10}x \ \mathrm{tr} \left(-\frac{1}{4} F^{MN} F_{MN} + \ \frac{i}{2} \ \bar{\psi} \Gamma^M D_M \psi \right) \ . \tag{2.1}$$

The capital indices are ten-dimensional space-time indices. F_{MN} is the ten-dimensional field strength

$$F_{MN} = \partial_M A_N - \partial_N A_M - ig \Big[A_M, A_N \Big] \ , \tag{2.2}$$

with the covariant derivative

$$D_M = \partial_M - ig \Big[A_M, \ . \ \Big] \ . \tag{2.3}$$

For the action to be super-symmetric the spinor field ψ has to satisfy both the Majorana

$$\psi = C \bar{\psi}^T \tag{2.4}$$

and the Weyl condition

$$\Gamma_{11} \psi = \psi \ , \quad \Gamma_{11} = \Gamma^0 \Gamma^1 \ldots \Gamma^9 \ . \tag{2.5}$$

In order to go to four dimensions one can use the following representation of Γ-matrices

$$\Gamma^\mu = \gamma^\mu \otimes \mathbb{1}_8 \ , \quad \mu \in \{0, 1, 2, 3\} \ , \tag{2.6}$$

and

$$\Gamma^{m+3} = \gamma^5 \otimes \Gamma^m_6 \ , \quad m \in \{1, \ldots, 6\} \ , \tag{2.7}$$

where Γ^m_6 is a representation of the gamma matrices for the six-dimensional Euclidean space. One can choose

$$\Gamma^m_6 = \begin{pmatrix} 0 & \rho_m \\ \rho_m^{-1} & 0 \end{pmatrix} \ , \tag{2.8}$$

where the ρ_m are the 4×4 matrices given by

$$(\rho_{ij})_{kl} = \delta_{ik}\delta_{jl} - \delta_{jk}\delta_{il} \ , \quad i,j \in \{1,2,3,4\} \tag{2.9}$$

with the identification of $m \in \{1,\dots,6\}$ with the antisymmetric pairs $(i,j) \in \{1,2,3,4\}$. The dimensional reduction is performed by demanding that the fields just depend on four space-time dimensions

$$\partial_{m+3}\{A,\psi,\bar{\psi}\} = 0 \ , \quad m \in \{1,\dots,6\} \ . \tag{2.10}$$

The four dimensional gauge field is built out of the first four components of the ten dimensional field. Then six scalar fields are defined via

$$\phi_m = A_{m+3} \ , \quad \phi_{ij} = -\frac{1}{2}A_m(\rho_m)_{ij} = -\phi_{ji} \ . \tag{2.11}$$

Decomposing the ten dimensional Lagrangian into the four dimensional fields, the Lagrangian is given by

$$\begin{aligned}\mathcal{L} = \mathrm{tr}\Big(&-\frac{1}{4}F_{\mu\nu}F^{\mu\nu} + \frac{1}{2}D^\mu\phi^{ij}D_\mu\phi_{ij} + i\lambda^i\sigma^\mu D_\mu\bar{\lambda}_i \\ &+ ig\lambda_i[\lambda_j,\phi^{ij}] + ig\bar{\lambda}^i[\bar{\lambda}^j,\phi_{ij}] + \frac{g^2}{4}[\phi_{ij},\phi_{kl}][\phi^{ij},\phi^{kl}]\Big) \ .\end{aligned} \tag{2.12}$$

2.1 Wilson loops

In SU(N) gauge theory the Wilson loop operator is the parallel transport of the gauge field $A^\mu(x)$ along a closed line C. The parallel transport is defined by

$$\mathcal{U}(\mathcal{C}) := \frac{1}{N}\ \mathrm{tr}\ \mathcal{P}\exp\left(ig\oint_{\mathcal{C}} A_\mu \mathrm{d}x^\mu\right) \ . \tag{2.13}$$

For the duality between scattering amplitudes and Wilson loops we are interested in the vacuum expectation value

$$\mathcal{W}_{\mathcal{C}} = \langle 0 \mid \ \mathcal{U}(\mathcal{C}) \ \mid 0\rangle \ . \tag{2.14}$$

In $\mathcal{N}=4$ sYM it is natural to examine the supersymmetric generalisation of 2.14 proposed in [2] which is

$$\tilde{\mathcal{W}}_{\mathcal{C}} = \langle 0 \mid \ \frac{1}{N}\ \mathrm{tr}\ \mathcal{P}\exp\left(ig\oint_{\mathcal{C}} \mathrm{d}\tau\left(A_\mu \dot{x}^\mu + \mid \dot{x} \mid \Theta^I\phi_I(x(\tau))\right)\right) \ \mid 0\rangle \ , \tag{2.15}$$

with $\Theta_I\Theta^I = 1$ being the coordinates of a contour on the 5-sphere and ϕ_I the six scalar fields. Here, we are primarily interested in light-like Wilson loops.

In this case the supersymmetric Wilson loops coincides with the ordinary Wilson loop 2.14. Up to one-loop the expression (2.14) can be expanded

$$\mathcal{W}_{\mathcal{C}} = 1 - \frac{g^2}{2} C_f \oint_C \mathrm{d}x^\mu \oint_C \mathrm{d}y^\nu D_{\mu\nu}(x-y) + \mathcal{O}(g^4) \ . \tag{2.16}$$

Here, $C_f = (N^2-1)/(2N)$ is the quadratic Casimir of SU(N) in fundamental representation. We use the propagator in Feynman gauge and dimensional regularisation

$$D_{\mu\nu}(x) = \eta_{\mu\nu} D(x) \ , \quad D(x) = -\frac{\Gamma(1-\epsilon)}{4\pi^{2-\epsilon}(-x^2+i\varepsilon)^{1-\epsilon}} \ , \tag{2.17}$$

with the metric convention $\eta_{\mu\nu} = \mathrm{diag}(+,-,-,-)$.

2.1.1 The anomalous dimension of the cusped Wilson line

Let us first consider the cusped Wilson line. The cusp is spanned by the vectors p and q with $pq < 0$. The Wilson loop can be renormalised by sepatrating the divergences into the $\mathcal{Z}$ factor

$$\mathcal{W} = \mathcal{Z}_{\text{cusp}} \ \mathcal{W}^{\text{ren.}} \ . \tag{2.18}$$

We work in dimensional regularisation. In order to keep the dimension of the action unchanged one has to replace $g \to \mu^\epsilon g$ introducing an energy scale μ. The unrenormalised Wilson loop has to be independent of μ and thus

$$\mu \frac{\mathrm{d}}{\mathrm{d}\mu} \mathcal{W} = 0 = \mathcal{Z}_{\text{cusp}} \ \mu \frac{\mathrm{d}}{\mathrm{d}\mu} \mathcal{W}^{\text{ren.}} \ + \ \mathcal{W}^{\text{ren.}} \ \mu \frac{\mathrm{d}}{\mathrm{d}\mu} \mathcal{Z}_{\text{cusp}} \ . \tag{2.19}$$

Multiplying with $\mathcal{Z}_{\text{cusp}}^{-1}$ leads to the renormalisation group equation

$$\mu \frac{\mathrm{d}}{\mathrm{d}\mu} \mathcal{W}^{\text{ren.}} = -\mathcal{Z}_{\text{cusp}}^{-1} \mu \frac{\mathrm{d}}{\mathrm{d}\mu} \mathcal{Z}_{\text{cusp}} \mathcal{W}^{\text{ren.}} = -\Gamma_{\text{cusp}}(g,\gamma) \ \mathcal{W}^{\text{ren.}} \ , \tag{2.20}$$

where

$$\Gamma_{\text{cusp}}(g,\gamma) \ = \ \mathcal{Z}_{\text{cusp}}^{-1} \ \mu \frac{\mathrm{d}}{\mathrm{d}\mu} \ \mathcal{Z}_{\text{cusp}} \ \ |_{g_{\text{bare}} \text{ fixed}} \tag{2.21}$$

is called the anomalous dimension. Here, γ is angle between p and q with $\cosh\gamma = \frac{-pq}{\sqrt{p^2 q^2}}$. It is convenient to express the renormalisation group equation using the β-function $\beta(g) = \frac{\mathrm{d}}{\mathrm{d}\log\mu} \ g$

$$\left(\mu \frac{\partial}{\partial \mu} + \beta(g) \frac{\partial}{\partial g} \right) \mathcal{W}^{\text{ren.}} = \ - \ \Gamma_{\text{cusp}}(g,\gamma) \ \mathcal{W}^{\text{ren.}} \ . \tag{2.22}$$

The divergent part of the Wilson line in dimensional regularisation then reads

$$\mathcal{W}^{(1)}_{\text{cusp}} = \frac{g^2 C_f}{4\pi^2}\frac{1}{2\epsilon}(1-\gamma\coth\gamma) + \text{finite}\ . \tag{2.23}$$

The computation is available in appendix 8.8. The renormalised Wilson line obeys the renormalisation group equation 2.22 with

$$\Gamma^{(1)}_{\text{cusp}}(g,\gamma) = \frac{g^2 C_f}{4\pi^2}\left(\gamma\coth\gamma - 1\right)\ . \tag{2.24}$$

Aiming at light-like Wilson loops we are interested in the large γ behaviour of $\Gamma_{\text{cusp}}(g,\gamma)$. It was shown in [21] that for $\gamma\to\infty$

$$\Gamma_{\text{cusp}}(g,\gamma) \overset{\gamma\to\infty}{=} \frac{\gamma}{2}\Gamma_{\text{cusp}}(g) \tag{2.25}$$

at all loops. We shall refer to $\Gamma_{\text{cusp}}(g)$ as the cusp anomalous dimension from now on. This property is very important for our Ansatz of the crossing anomalous dimension matrix in the chapters 6 and 7. Being interested in the large γ (near light-like) regime we can substitute

$$\gamma = \operatorname{arccosh}\left(\frac{-pq}{\sqrt{p^2q^2}}\right) = \log\left(\frac{-pq}{\sqrt{p^2q^2}} - \sqrt{\frac{(pq)^2}{p^2q^2}-1}\right) \approx \log\left(\frac{-2pq}{\sqrt{p^2q^2}}\right)$$

However, calculating the light-like cusp we find that the divergence is more severe. At one loop the divergent contribution in dimensional regularisation reads

$$\mathcal{W}^{(1)}_{\text{light-like cusp}} = -\frac{g^2 C_f}{8\pi^2}\left(\frac{1}{\epsilon^2} + \log(-2\mu^2 p\cdot q \pm i\varepsilon)\frac{1}{\epsilon}\right) + \text{finite}\ . \tag{2.26}$$

Now the anomalous dimension on the left hand side in eq. (2.25) formally diverges in the light-like limit. The suitable cusp anomalous dimension for light-like Wilson loop can then be constructed by replacing

$$\begin{aligned}\log\left(-\frac{2pq}{\sqrt{p^2q^2}}\right) &\longrightarrow \log\left(-2pq\ \mu^2\right)\\ \Rightarrow \Gamma_{\text{light-like}}(g) &= \frac{1}{2}\log\left(-2pq\ \mu^2 \pm i\varepsilon\right)\Gamma_{\text{cusp}}(g)\ .\end{aligned} \tag{2.27}$$

In their work in [20] the authors demontrate this replacement using a differentiation with respect to $p\cdot q$. The divergent part of the polygonal closed light-like Wilson loop at one loop is the sum of all cusp divergences

$$\mathcal{W}^{(1)}_{\text{light-like}} = -\frac{g^2 C_f}{4\pi^2}\frac{1}{2\epsilon^2}\sum_{k=1}^{n}(-2p_k\cdot p_{k+1}\pm i\varepsilon)^{\epsilon} + \text{finite}\ . \tag{2.28}$$

The $i\varepsilon$ pole prescription originates from the gluon propagator and is often omitted, when only Euclidean Wilson loops (i.e. where the distances between all cusps that are not adjacent are space-like) are considered. As self-crossing Wilson loops do not fall into that category in general, we keep the $i\varepsilon$ prescription here.

2.1.2 Anomalous conformal Ward-identities

Due to the singularities coming from the cusps and the light-likeness of the Wilson loop, it needs to be regularised. As mentioned earlier, the action of $\mathcal{N}=4$ sYM is invariant under conformal transformations in four dimensions. However, in $D=4-2\epsilon$ dimensions the action is not invariant under dilatation and special conformal transformations. This leads to anomalous conformal Ward identities for light-like polygonal Wilson loops that have been studied in [17, 19]. The Ward identities read

$$\begin{aligned} D\log\langle\mathcal{W}(\mathcal{C}_n)\rangle &= -\frac{2i\epsilon}{g^2\mu^{2\epsilon}}\int \mathrm{d}^D x \frac{\langle\mathcal{L}(x)\mathcal{W}(\mathcal{C}_n)\rangle}{\langle\mathcal{W}(\mathcal{C}_n)\rangle} \ , \\ K^\mu\log\langle\mathcal{W}(\mathcal{C}_n)\rangle &= -\frac{4i\epsilon}{g^2\mu^{2\epsilon}}\int \mathrm{d}^D x x^\mu \frac{\langle\mathcal{L}(x)\mathcal{W}(\mathcal{C}_n)\rangle}{\langle\mathcal{W}(\mathcal{C}_n)\rangle} \ . \end{aligned} \tag{2.29}$$

The Wilson loop can be split

$$\log\langle\mathcal{W}(\mathcal{C}_n)\rangle = \log\mathcal{Z}_n + \log F_n \ , \tag{2.30}$$

into the divergent part $\mathcal{Z}_n$ and the finite part F_n. As a consequence of non-abelian exponentiation, the divergences exponentiate and have the all-loop structure [20].

$$\log\mathcal{Z}_n = -\frac{1}{4}\sum_{l=1}^{\infty}\sum_{i=1}^{n}(-x_{i-1,i+1}^2\mu^2)^{l\epsilon}\left(\frac{\Gamma_{\text{cusp}}^{(l)}}{(l\epsilon)^2}+\frac{\Gamma^{(l)}}{l\epsilon}\right) \ , \tag{2.31}$$

where $\Gamma^{(l)}$ are the expansion coefficients of the so-called collinear anomalous dimension and $a=\frac{g^2N}{8\pi^2}$. The position of the n cusps is given by the vector x_i^μ. Additionally, $x_{ik}=(x_i-x_k)$ and $x_i=x_{i+n}$. In [19] the authors examine the term containing the insertion of the Lagrangian for the special conformal Ward identity (2.29) for the finite part of the Wilson loop F_n in the limit $\epsilon\to 0$ and find

$$\sum_{i=1}^{n}(2x_i^\nu x_i\cdot\partial_i - x_i^2\partial_i^\nu)\log F_n = \frac{1}{2}\Gamma_{\text{cusp}}(a)\sum_{i=1}^{n}\log\frac{x_{i,i+2}^2}{x_{i-1,i+1}^2}x_{i,i+1}^\nu \ . \tag{2.32}$$

For $n = 4, 5$ this differential equation for the finite part can be solved up to a constant and gives

$$\log F_4 = \frac{1}{4}\Gamma_{\text{cusp}}(a) \log^2\left(\frac{x_{13}^2}{x_{24}^2}\right) + \text{const.} \,, \tag{2.33}$$
$$\log F_5 = -\frac{1}{8}\Gamma_{\text{cusp}}(a) \sum_{i=1}^{5} \log\left(\frac{x_{i,i+2}^2}{x_{i,i+3}^2}\right) \log\left(\frac{x_{i+1,i+3}^2}{x_{i+2,i+4}^2}\right) + \text{const.} \,.$$

Starting at six cusps (separated light-likely), it is possible to build cross ratios

$$u = \frac{x_{ij}^2 x_{kl}^2}{x_{ik}^2 x_{jl}^2} \tag{2.34}$$

that are invariant under conformal transformations. Thus, it is possible to add a function of these cross ratios to the $\log F_n$, which is annihilated by the conformal generator and therefore not visible in the anomalous conformal Ward identity. This additional function is called *remainder* function.

2.2 Gluon scattering amplitudes

In gauge theories it is convenient to sort gluon scattering amplitudes according to their colour structure. It can be seen that gluon scattering amplitudes with n external legscan be decomposed in the planar limit

$$\mathcal{A}_n(\{p_i, h_i, a_i\}) = \sum_{\sigma \in S_n/Z_n} \text{tr}\left(t^{a_{\sigma(1)}} \dots t^{a_{\sigma(n)}}\right) \mathcal{A}_n(\sigma(1)^{h_{\sigma(1)}}, \dots, \sigma(n)^{h_{\sigma(n)}}) \,, \tag{2.35}$$

with p_i being the momentum, a_i is the colour index and h_i the helicity of the ith particle. Multi-trace contributions are supressed in the planar limit. S_n is the group of all permutations of n elements and Z_n the cyclic subgroup. The $\mathcal{A}_n$ are called colour ordered partial amplitudes. It can be shown that

$$\mathcal{A}_n^{\text{tree}}(1^{\pm}, 2^{+}, \dots, n^{+}) = 0 \,. \tag{2.36}$$

2.2.1 Spinor helicity formalism

As this method plays an important role in computing scattering amplitudes we mention it here. The idea is to express four-dimensional massless momenta in terms of two commuting, two-component complex Weyl-spinors.

$$p_i^{\mu} \leftrightarrow p_i^{\alpha\dot{\alpha}} = p_i^{\mu}(\sigma_{\mu})^{\alpha\dot{\alpha}} =: \lambda_i^{\alpha}\tilde{\lambda}_i^{\dot{\alpha}} \,, \tag{2.37}$$

where $\sigma^\mu = (\mathbb{1}, \vec{\sigma})$ are the Pauli matrices. The spinor indices are raised and lowered with the two-dimensional antisymmetric ϵ-tensor with $\epsilon_{\alpha\beta} = -\epsilon^{\alpha\beta}$ and $\epsilon_{\dot{\alpha}\dot{\beta}} = -\epsilon^{\dot{\alpha}\dot{\beta}}$. Then the contractions

$$\langle ij\rangle := (\lambda_i)^\alpha(\lambda_j)_\alpha = (\lambda_i)^\alpha(\lambda_j)^\beta\epsilon_{\alpha\beta} \ , \quad [ij] := (\tilde{\lambda}_i)_{\dot{\alpha}}(\tilde{\lambda}_j)^{\dot{\alpha}} = (\tilde{\lambda}_i)_{\dot{\alpha}}(\tilde{\lambda}_j)_{\dot{\beta}}\epsilon^{\dot{\alpha}\dot{\beta}} \tag{2.38}$$

are invariant under Lorentz transformations. The scalar product can be reformulated using the spinor products

$$(p_i)^\mu(p_j)_\mu = -\frac{1}{2}\langle ij\rangle[ij] \ . \tag{2.39}$$

2.2.2 MHV amplitudes

Colour ordering provides a natural way to organise scattering amplitudes. The simplest colour ordered amplitudes that do not vanish are MHV (maximally helicity violating) amplitudes which have two flipped helicities. Further colour ordered partial amplitudes include the next-to-MHV amplitude (NMHV), $\mathrm{N^2MHV}$, up to the $\overline{\mathrm{MHV}}$ amplitude which has with $n-2$ flipped helicities. Thus, the simplest MHV amplitude (for real momenta) is the four-point amplitude. The MHV amplitude has a very simple form and can be expressed using the spinor products introduced before

$$\mathcal{A}_n^{\mathrm{MHV,\ tree}}(i^-, j^-) = \frac{\langle ij\rangle^4}{\langle 12\rangle\langle 23\rangle\ldots\langle n1\rangle} i\delta^{(4)}\left(\sum_{i=1}^n p_i\right) \ . \tag{2.40}$$

This result was first obtained in [30] and is therefore called Parke-Taylor formula. In order to prove the above formula R. Britto, F. Cachazo, B. Feng and E. Witten proposed a recursive method that has become famous as BCFW recursion [31, 32], that involves a generalised three-point amplitude for complex momenta.

2.2.3 Duality between Wilson loops and gluon scattering amplitudes

The duality between light-like polygonal Wilson loops and gluon scattering amplitudes first became visible when Alday and Maldacena proposed the calculation of a n point gluon amplitude at strong coupling by calculating certain minimal surfaces in AdS_5 in [4, 6]. This formally resembles the calculation of the strong coupling limit of a light-like polygonal Wilson loop [2]. Surprisingly, also at weak coupling the correspondence was checked in several

cases and validated, [15, 16, 18, 19]. The correspondence is formulated using the dual coordinates

$$p_i = (x_{i+1} - x_i) \ . \tag{2.41}$$

Thus, the positions of the cusps of the Wilson loop x_i are defined by the momenta p_i on the amplitude side. By

$$\mathcal{M} = \frac{\mathcal{A}_n^{\text{MHV}}}{\mathcal{A}_n^{\text{MHV, tree}}} \ , \tag{2.42}$$

we denote the rescaled, planar MHV amplitude. Then[1]

$$\log \mathcal{M}_n = \log\langle \mathcal{W}(\mathcal{C}_n)\rangle \ + \ \text{const.} \ + \ \mathcal{O}(\epsilon) \tag{2.43}$$

in the planar limit. $\mathcal{C}_n$ is the closed polygonal countour which is spanned by the momenta p_i and has cusps at x_i. This duality also introduces a new set of symmetries. Wilson loops obey the usual conformal symmetry, as well as a dual conformal symmetry. This dual conformal symmetry is referred to as a hidden symmetry, as this symmetry is not present in the action.

[1]Under the duality $\mu_{UV} = \mu_{IR}$ and $\epsilon_{UV} = -\epsilon_{IR}$

Part I
Strong coupling

The aim of this first section is to use a Pohlmeyer reduction to examine space-like classical strings in $AdS_3 \times S^3$, eventually providing a complete classification of all flat minimal surfaces in $AdS_3 \times S^3$. A lot of previous work has been concerned with the study of minimal surfaces in AdS_5 with a light-like closed polygon on its conformal boundary. However, the only explicit minimal surface with use in the amplitudes/strings duality is a surface presented in [4, 5] which corresponds to the four-gluon amplitude. This surface has the unique property of being the only *flat* minimal surface in AdS_n up to isometries, [33]. For flat minimal surfaces it is possible to find an explicit realization in AdS space. As the background space for the string theory is $AdS_5 \times S^5$ it is natural to also examine the flat minimal surfaces in the product space. In the appendix we present a brief note on minimal surfaces in general (see appendix 8.3) and on the conformal boundary of AdS (see appendix 8.4).

3 Introduction

One of the most important features in AdS/CFT duality is the possibility of calculating certain observables at strong coupling using geometric calculations on AdS.

3.1 Scattering amplitudes at strong coupling

In order to establish the correspondence between strings and gluon scattering amplitudes, in [4, 6, 7] Alday and Maldacena consider open string states that start and end on a D3 brane located at $z = z_{IR}$ in Poincaré coordinates. The proper momentum of the strings is $k_{pr} = z_{IR}k/R$, where k is the momentum in the gauge theory and is kept fixed if we take $z_{IR} \to \infty$. R is the radius of AdS space. So the proper momentum of the strings is very large if we take away the regulator. In this regime, string amplitudes were studied in [3] and shown to be dominated by a saddle point of the classical action. Thus we have to consider a world-sheet with disk topology inside AdS with vertex operator insertions at the boundary, that correspond to the external states. After

introducing T-dual coordinates the problem is equivalent to study minimal surfaces in a T-dual AdS space that end on a brane at $r = R^2/z_{IR}$. For every vertex operator insertion with momentum k^μ, the location of this point is shifted by

$$\Delta y^\mu = 2\pi k^\mu \ . \tag{3.1}$$

This relation is similar to the dual coordinates at weak coupling (2.41). Taking away the regulator $z_{IR} \to \infty$ we approach the conformal boundary in the T-dual coordinates. On the conformal boundary the boundary is now a closed light-like polygon, with cusps at y_i^μ. The momenta of the gluon amplitude is then related to the cusps via eq. (3.1). The leading exponential behaviour of the scattering amplitude is then given by

$$\mathcal{A}_n \propto e^{-\frac{\sqrt{\lambda}}{2\pi} A(k_1,\ldots,k_n)} \ , \quad \lambda = g^2 N \ , \tag{3.2}$$

where $A(k_1, \ldots, k_n)$ is the area of a space-like minimal surface that ends on a polygon that is spanned by the vectors k_i on the conformal boundary.

3.2 The four gluon amplitude at strong coupling

The first explicit calculations have been performed for the closed light-like tetragon in [4]. As our analysis is inspired by their calculation we review some details here. The authors first consider a minimal surface spanned by a light-like cusp. They find the explicit parametrisation

$$x_0 = e^\tau \cosh\sigma \ , \quad x_1 = e^\tau \sinh\sigma \ , \quad r = \sqrt{2} e^\tau \tag{3.3}$$

using Poincaré coordinates that we introduce in the appendix 8.4. Going to embedding coordinates of AdS_3 the authors realise that the explicit solution for the light-like cusp is given by a quadratic relation, additionally to the quadric that defines AdS. They show that

$$M_{\text{cusp}} = \{Y \in \mathbb{R}^{2,2} \mid Y^A Y_A = -1 \text{ and } Y_0^2 - Y_{-1}^2 = Y_1^2 - Y_2^2\} \ . \tag{3.4}$$

However, not constrained to the Poincaré patch they started in, this quadric also defines a minimal surface in the total AdS space. Surprisingly, defining a surface in AdS using the quadric found for the one-cusp surface leads to a minimal surface containing four cusps. Only one cusp has been in a finite position in the Poincaré patch that has been considered before.

In order to relate this surface to the four gluon amplitude at strong coupling it needs a regularisation which is realised via a cut-off in the radial coordinate in a Poincaré patch. Therefore it is necessary to shift the whole surface into

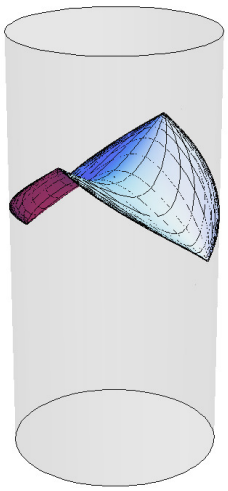

Figure 1: Extended to AdS_3 the minimal surface has four cusps and corresponds to the four gluon scattering amplitude at strong coupling. In this and similar plots the conformal boundary of AdS_3, which is $S^1 \times S^1$, is cut open in time direction. To get an impression of the embedding in AdS, one should identify the top with the bottom.

a single Poincaré patch. This is done by embedding AdS_3 into AdS_4 and then using global isometries of AdS_4 in order to shift the surface into a single Poincaré patch of AdS_4.

Up to now this surface merely represents a specific momentum alignment of the four gluon amplitude. To get a general result the authors use a two-parameter isometry transformation to be able to adjust the kinematic invariants s, t to any value. Then they calculate the regularised area of the tetragon minimal surface in [8]

$$\begin{aligned} iS &= -\frac{\sqrt{\lambda}}{2\pi} A \ , \\ A &= \frac{1}{4}\left(\log^2\left(\frac{r_c}{-8\pi^2 s}\right) + \log^2\left(\frac{r_c}{-8\pi^2 t}\right) - \log^2\left(\frac{s}{t}\right)\right) + \text{const.} \ , \end{aligned} \tag{3.5}$$

where r_c is a cut-off in the radial coordinate of a Poincaré patch of AdS. As we have commented earlier, no further explicit surfaces with light-like boundaries that are relevant to the study gluon scattering amplitudes have been constructed yet. However, in [33] we prove, that the tetragon surface, which as first constructed in [5] with no relation to scattering amplitudes, is the only flat minimal surface in AdS for general dimensions. The condition

flat is necessary to integrate the linear system in the Pohlmeyer approach to find an explicit embedding. The idea in the next section is to explore all space-like flat minimal surfaces in $AdS_3 \times S^3$ to give a extended set of explicit classical string solutions that may find their interpretation within the AdS/CFT correspondence. The classification is a combined work form [34, 35]. In [34] the authors focus on minimal surfaces in $AdS_3 \times S^3$ with a space-like AdS projection. Our work [35] also focuses on time-like and degenerated AdS projections, using a description in group variables which is equivalent to a Pohlmeyer reduction. Here, we will review the classification in terms of the Pohlmeyer construction.

4 Pohlmeyer reduction for space-like minimal surfaces

We consider $Y \in \mathbb{R}^{2,4}$ and $X \in \mathbb{R}^6$. Then, AdS_5 and S^5 are given by

$$Y \cdot Y = Y^A Y_A = -1 \ , \quad X \cdot X = X^A X_A = 1 \ , \ A = 1 \dots 6 \ . \tag{4.1}$$

Furthermore, $Y(\sigma, \tau)$ and $X(\sigma, \tau)$ are functions of the world-sheet coordinates. We consider a string in conformal gauge, i.e. the metric has the form

$$g_{ab} = \partial_a(Y, X) \cdot \partial_b(Y, X) = f(\sigma, \tau) \begin{pmatrix} 1 & 0 \\ 0 & 1 \end{pmatrix} \ , \quad a, b \in \{\sigma, \tau\} \ . \tag{4.2}$$

Introducing the complex world-sheet coordinates

$$\begin{aligned} z = \frac{1}{2}(\sigma + i\tau) \ , \quad \bar{z} = \frac{1}{2}(\sigma - i\tau) \ , \\ \partial := \partial_z = \partial_\sigma - i\partial_\tau \ , \quad \bar{\partial} := \partial_{\bar{z}} = \partial_\sigma + i\partial_\tau \ . \end{aligned} \tag{4.3}$$

Then, the bosonic part of the string action on $\mathrm{AdS}_5 \times \mathrm{S}^5$ in conformal gauge is given by

$$S_b = \frac{\sqrt{\lambda}}{4\pi} \int \mathrm{d}\sigma \mathrm{d}\tau \left(\partial Y \cdot \bar{\partial} Y + \partial X \cdot \bar{\partial} X + \Lambda_1 (Y \cdot Y + 1) + \Lambda_2 (X \cdot X - 1) \right) , \tag{4.4}$$

where Λ_1 and Λ_2 are two Lagrange multipliers. The variation of the action leads to the equations

$$\bar{\partial}\partial Y = \Lambda_1 Y \ , \quad Y \cdot Y = -1 \ , \quad \bar{\partial}\partial X = \Lambda_2 X \ , \quad X \cdot X = 1 \ . \tag{4.5}$$

Using those equations we further find

$$Y \cdot \partial Y = Y \cdot \bar{\partial} Y = 0 \ , \quad X \cdot \partial X = X \cdot \bar{\partial} X = 0 \ , \tag{4.6}$$

the holomorphicity of $\partial Y \cdot \partial Y$ and $\partial X \cdot \partial X$

$$\bar{\partial}(\partial Y \cdot \partial Y) = \bar{\partial}(\partial X \cdot \partial X) = 0 \tag{4.7}$$

and the expression for the Lagrange multipliers

$$\Lambda_1 = \partial Y \cdot \bar{\partial} Y \ , \quad \Lambda_2 = -\partial X \cdot \bar{\partial} X \ . \tag{4.8}$$

There is the gauge freedom to impose a holomorphic change of variables $z \longmapsto h(z)$. We use this freedom to render the holomorphic quantity

$$\partial Y \cdot \partial Y = -1 \ . \tag{4.9}$$

This in turn implies $\partial X \cdot \partial X = 1$. Further, one can verify that with the above definitions

$$2f(\sigma,\tau) = \Lambda_1 + \Lambda_2 \ . \tag{4.10}$$

From now on we consider AdS_3 and S^3. This implies $X \in \mathbb{R}^4$ and $Y \in \mathbb{R}^{2,2}$. Minimal surfaces in this lower dimensional subspace are automatically also minimal in $\mathrm{AdS}_5 \times \mathrm{S}^5$, as the embedding is totally geodesic (see appendix 8.4.3).

4.1 Projection on S^3

We start the spherical part of the problem. As the spherical part of the surface is space-like, we have

$$\begin{aligned} 0 \leq \partial_\tau X \cdot \partial_\tau X &= -\frac{1}{4}\left(\partial X \cdot \partial X + \bar\partial X \cdot \bar\partial X - 2\partial X \cdot \bar\partial X\right) \\ &= -\frac{1}{2}\left(1 - \partial X \cdot \bar\partial X\right) \ , \end{aligned} \tag{4.11}$$

which implies that $\partial X \cdot \bar\partial X \geq 1$ and thus we can parametrise

$$\cosh\beta := \partial X \cdot \bar\partial X \ , \quad \beta \in \mathbb{R} \ . \tag{4.12}$$

We now introduce a set of basis vectors in $\mathbb{R}^4$, namely $\mathcal{B} = \{X, \partial X, \bar\partial X, M\}$, where M is chosen orthogonal to the first three vectors and has unit length. Now we express the ∂ derivative of the basis vector fields $\mathcal{B}$ in terms of the basis $\mathcal{B}$. Using the parametrisation $v = \partial\partial X \cdot M$ we find

$$\begin{aligned} \partial^2 X &= -X + \frac{\partial\beta}{\sinh\beta}\left(\cosh\beta\partial X - \bar\partial X\right) + v\ M \ , \\ \partial\bar\partial X &= -\cosh\beta X \ , \\ \partial M &= \frac{v}{\sinh^2\beta}\left(\partial X - \cosh\beta\bar\partial X\right) \ , \end{aligned} \tag{4.13}$$

plus their complex conjugated counterparts. The functions β and v have a geometrical meaning. The real function β encodes the metric $h_{ab} = \partial_a X \cdot \partial_b X \ , \ a,b \in \{\sigma,\tau\}$ on the surface's projection to S^3

$$\begin{aligned} &\partial_\sigma X \cdot \partial_\sigma X = \frac{1}{2}\left(\cosh\beta + 1\right) \ , \ \partial_\tau X \cdot \partial_\tau X = \frac{1}{2}\left(\cosh\beta - 1\right) \ , \\ &\partial_\sigma X \cdot \partial_\tau X = 0 \ . \end{aligned} \tag{4.14}$$

The complex function v encodes the second fundamental form of the spherical projection of the surface inside S^3. The definition of the second fundamental form reads

$$\mathrm{II}(V,W) := (\nabla_V W)^\perp \ , \tag{4.15}$$

where V and W are two tangential vector fields and $(.)^{\perp}$ denotes the normal projection. If we evaluate the second fundamental form for the base of the tangential space $\{\partial_\sigma X, \partial_\tau X\}$ of the surface we find

$$\mathrm{II} = \begin{pmatrix} \partial_\sigma^2 X \cdot M & \partial_\sigma \partial_\tau X \cdot M \\ \partial_\sigma \partial_\tau X \cdot M & \partial_\tau^2 X \cdot M \end{pmatrix} . \tag{4.16}$$

Because of (4.13) we know that

$$0 = \partial\bar{\partial} X \cdot M = \left(\partial_\tau^2 + \partial_\sigma^2\right) X \cdot M , \tag{4.17}$$

and therefore II is traceless and we have

$$\mathrm{II} = \begin{pmatrix} a & b \\ b & -a \end{pmatrix} . \tag{4.18}$$

Furthermore,

$$v = \partial\partial X \cdot M = \left(\partial_\sigma^2 X - \partial_\tau^2 X - 2i\,\partial_\sigma \partial_\tau X\right) \cdot M = 2a - 2ib , \tag{4.19}$$

and thus

$$\mathrm{II} = \frac{1}{2} \begin{pmatrix} \mathrm{Re}(v) & -\mathrm{Im}(v) \\ -\mathrm{Im}(v) & -\mathrm{Re}(v) \end{pmatrix} . \tag{4.20}$$

The linear system (4.13) can be rephrased

$$\partial \mathcal{B} = \mathcal{A} \cdot \mathcal{B} , \tag{4.21}$$

with $\mathcal{A}$ being the coefficient functions in (4.13). The explicit expression for $\mathcal{A}$ is given by

$$\begin{aligned} \mathcal{A} &= \begin{pmatrix} 0 & 1 & 0 & 0 \\ -1 & \frac{\cosh\beta \partial\beta}{\sinh\beta} & -\frac{\partial\beta}{\sinh\beta} & v \\ -\cosh\beta & 0 & 0 & 0 \\ 0 & \frac{v}{\sinh^2\beta} & -\frac{v\cosh\beta}{\sinh^2\beta} & 0 \end{pmatrix} , \\ \bar{\mathcal{A}} &= \begin{pmatrix} 0 & 0 & 1 & 0 \\ -\cosh\beta & 0 & 0 & 0 \\ -1 & -\frac{\bar{\partial}\beta}{\sinh\beta} & \frac{\cosh\beta \bar{\partial}\beta}{\sinh\beta} & \bar{v} \\ 0 & -\frac{\bar{v}\cosh\beta}{\sinh^2\beta} & \frac{\bar{v}}{\sinh^2\beta} & 0 \end{pmatrix} . \end{aligned} \tag{4.22}$$

The consistency condition $\partial\bar{\partial}\mathcal{B} = \bar{\partial}\partial\mathcal{B}$ is equivalent to

$$\partial\bar{\mathcal{A}} - \bar{\partial}\mathcal{A} - \left[\mathcal{A}, \bar{\mathcal{A}}\right] = 0 . \tag{4.23}$$

These consistency conditions[2] are equivalent to

$$\partial\bar{\partial}\beta = \frac{v\bar{v}}{\sinh\beta} - \sinh\beta \ , \quad \bar{\partial}v = \frac{\partial\beta}{\sinh\beta}\bar{v} \ , \quad \partial\bar{v} = \frac{\bar{\partial}\beta}{\sinh\beta}v \ . \tag{4.24}$$

In principle, one has to solve these differential equations for $v, \bar{v}$ and β and then plug the solutions into the linear system (4.13) and solve it. Here, we concentrate on the constant solutions of (4.24). The constant solutions are

$$v = v_0 \ , \quad \sinh^2\beta_0 = |v_0|^2 \ . \tag{4.25}$$

Now it is convenient to introduce the parameters ρ_s and ϕ_s via

$$v_0 = \frac{2}{i}\rho_s\sqrt{1+\rho_s^2}e^{2i\phi_s} \ , \quad \sinh^2\beta_0 = 4\rho_s^2\left(1+\rho_s^2\right) \ . \tag{4.26}$$

With this choice the metric on the spherical part $h_{ab} = \partial_a X \cdot \partial_b X \ , \ a, b \in \{\sigma, \tau\}$ and the second fundamental form are

$$h = \begin{pmatrix} \rho_s^2+1 & 0 \\ 0 & \rho_s^2 \end{pmatrix} \ , \quad \mathrm{II} = \rho_s\sqrt{1+\rho_s^2}\begin{pmatrix} \sin 2\phi_s & \cos 2\phi_s \\ \cos 2\phi_s & -\sin 2\phi_s \end{pmatrix} \ . \tag{4.27}$$

We can also express the mean curvature

$$H_s = \frac{1}{2}(h^{-1})_{ab}\mathrm{II}_{ba} = -\frac{\sin 2\phi_s}{2\rho_s\sqrt{1+\rho_s^2}} \ . \tag{4.28}$$

The integration of the linear system is performed in the next section.

4.1.1 Integration of the linear system for S^3

We rewrite the linear system (4.13) using real world-sheet coordinates. Therefore, we use a real orthonormal base

$$\begin{aligned} e &= \left\{ M, X, \frac{\partial_\sigma X}{\sqrt{\partial_\sigma X \cdot \partial_\sigma X}}, \frac{\partial_\tau X}{\sqrt{\partial_\tau X \cdot \partial_\tau X}} \right\} \\ &= \left\{ M, X, \frac{\partial_\sigma X}{\sqrt{\rho_s^2+1}}, \frac{\partial_\tau X}{\rho_s} \right\} \ . \end{aligned} \tag{4.29}$$

Now the vectors in e form an orthonormal system, i.e. $e \in \mathrm{O}(4)$. We will then write down the linear system using e

$$\partial_a e_J{}^K = (\mathcal{A}_a)_J{}^I e_I{}^K \ , \tag{4.30}$$

[2]Geometrically those equations are equivalent to the Gauss- and Codazzi-Mainardi-equation. In higher dimensional spheres (and also AdS) this consistency condition will also yield the Ricci-equation.

with

$$\mathcal{A}_1 = \begin{pmatrix} 0 & -B_1^T \\ B_1 & 0 \end{pmatrix} \ , \quad \mathcal{A}_2 = \begin{pmatrix} 0 & -B_2^T \\ B_2 & 0 \end{pmatrix} \ , \tag{4.31}$$

and

$$\begin{aligned} B_1 &= \begin{pmatrix} \rho_s \sin 2\phi_s & -\sqrt{1+\rho_s^2} \\ \sqrt{1+\rho_s^2}\cos 2\phi_s & 0 \end{pmatrix} \ , \\ B_2 &= \begin{pmatrix} \rho_s \cos 2\phi_s & 0 \\ -\sqrt{1+\rho_s^2}\sin 2\phi_s & -\rho_s \end{pmatrix} \ , \end{aligned} \tag{4.32}$$

In order to integrate (4.30) we have to calculate

$$e = C \cdot \exp\left(\mathcal{A}_\sigma \sigma + \mathcal{A}_\tau \tau\right) \ , \tag{4.33}$$

where C is a constant SO(4) matrix. In order to calculate this exponentiation it is useful to recall that $\mathcal{A}_\sigma\sigma + \mathcal{A}_\tau\tau \in \mathfrak{so}(4)$ and $\mathfrak{so}(4) = \mathfrak{so}(3)_L \oplus \mathfrak{so}(3)_R$. We use the following matrices as a base of $\mathfrak{so}(3)_L$ and $\mathfrak{so}(3)_R$ in $\mathfrak{so}(4)$

$$L_1 = \begin{pmatrix} 0 & \mathbf{t}_1 \\ -\mathbf{t}_1 & 0 \end{pmatrix} \ , \quad L_2 = \begin{pmatrix} 0 & \mathbf{t}_2 \\ -\mathbf{t}_2 & 0 \end{pmatrix} \ , \quad L_3 = \begin{pmatrix} \mathbf{t}_0 & 0 \\ 0 & \mathbf{t}_0 \end{pmatrix} \ , \tag{4.34}$$

and

$$R_1 = \begin{pmatrix} 0 & \mathbf{t}_0 \\ \mathbf{t}_0 & 0 \end{pmatrix} \ , \quad R_2 = \begin{pmatrix} 0 & -\mathbb{1} \\ \mathbb{1} & 0 \end{pmatrix} \ , \quad R_3 = \begin{pmatrix} \mathbf{t}_0 & 0 \\ 0 & -\mathbf{t}_0 \end{pmatrix} \ , \tag{4.35}$$

where the $\mathbf{t}_i$ are the $\mathfrak{sl}(2,\mathbb{R})$ generators

$$\mathbf{t}_0 = \begin{pmatrix} 0 & 1 \\ -1 & 0 \end{pmatrix} \ , \quad \mathbf{t}_1 = \begin{pmatrix} 0 & 1 \\ 1 & 0 \end{pmatrix} \ , \quad \mathbf{t}_2 = \begin{pmatrix} 1 & 0 \\ 0 & -1 \end{pmatrix} \ . \tag{4.36}$$

The L_i and R_i are generators of $\mathfrak{so}(3)$ and $[L_i, R_j] = 0$. We denote by π_L and π_R the projections on the sub-algebras. Then

$$\exp\left(\mathcal{A}_a \xi^a\right) = \exp\left(\pi_L\left(\mathcal{A}_a\xi^a\right)\right) \cdot \exp\left(\pi_R\left(\mathcal{A}_a\xi^a\right)\right) \tag{4.37}$$

The projections on the left and right subspaces read

$$\begin{aligned} \mathcal{A}_2^L &= \begin{pmatrix} \sqrt{\rho_s^2+1}\sin\phi_s\cos\phi_s \\ -\rho_s\cos^2\phi_s \\ 0 \end{pmatrix} \ , \quad \mathcal{A}_1^L = \begin{pmatrix} \sqrt{\rho_s^2+1}\sin^2\phi_s \\ -\rho_s\sin\phi_s\cos\phi_s \\ 0 \end{pmatrix} \\ \mathcal{A}_2^R &= \begin{pmatrix} \sqrt{\rho_s^2+1}\sin\phi_s\cos\phi_s \\ -\rho_s\sin^2\phi_s \\ 0 \end{pmatrix} \ , \quad \mathcal{A}_1^R = \begin{pmatrix} -\sqrt{\rho_s^2+1}\cos^2\phi_s \\ \rho_s\sin\phi_s\cos\phi_s \\ 0 \end{pmatrix} \ . \end{aligned} \tag{4.38}$$

One observes that $\mathcal{A}_1^L \propto \mathcal{A}_2^L$ and $\mathcal{A}_1^R \propto \mathcal{A}_2^R$. Thus, with a redefinition of the world-sheet coordinates $(\tilde{\eta}, \tilde{\xi})$, which are linear combinations of (σ, τ), we have to calculate

$$\exp\left(\mathcal{A}_2^L \tilde{\eta} + \mathcal{A}_2^R \tilde{\xi}\right) \ . \tag{4.39}$$

Via a suitable rotation around the 3-axis in the left and in the right algebra both projections can be made parallel to L_1 and R_1. Thus with suitable rotation angles (θ_L, θ_R) and coordinates on the surface $\xi = \|\mathcal{A}_2^R\|\tilde{\xi}$ and $\eta = \|\mathcal{A}_2^L\|\tilde{\eta}$ we are left with

$$e = \exp(\theta_L L_3)\exp(\theta_R R_3)\exp(\eta L_1)\exp(\xi R_1)\exp(-\theta_R R_3)\exp(-\theta_L L_3) \ . \tag{4.40}$$

The factor $\exp(\theta_L L_3)\exp(\theta_R R_3)$ can be brought to the left hand side and is a SO(4) transformation (i.e. an isometry). So we are only interested in calculating

$$\exp(\eta L_1)\exp(\xi R_1)\exp(-\theta_R R_3)\exp(-\theta_L L_3) \ , \tag{4.41}$$

and more precisely, the second row thereof, as it gives the embedding coordinates, see eq. (4.29). The solution reads

$$\begin{aligned} X^1 &= \cos\xi_+ \sin\theta \ , \ X^2 = \cos\xi_- \cos\theta \ , \\ X^3 &= \sin\xi_- \cos\theta \ , \ X^4 = \sin\xi_+ \sin\theta \ , \end{aligned} \tag{4.42}$$

where $\theta = -(\theta_L + \theta_R)$ and $\xi_\pm = \xi \pm \eta$. This solution is a torus.[3]

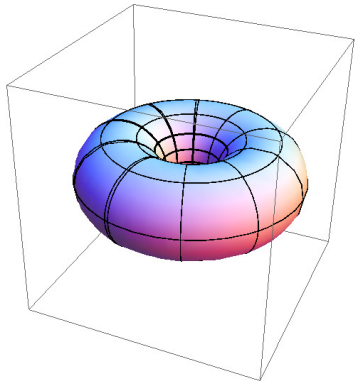

Figure 2: The S^3-projection of the minimal surfaces is a torus.

The mean curvature reads

$$H_s = \cot 2\theta \ , \quad \theta \in (0, \frac{\pi}{2}) \ . \tag{4.43}$$

[3]The plot has been taken from [34].

4.2 Pohlmeyer reduction for a time-like AdS_3 projection

Similarly to the spherical projection we embed AdS_3 into $\mathbb{R}^{2,2}$

$$Y \cdot Y = -1 \ . \tag{4.44}$$

Using conformal world-sheet coordinates we arrive at the following expression for the embedding coordinates (see eq. (4.5) and (4.8))

$$\partial\bar{\partial}Y = \left(\partial Y \cdot \bar{\partial}Y\right) Y \ . \tag{4.45}$$

Writing the gauge fixing conditions $\partial Y \cdot \partial Y = \bar{\partial}Y \cdot \bar{\partial}Y = -1$ in real world-sheet coordinates (σ, τ) this means

$$(\partial_\tau Y)^2 - (\partial_\sigma Y)^2 = 1 \tag{4.46}$$

As we are considering the AdS projection to be time-like here, we can assume that $\partial_\sigma Y$ is time-like and $\partial_\tau Y$ is space-like. Using this assumption and (4.46) we can show that

$$-1 < \partial Y \cdot \bar{\partial}Y < 1 \tag{4.47}$$

and thus we can parametrise

$$\partial Y \cdot \bar{\partial}Y = \cos\alpha \ . \tag{4.48}$$

Following the scheme of Pohlmeyer reduction, we introduce the basis $\mathcal{B} = \{Y, \partial Y, \bar{\partial}Y, N\}$ in $\mathbb{R}^{2,2}$, where N is the normalised orthogonal vector to the surface

$$N \cdot N = 1 \ , \qquad Y \cdot N = 0 = \partial Y \cdot N = \bar{\partial}Y \cdot N \ . \tag{4.49}$$

The real vector N has to be space-like, since the world-sheet in AdS_3 is time-like. These basis vectors satisfy the linear equations

$$\partial^2 Y = -Y + \frac{\partial\alpha}{\sin\alpha}(\cos\alpha\ \partial Y + \bar{\partial}Y) + uN \ , \tag{4.50}$$

$$\partial\bar{\partial}Y = \cos\alpha\ Y \ , \tag{4.51}$$

$$\partial N = \frac{u}{\sin^2\alpha}\left(\partial Y + \cos\alpha\ \bar{\partial}Y\right) \ , \tag{4.52}$$

where

$$u = \partial^2 Y \cdot N \tag{4.53}$$

is the zz-component of the second fundamental form. Also introducing the equations complex conjugated to (4.50), one finds the consistency conditions for the linear system

$$\partial\bar{\partial}\alpha = \sin\alpha - \frac{u\bar{u}}{\sin\alpha}, \tag{4.54}$$

$$\bar{\partial}u = -\frac{\partial\alpha}{\sin\alpha}\,\bar{u}\ , \qquad \partial\bar{u} = -\frac{\bar{\partial}\alpha}{\sin\alpha}\,u. \tag{4.55}$$

In the next subsection we describe the constant solutions of these equations and integrate the corresponding linear system (4.50).

4.2.1 Integration of the linear system

The consistency conditions (4.54) have a $(z,\bar{z})$-independent solution

$$u = u_0\ , \qquad \sin^2\alpha = |u_0|^2\ , \tag{4.56}$$

which we parametrise by

$$u_0 = \frac{2}{i}\,\rho\,\sqrt{1-\rho^2}\;e^{2i\phi} \qquad (0<\rho<1)\ . \tag{4.57}$$

The world-sheet metric tensor $f_{ab} = \partial_a Y\cdot\partial_b Y$ and the second fundamental form $\mathrm{II}_{ab} = \partial^2_{ab}Y\cdot N$ corresponding to the solution (4.56)-(4.57) read

$$f_{ab} = \begin{pmatrix} \rho^2-1 & 0\\ 0 & \rho^2\end{pmatrix}, \quad \mathrm{II}_{ab} = \rho\,\sqrt{1-\rho^2}\begin{pmatrix} \sin 2\phi & \cos 2\phi\\ \cos 2\phi & -\sin 2\phi\end{pmatrix}\ . \tag{4.58}$$

This implies for the mean curvature of the AdS_3 projection [4]

$$H \;=\; \frac{1}{2}(f^{-1})_{ab}\mathrm{II}_{ab} \;=\; -\,\frac{\sin 2\phi}{2\rho\sqrt{1-\rho^2}}\ . \tag{4.59}$$

These conventions have the consequence that σ is the time-like coordinate. Let us introduce the following real orthonormal basis vectors

$$\mathcal{E} = \left\{ Y, \frac{\partial_1 Y}{\sqrt{1-\rho^2}}, N, \frac{\partial_2 Y}{\rho}\right\}\ . \tag{4.60}$$

Thus, the matrix $\mathcal{E}_J{}^K$ is in $\mathrm{O}(2,2)$. The system (4.50) is then equivalent to the matrix equations

$$\partial_a\mathcal{E} = \mathcal{A}_a\,\mathcal{E}\ , \qquad (a=1,2)\ . \tag{4.61}$$

[4] Taking the conformal metric of the surface instead of f_{ab} will of course provide a vanishing mean curvature due to minimality of the surface as a whole.

The matrices $\mathcal{A}_a$ belong to the $\mathfrak{so}(2,2)$ algebra and they have the following block structure

$$\mathcal{A}_1 = \begin{pmatrix} C_1 & B_1 \\ B_1^T & D_1 \end{pmatrix}, \qquad \mathcal{A}_2 = \begin{pmatrix} 0 & B_2 \\ B_2^T & D_2 \end{pmatrix}, \tag{4.62}$$

with 2×2 matrices

$$B_1 = \begin{pmatrix} 0 & 0 \\ \rho \sin 2\phi & 0 \end{pmatrix}, \quad B_2 = \begin{pmatrix} 0 & \rho \\ \rho \cos 2\phi & 0 \end{pmatrix}, \tag{4.63}$$

$$C_1 = \sqrt{1-\rho^2}\,\mathbf{t}_0\ , \quad D_1 = -\sqrt{1-\rho^2}\,\cos 2\phi\,\mathbf{t}_0\ , \quad D_2 = \sqrt{1-\rho^2}\,\sin 2\phi\,\mathbf{t}_0\ . \tag{4.64}$$

The integrability of the system (4.61) is provided by $[\mathcal{A}_1, \mathcal{A}_2] = 0$, and one obtains

$$\mathcal{E} = C \cdot \exp(\xi^a \mathcal{A}_a)\ , \tag{4.65}$$

where C is a constant $\mathrm{O}(2,2)$ matrix. The world-sheet $Y(\sigma, \tau)$ can be read off from the first row of this solution. In order to perform the exponentiation we remark that there is a decomposition of the Lie algebra $\mathfrak{so}(2,2) = \mathfrak{sl}(2,\mathbb{R}) \oplus \mathfrak{sl}(2,\mathbb{R})$. One can construct the four dimensional representation of $\mathfrak{sl}(2,\mathbb{R})_L$ and $\mathfrak{sl}(2,\mathbb{R})_R$.

$$L_0 = \begin{pmatrix} \mathbf{t}_0 & 0 \\ 0 & \mathbf{t}_0 \end{pmatrix}, \qquad L_1 = \begin{pmatrix} 0 & \mathbf{t}_2 \\ \mathbf{t}_2 & 0 \end{pmatrix}, \qquad L_2 = \begin{pmatrix} 0 & \mathbf{t}_1 \\ \mathbf{t}_1 & 0 \end{pmatrix}, \tag{4.66}$$

$$R_0 = \begin{pmatrix} -\mathbf{t}_0 & 0 \\ 0 & \mathbf{t}_0 \end{pmatrix}, \quad R_1 = \begin{pmatrix} 0 & -\mathbb{1} \\ -\mathbb{1} & 0 \end{pmatrix}, \quad R_2 = \begin{pmatrix} 0 & -\mathbf{t}_0 \\ \mathbf{t}_0 & 0 \end{pmatrix}.$$

The left and right elements commute. Now we need to compute the projections of $\mathcal{A}_a$ on the left and right subspace of $\mathfrak{so}(2,2)$. We find

$$\mathcal{A}_1^L = \begin{pmatrix} +\sqrt{1-\rho^2}\sin^2\phi \\ 0 \\ \rho\cos\phi\sin\phi \end{pmatrix}, \quad \mathcal{A}_2^L = \begin{pmatrix} \sqrt{1-\rho^2}\sin\phi\cos\phi \\ 0 \\ \rho\cos^2\phi \end{pmatrix}, \tag{4.67}$$

$$\mathcal{A}_1^R = \begin{pmatrix} -\sqrt{1-\rho^2}\cos^2\phi \\ 0 \\ \rho\cos\phi\sin\phi \end{pmatrix}, \quad \mathcal{A}_2^R = \begin{pmatrix} \sqrt{1-\rho^2}\sin\phi\cos\phi \\ 0 \\ -\rho\sin^2\phi \end{pmatrix}. \tag{4.68}$$

From these projections we see that $\mathcal{A}_1^L \propto \mathcal{A}_2^L$ and $\mathcal{A}_1^R \propto \mathcal{A}_2^R$ with different proportionality factors. So there are two linear combinations $\tilde{\xi}$ and $\tilde{\eta}$ of σ and τ, that we can treat as new coordinates for the surface, such that the remaining exponentiation problem is

$$\mathcal{E} = \exp(\mathcal{A}_2^L \tilde{\xi} + \mathcal{A}_2^R \tilde{\eta})\ . \tag{4.69}$$

The algebra $\mathfrak{so}(2,2)$ carries a metric induced by the Killing form

$$g(X,Y) \;=\; \frac{1}{4}\,\mathrm{tr}(X\cdot Y)\;. \tag{4.70}$$

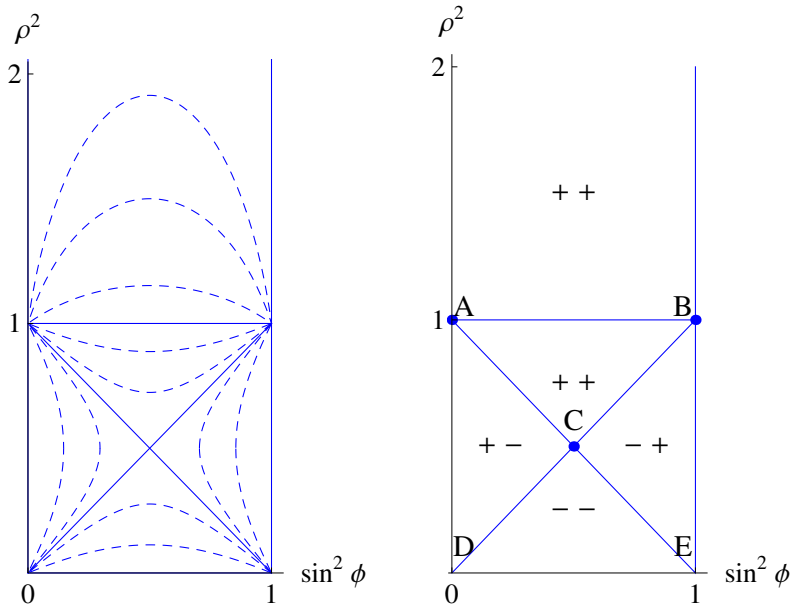

Figure 3: The dashed lines in the first plot correspond to constant θ. The definition of θ is given seperately for each class of surfaces in the following sections. The left and right signs in the second plot correspond to the signs of $\left(\mathcal{A}_2^L\right)^2$ and $\left(\mathcal{A}_2^R\right)^2$, respectively. $\left(\mathcal{A}_2^L\right)^2$ vanishes at the diagonal BD and $\left(\mathcal{A}_2^R\right)^2$ at AE. The area above the line AB represents surfaces with space-like AdS projection - below the line AB the surfaces' AdS projections are time-like. On line AB the AdS projection has a degenerated metric.

The generators given in eq. (4.66) are orthogonal with respect to this metric. Furthermore, the induced metric on the left and right sub-algebras is Minkowskian, with the time-like direction being the 0-direction. Naturally, here arises a subdivision depending on whether the left and right projections of $\mathcal{A}_2$ are space-like, time-like or light-like. The norm of $\mathcal{A}_2^L$ and $\mathcal{A}_2^R$ is

$$\begin{aligned}\|\mathcal{A}_2^L\| &= \frac{\cos\phi}{\sqrt{2}}\sqrt{-1+2\rho^2+\cos 2\phi} \;=\; \cos\phi\sqrt{\rho^2-\sin^2\phi}\;, \\ \|\mathcal{A}_2^R\| &= \frac{\sin\phi}{\sqrt{2}}\sqrt{-1+2\rho^2-\cos 2\phi} \;=\; \sin\phi\sqrt{\rho^2-1+\sin^2\phi}\;.\end{aligned} \tag{4.71}$$

In the next section we will present the surfaces in embedding coordinates in $\mathbb{R}^{(2,2)}$ that correspond to these cases, see fig. 3.

4.2.2 Space-like - Space-like case (inside the triangle ABC)

We assume that both projections of $\mathcal{A}_2$ are space-like, thus the parameters $(\rho,\ \phi)$ are such that they lie inside the triangle ABC (see fig. 3). Then in both Lie algebras there are boosts with the angles θ_L and θ_R such that both projections are proportional to R_2 or L_2. Defining $\xi = \|\mathcal{A}_2^L\|\tilde{\xi}$ and $\eta = \|\mathcal{A}_2^R\|\tilde{\eta}$ we have

$$\begin{aligned}\mathcal{E} &= \exp(\mathcal{A}_2^L\tilde{\xi} + \mathcal{A}_2^R\tilde{\eta}) &(4.72)\\ &= \exp(\theta_L L_1)\exp(\theta_R R_1)\exp(\xi L_2)\exp(\eta R_2)\exp(-\theta_R R_1)\exp(-\theta_L L_1)\ . &(4.73)\end{aligned}$$

The factor $\exp(\theta_L L_1)\exp(\theta_R R_1)$ is in $\mathrm{SO}_\uparrow(2,2)$ and can be absorbed into the constant of integration which is an isometry transformation on AdS_3. We compute

$$\exp(\xi L_2)\exp(\eta R_2)\exp(-\theta_R R_1)\exp(-\theta_L L_1)\ , \tag{4.74}$$

where the first row provides the embedding coordinates

$$\begin{aligned} Y^{0'} &= \cosh\theta\cosh\xi_-\ ,\ Y^0 = \sinh\theta\sinh\xi_+\ , \\ Y^1 &= \sinh\theta\cosh\xi_+\ ,\ Y^2 = \cosh\theta\sinh\xi_-\ , \end{aligned} \tag{4.75}$$

with $\xi_\pm = \xi \pm \eta$ and $\theta = \theta_R - \theta_L$. The embedding coordinates of this surface fulfil the quadratic relation

$$(Y^{0'})^2 - (Y^2)^2 = \cosh^2\theta\ . \tag{4.76}$$

The conformal boundary of AdS_3 is $\mathrm{S}^1\times\mathrm{S}^1$. Calculating θ explicitly we find that

$$\coth\ 2\theta = \frac{\sin(2\phi)}{2\rho\sqrt{1-\rho^2}} \tag{4.77}$$

which means by eq. (4.59) that the mean curvature is given via

$$H = -\coth\ 2\theta\ . \tag{4.78}$$

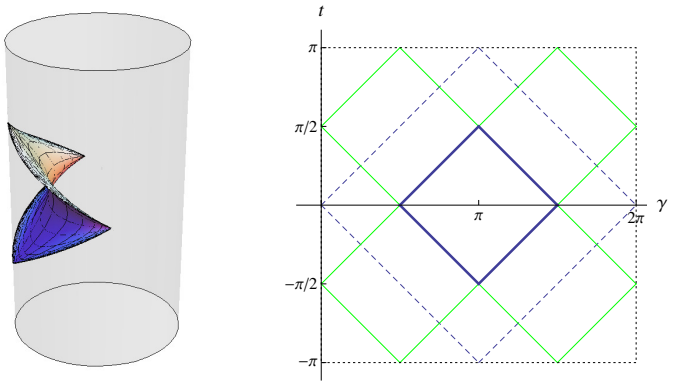

Figure 4: The tetragon with time-like AdS projection. The dashed line corresponds to the boundary of a Poincaré patch of AdS_3. The green and blue lines correspond to the boundaries generated by the quadratic relation eq. (4.76). If we are only interested in a single connected part of the surface (which is the parametrised solution eq. (4.75)) the boundary of the surface is depicted blue. The boundary of AdS_3 is a torus with periodic time t and a periodic spatial direction γ. The precise definition of these parameters can be found in 8.6.

4.2.3 Light-like - Light-like case (Point C)

We assume that both projections of $\mathcal{A}_2$ are light-like. This implies that

$$\phi = \frac{\pi}{4} \,, \qquad \rho^2 = \frac{1}{2} \,, \tag{4.79}$$

which means that we are looking on point C in the parameter space (see fig. 3).Then we have to calculate

$$\exp\left(\frac{\sigma+\tau}{2\sqrt{2}}\,(L_0+L_2)\right)\exp\left(-\frac{\sigma-\tau}{2\sqrt{2}}\,(R_0-R_2)\right) \,. \tag{4.80}$$

The first row then gives the embedding coordinates

$$Y^{0'} = \frac{1}{4}(4-\sigma^2+\tau^2) \,,\; Y^0 = \frac{-\sigma}{\sqrt{2}} \,,\; Y^1 = -\frac{1}{4}(\sigma^2-\tau^2) \,,\; Y^2 = \frac{\tau}{\sqrt{2}} \,. \tag{4.81}$$

Contrary to most other solutions that we present here, this surfaces is isolated and not embedded into any one parameter family of solutions. It can be realised as the intersection of AdS_3 with the linear relation

$$Y^{0'} - Y^1 = 1 \,. \tag{4.82}$$

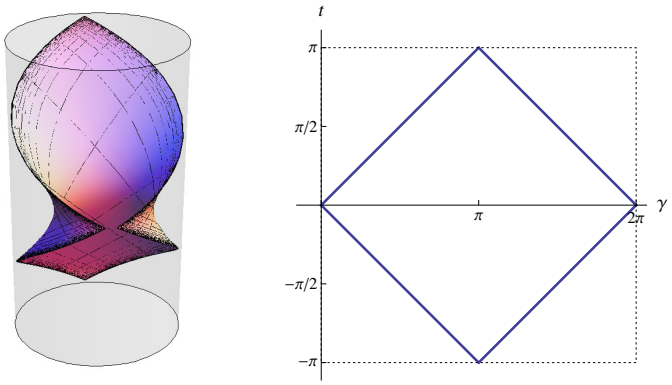

Figure 5: The boundary for the "giant" solution coincides with the boundary of a Poincaré patch. As the defining relation (4.82) is linear, the surface consists of a single connected part.

The mean curvature for this surface is

$$H = -1 \ . \tag{4.83}$$

4.2.4 Time-like - Time-like case (inside the triangle CDE)

Assuming that both projections of $\mathcal{A}_2$ are time-like, we can similarly to a previous case introduce two boost angles θ_R and θ_L and calculate

$$\exp(\xi L_0)\exp(\eta R_0)\exp(-\theta_R R_1)\exp(-\theta_L L_1) \ . \tag{4.84}$$

The first row then gives the embedding coordinates

$$\begin{aligned} Y^{0'} &= \cos\xi_- \cosh\theta \ , \quad Y^0 = \sin\xi_- \cosh\theta \ , \\ Y^1 &= \cos\xi_+ \sinh\theta \ , \quad Y^2 = \sin\xi_+ \sinh\theta \ , \end{aligned} \tag{4.85}$$

with $\theta = \theta_R - \theta_L$, $\xi_\pm = -(\xi \pm \eta)$.
Here, θ determines the diameter of the torus. The quadratic relation defining this surface is

$$(Y^{0'})^2 + (Y^0)^2 = \cosh^2\theta \ . \tag{4.86}$$

Calculating θ explicitly we find that

$$\coth\ 2\theta = \frac{\sin(2\phi)}{2\rho\sqrt{1-\rho^2}} \tag{4.87}$$

which means by eq. (4.59) that the mean curvature is given by

$$H = -\coth\ 2\theta \ . \tag{4.88}$$

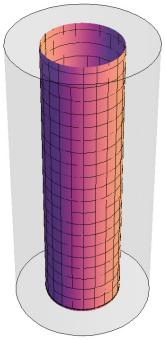

Figure 6: This solution describes a torus in AdS does not approach the conformal boundary of AdS_3.

4.2.5 Time-like - Space-like case (inside triangle ACD or BCE)

We assume that one of the projections of $\mathcal{A}_2$ is time-like while the other is space-like. Then we can choose boosts in both planes such that the vectors then are proportional to one generator. Then we calculate

$$\exp(\xi L_2)\exp(\eta R_0)\exp(-\theta_R R_1)\exp(-\theta_L L_1)\ , \tag{4.89}$$

and the first row then gives the embedding coordinates

$$\begin{aligned} Y^{0'} &= \sin(\eta)\sinh(\theta)\sinh(\xi) + \cos(\eta)\cosh(\theta)\cosh(\xi)\ , \\ Y^{0} &= \sin(\eta)\cosh(\theta)\cosh(\xi) - \cos(\eta)\sinh(\theta)\sinh(\xi)\ , \\ Y^{1} &= \sin(\eta)\cosh(\theta)\sinh(\xi) - \cos(\eta)\sinh(\theta)\cosh(\xi)\ , \\ Y^{2} &= \sin(\eta)\sinh(\theta)\cosh(\xi) + \cos(\eta)\cosh(\theta)\sinh(\xi)\ , \end{aligned} \tag{4.90}$$

with $\theta = \theta_L - \theta_R$. Setting the other projection time-like, we obtain a similar expression that is connected via $\xi \to \eta$ and $\eta \to -\xi$. So there are no further solutions. The quadratic relation that is satisfied by eq. (4.90) is

$$-Y^{0'}Y^1 + Y^0 Y^2 = \frac{1}{2}\sinh 2\theta\ . \tag{4.91}$$

Calculating θ explicitly we find that

$$\tanh\ 2\theta = \frac{\sin(2\phi)}{2\rho\sqrt{1-\rho^2}} \tag{4.92}$$

which means by eq. (4.59) that the mean curvature is given by

$$H = -\tanh\ 2\theta\ . \tag{4.93}$$

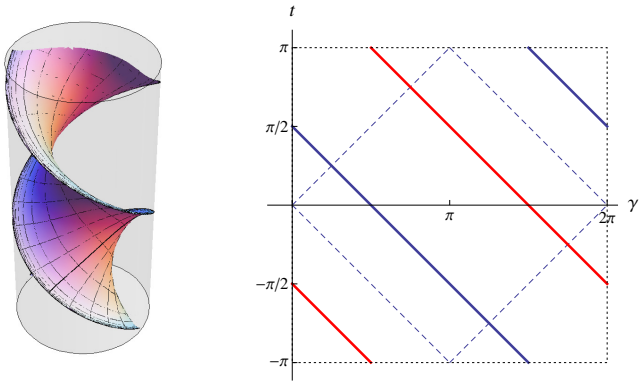

Figure 7: This surface describes a infinite spinning string that starts and ends on the conformal boundary of AdS_3 and creates two light-like traces there. These light-like traces are the blue and red lines in the boundary plot.

4.2.6 Light-like - Space-like case (line AC or BC)

If one of the projections of $\mathcal{A}_2$ is light-like while the other is space-like we can choose a boost similarly to previous cases and calculate

$$\exp(\eta e^{2\theta_R}(L_0 + L_2)) \exp(\xi R_2) \exp(-\theta_R R_1) \ . \tag{4.94}$$

Here η is rescaled for convenience. The first row then gives the embedding coordinates

$$\begin{aligned} \tilde{Y}^{0'} &= -\eta e^{\theta_R} \sinh\xi + \cosh\theta_R \cosh\xi \ , \\ \tilde{Y}^{0} &= -\eta e^{\theta_R} \cosh\xi + \sinh\theta_R \sinh\xi \ , \\ \tilde{Y}^{1} &= -\eta e^{\theta_R} \sinh\xi + \sinh\theta_R \cosh\xi \ , \\ \tilde{Y}^{2} &= +\eta e^{\theta_R} \cosh\xi - \cosh\theta_R \sinh\xi \ . \end{aligned} \tag{4.95}$$

Applying the isometry

$$Y = \exp(-\theta_R L_1)\tilde{Y} \ , \tag{4.96}$$

the solution simplifies to

$$Y = (\cosh\xi - \eta\sinh\xi, -\eta\cosh\xi, -\eta\sinh\xi, \eta\cosh\xi - \sinh\xi) \ , \tag{4.97}$$

so this surface does not come as a one-parameter family. Alternatively, one can set the right part light-like and obtain a solution by replacing

$$Y^0 \to -Y^0 \ , \quad Y^1 \to -Y^1 \ , \quad Y^2 \to -Y^2$$

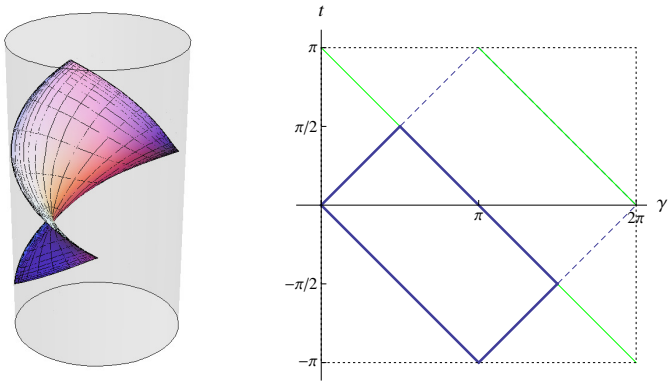

Figure 8: This surface can not be contained in a single Poincaré patch, as it contains antipodal points. The defining quadratic relation (4.98) also creates a second non-connected part of the surface whose boundary is depicted in green in the boundary plot.

in eq. (4.97).
The defining quadratic relation for these surfaces is

$$(Y^{0'} + Y^1)^2 - (Y^0 + Y^2)^2 = 1 \ . \tag{4.98}$$

The mean curvature of the projection inside AdS_3 is

$$H = -1 \ . \tag{4.99}$$

4.2.7 Light-like - Time-like case (line DC or EC)

The last remaining case is where one of the projections of $\mathcal{A}_2$ is light-like while the other is time-like. Again, we can choose a boost similarly to previous cases and calculate

$$\exp(\eta e^{2\theta_R}(L_0 + L_2)) \exp(\xi R_0) \exp(-\theta_R R_1) \ , \tag{4.100}$$

where we have rescaled η for convenience. The first row then gives the embedding coordinates

$$\begin{aligned}
\tilde{Y}^{0'} &= \eta \sinh\theta_R \sin\xi + \cosh\theta_R(\eta \sin\xi + \cos\xi) \ , \\
\tilde{Y}^{0} &= -\eta \sinh\theta_R \cos\xi - \cosh\theta_R(\eta \cos\xi - \sin\xi) \ , \\
\tilde{Y}^{1} &= \eta \cosh\theta_R \sin\xi + \sinh\theta_R(\eta \sin\xi + \cos\xi) \ , \\
\tilde{Y}^{2} &= \eta \cosh\theta_R \cos\xi + \sinh\theta_R(\eta \cos\xi - \sin\xi) \ ,
\end{aligned} \tag{4.101}$$

Using the isometry transformation

$$Y = \exp(-\theta_R L_1)\tilde{Y} \ , \tag{4.102}$$

the solution simplifies and becomes θ-independent

$$Y = (\cos\xi + \eta\sin\xi, \sin\xi - \eta\cos\xi, \eta\cos\xi, \eta\sin\xi) \tag{4.103}$$

Setting the right part light-like, one obtains a solution that by setting

$$Y^0 \to -Y^0 \ , \quad Y^1 \to -Y^1 \ , \quad Y^2 \to -Y^2$$

is connected to (4.103). The defining quadratic relation for these surfaces is

$$(Y^{0'} - Y^1)^2 + (Y^0 + Y^2)^2 = 1 \ . \tag{4.104}$$

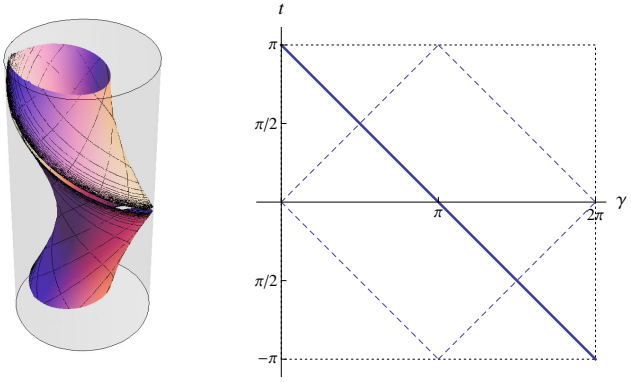

Figure 9: This surface describes an open spinning string whose two end points coincide at the conformal boundary.

The mean curvature of this string is

$$H = -1 \ . \tag{4.105}$$

4.3 Generic solution for time-like AdS projection

The integration of the linear system (4.61) can also be done for all flat minimal surfaces with time-like AdS projection in general. Of course the resulting embedding coordinates are more complicated, but we can see that they are all smoothly connected if we are moving from one region in fig. 3 to another. We will need the length of the projections of the Matrices $\mathcal{A}_1$ and $\mathcal{A}_2$.

$$\begin{aligned}
\|\mathcal{A}_1^L\| &= \frac{\sin\phi}{\sqrt{2}}\sqrt{-1+2\rho^2+\cos 2\phi}\ , \quad \|\mathcal{A}_1^R\| = \frac{\cos\phi}{\sqrt{2}}\sqrt{-1+2\rho^2-\cos 2\phi}\ , \\
\|\mathcal{A}_2^L\| &= \frac{\cos\phi}{\sqrt{2}}\sqrt{-1+2\rho^2+\cos 2\phi}\ , \quad \|\mathcal{A}_2^R\| = \frac{\sin\phi}{\sqrt{2}}\sqrt{-1+2\rho^2-\cos 2\phi}.
\end{aligned} \tag{4.106}$$

Then calculating $\exp(\mathcal{A}_1\sigma + \mathcal{A}_2\tau)$ leads to

$$\begin{aligned}
Y^{0'} &= \cosh\eta\cosh\xi - \frac{\sin^2 2\phi}{4\|\mathcal{A}_1^L\|\|\mathcal{A}_1^R\|}\sinh\eta\sinh\xi \\
Y^0 &= \sqrt{1-\rho^2}\left(\frac{\cos^2\phi}{\|\mathcal{A}_1^R\|}\cosh\eta\sinh\xi + \frac{\sin^2\phi}{\|\mathcal{A}_1^L\|}\sinh\eta\cosh\xi\right) \\
Y^1 &= \rho\left(\frac{\sin^2\phi}{\|\mathcal{A}_2^R\|}\cosh\eta\sinh\xi - \frac{\cos^2\phi}{\|\mathcal{A}_2^L\|}\sinh\eta\cosh\xi\right) \\
Y^2 &= -\frac{\rho\sqrt{1-\rho^2}\,\sin 2\phi}{2\|\mathcal{A}_1^L\|\|\mathcal{A}_1^R\|}\sinh\eta\sinh\xi\ ,
\end{aligned} \tag{4.107}$$

with the redefinition of word sheet coordinates

$$\eta = \|\mathcal{A}_1^L\|\sigma + \|\mathcal{A}_2^L\|\tau\ , \quad \xi = \|\mathcal{A}_1^R\|\sigma - \|\mathcal{A}_2^R\|\tau\ . \tag{4.108}$$

Some comments are in order here. The above equation is fine as it stands if all projections of $\mathcal{A}$ are space-like, which means that we are in the (++)-region in fig. 3. If either the left or right projection is time-like there is a continuation from the hyperbolic to a trigonometric function. Therefore, one has to generate a complex i in the denominator for every sinh-function in the numerator to keep the embedding coordinates real. From the definition of $(\eta,\ \xi)$, we see that η is a *left* variable and ξ is *right*. So $\sinh(\eta)$ has to be paired with $\frac{1}{\|\mathcal{A}^L\|}$ and $\sinh(\xi)$ with $\frac{1}{\|\mathcal{A}^R\|}$ - just as it is realised in the formula.

The continuation of formula (4.107) to a light-like case is also well defined. In this case, for every sinh term the denominator and numerator are zero and the application of de l'Hospital rule yields a linear term.

4.4 Degenerated AdS_3 projection

In this section we present a Pohlmeyer reduction for the case where the induced metric for the AdS_3 projection of the surface is degenerated. However, these surfaces are still space-like inside $AdS_3 \times S^3$. If the AdS_3 projection is degenerated, the induced metric on the AdS_3 projection reads

$$f_{ab} = \begin{pmatrix} 0 & 0 \\ 0 & 1 \end{pmatrix} . \tag{4.109}$$

This assumption renders the mean curvature ill-defined as f_{ab} cannot be inverted, see eq. (4.59). The normal vector of the surface inside AdS_3 is then also light-like. We fix the normal vector N by demanding

$$N \cdot Y = N \cdot \partial_2 Y = N \cdot N = 0 , \tag{4.110}$$

together with the normalisation

$$(N \cdot \partial_1 Y) = 1 . \tag{4.111}$$

To express the linear system we choose the orthonormal basis

$$\mathcal{E} := \{Y, Z_-, \partial_2 Y, Z_+\} \tag{4.112}$$

where

$$Z_+ = \frac{1}{\sqrt{2}}(\partial_1 Y + N) , \qquad Z_- = \frac{1}{\sqrt{2}}(\partial_1 Y - N) . \tag{4.113}$$

Then one can check that these basis vectors satisfy

$$\partial_a \mathcal{E} = \mathcal{A}_a \mathcal{E} , \tag{4.114}$$

with

$$\mathcal{A}_1 = \begin{pmatrix} 0 & \frac{1}{\sqrt{2}} & 0 & \frac{1}{\sqrt{2}} \\ -\frac{1}{\sqrt{2}} & 0 & \frac{1}{\sqrt{2}}u_2 & u_1 \\ 0 & \frac{1}{\sqrt{2}}u_2 & 0 & \frac{1}{\sqrt{2}}u_2 \\ \frac{1}{\sqrt{2}} & u_1 & -\frac{1}{\sqrt{2}}u_2 & 0 \end{pmatrix} , \tag{4.115}$$

$$\mathcal{A}_2 = \begin{pmatrix} 0 & 0 & 1 & 0 \\ 0 & 0 & -\frac{1}{\sqrt{2}}u_1 & u_2 \\ 1 & -\frac{1}{\sqrt{2}}u_1 & 0 & -\frac{1}{\sqrt{2}}u_1 \\ 0 & u_2 & \frac{1}{\sqrt{2}}u_1 & 0 \end{pmatrix} , \tag{4.116}$$

where $u_1 = (N \cdot \partial_1 \partial_1 Y) = -(N \cdot \partial_2 \partial_2 Y)$ and $u_2 = (N \cdot \partial_2 \partial_1 Y)$ are coefficients of the second fundamental form. The vacuum solutions are obtained with constant u_1 and u_2. The integrability condition $[\mathcal{A}_1, \mathcal{A}_2] - \partial_1 \mathcal{A}_2 + \partial_2 \mathcal{A}_1$ then leads to

$$1 = u_1^2 + u_2^2 + \partial_2 u_2 + \partial_1 u_1 , \quad \partial_1 u_2 = \partial_2 u_1 . \tag{4.117}$$

4.4.1 Vacuum solutions

First, we consider the constant solutions of (4.117)

$$u_1^2 + u_2^2 = 1 \ . \tag{4.118}$$

We parametrise $u_1 = \cos\theta$ and $u_2 = \sin\theta$ with constant θ. The integration of the linear system is simple and does not require the splitting of $\mathfrak{so}(2,2) = \mathfrak{sl}(2,\mathbb{R}) \oplus \mathfrak{sl}(2,\mathbb{R})$. The embedding coordinates are given by the first row of $\exp(\mathcal{A}_a \xi^a)$ which is

$$\begin{aligned} Y^{0'} &= \cosh\tau \ , \quad Y^0 = \frac{e^{\varphi} - \cosh\tau - \sin\theta \sinh\tau}{\cos\theta\sqrt{2}} \ , \\ Y^1 &= \sinh\tau \ , \quad Y^2 = -\frac{e^{\varphi} - \cosh\tau - \sin\theta \sinh\tau}{\cos\theta\sqrt{2}} \ , \end{aligned} \tag{4.119}$$

with $\varphi = \sigma\cos\theta + \tau\sin\theta$. These surfaces satisfy the quadratic relation

$$(Y^{0'})^2 - (Y^1)^2 = 1 \ . \tag{4.120}$$

Therefore, the shape surface does not depend on the parameter θ. One can also verify that the limit $\theta \to \pm\frac{\pi}{2}$ of 4.119 exists and gives

$$Y^{0'} = \cosh\tau \ , \quad Y^0 = \frac{e^{\pm\tau}\sigma}{\sqrt{2}} \ , \quad Y^1 = \sinh\tau \ , \quad Y^2 = -\frac{e^{\pm\tau}\sigma}{\sqrt{2}} \ . \tag{4.121}$$

In this limit, surface has a closed light-like boundary with two cusps.

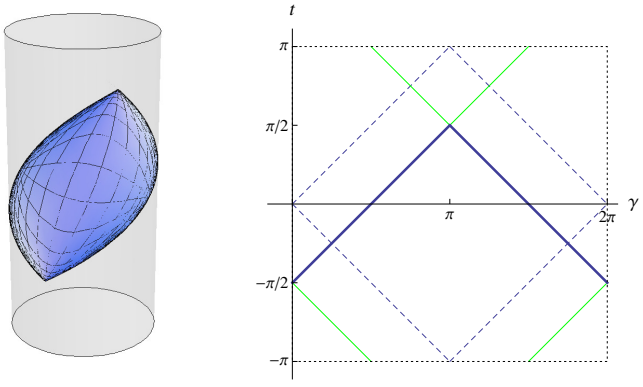

Figure 10: The plot corresponds to the limit $\theta \to \pm\frac{\pi}{2}$ and corresponds to the points A and B in fig. 3.

If, however, $\cos\theta \neq 0$, the surface is only a part of 4.121. Then, the AdS

projection contains a "boundary" which lies inside AdS. In the product space, this is not the case, as approaching the inner boundary in AdS results in infinite spinning around the torus in the spherical projection. The quadratic relation 4.120 also describes a solution obtained from 4.121 via a reflection. Thus, the whole intersection of AdS_3 with the quadratic relation 4.120 gives fig. 11.

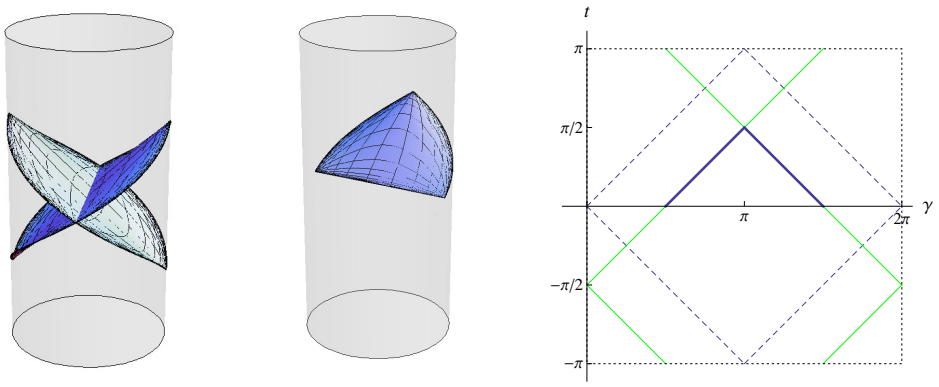

Figure 11: Each of these four leaves corresponds to a complete space-like minimal surface in $AdS_3 \times S^3$ without an internal boundary and with a single cusp. The position of the intersection line depends on the choice of θ.

4.4.2 Non-vacuum solutions

For a surface with an AdS projection that carries a degenerated metric (4.109), it is possible to integrate the linear system for non-constant solutions of the integrability conditions (4.117), as well. The linear system in complex variables reads

$$\begin{aligned} \partial^2 Y &= -Y + u(\partial Y + \bar{\partial} Y) \ , \\ \partial\bar{\partial} Y &= Y \ , \\ \partial N &= Y + \frac{u}{2}(\partial Y - \bar{\partial} Y) - uN \ , \end{aligned} \tag{4.122}$$

with $u = \frac{1}{2}\left(\partial^2 Y \cdot N\right)$. Inserting the second into the first equation we find

$$\partial\left(\bar{\partial} Y + \partial Y\right) = u(\bar{\partial} Y + \partial Y) \ , \tag{4.123}$$

and $(\bar{\partial} Y + \partial Y) = 2\partial_\sigma Y$. Therefore, we conclude that the light-like vector $\partial_\sigma Y$ can be written

$$\partial_\sigma Y = \psi(\sigma, \tau) e_+ \ , \tag{4.124}$$

where e_+ is a constant light-like vector and $\psi(\sigma,\tau)$ is a scalar function. The vector can be chosen to be $e_+ = (0,1,0,1)$, using a global isometry. Then, integrating eq. (4.124) the embedding coordinates have the structure

$$Y = \left(\cosh\left(\gamma(\tau)\right), F(\sigma,\tau), \sinh\left(\gamma(\tau)\right), F(\sigma,\tau)\right) \ , \tag{4.125}$$

with $\partial_\sigma F(\sigma,\tau) = \psi(\sigma,\tau)$. Using the second equation in (4.122) we conclude that $\gamma(\tau) = \tau$ and F satisfies the free field equation

$$\partial\bar{\partial}F = F \ . \tag{4.126}$$

The non-constant solutions have the embedding coordinates

$$Y = (\cosh\tau, F(\sigma,\tau), \sinh\tau, F(\sigma,\tau)) \tag{4.127}$$

with a suitable function F and thus satisfy the same quadratic relation (4.120) as the constant solutions.

The integrability condition is

$$\bar{\partial}u + u\bar{u} = 1 \ , \quad \partial\bar{u} + u\bar{u} = 1 \ , \tag{4.128}$$

which is via $u = u_1 - iu_2$ equivalent to the integrability condition (4.117). The conditions (4.128) are solved by setting $u = \partial\psi/\psi$.

4.5 Space-like AdS_3 projection

Here we follow the procedure in [34]. As the AdS-projection is space-like we have $\partial_a Y \cdot \partial_a Y > 0 \ , \quad a \in (\sigma,\tau)$. Therefore, together with eq. (4.9)

$$\partial Y \cdot \bar{\partial} Y > 1 \tag{4.129}$$

and we parametrise

$$\partial Y \cdot \bar{\partial} Y =: \cosh\alpha \ . \tag{4.130}$$

Following the Pohlmeyer receipt we introduce a set of basis vector fields in $\mathbb{R}^{2,2}$. $\mathcal{B} = \{N, Y, \partial Y, \bar{\partial} Y\}$ with N being the unit vector perpendicular to Y, ∂Y and $\bar{\partial} Y$. The differentials can be expressed as

$$\begin{aligned} \partial^2 Y &= -Y + \frac{\partial\alpha}{\sinh\alpha}\left(\cosh\alpha\partial Y + \bar{\partial} Y\right) + u\ N \ , \\ \partial\bar{\partial} Y &= \cosh\alpha Y \ , \\ \partial N &= \frac{u}{\sinh^2\alpha}\left(\partial Y \cosh\alpha\bar{\partial} Y\right) \ , \end{aligned} \tag{4.131}$$

together with their complex conjugated counterparts. As before,

$$u = -N \cdot \partial^2 Y \ , \quad \bar{u} = -N \cdot \bar{\partial}^2 Y \tag{4.132}$$

parametrise the second fundamental form. The consistency conditions ($\bar{\partial}\partial\mathcal{B} = \partial\bar{\partial}\mathcal{B}$) yield the equations

$$\begin{aligned} \partial\bar{\partial}\alpha &= \sinh\alpha - \frac{u\bar{u}}{\sinh\alpha} \ , \\ \bar{\partial}u &= -\frac{\partial\alpha}{\sinh\alpha}\bar{u} \ , \quad \partial\bar{u} = -\frac{\bar{\partial}\alpha}{\sinh\alpha}u \ . \end{aligned} \tag{4.133}$$

Looking for constant solutions we see that

$$u = u_0 \ , \quad \sinh^2\alpha = |u_0|^2 \ , \tag{4.134}$$

and can parametrise

$$u_0 \ = \ \frac{2}{i}\ \rho\ \sqrt{1+\rho^2}\ e^{2i\phi} \quad , \qquad \rho > 0 \ . \tag{4.135}$$

Then, the induced metric f_{ab} and the second fundamental form II_{ab} take the form

$$f_{ab} = \begin{pmatrix} \rho^2 & 0 \\ 0 & 1+\rho^2 \end{pmatrix} \ , \quad \mathrm{II}_{ab} = \rho\sqrt{1+\rho^2}\begin{pmatrix} \sin 2\phi & \cos 2\phi \\ \cos 2\phi & -\sin 2\phi \end{pmatrix} \ , \tag{4.136}$$

and thus the mean curvature becomes

$$H = \frac{1}{2}(f^{-1})_{ab}\mathrm{II}_{ba} = \frac{\sin 2\phi}{2\rho\sqrt{1+\rho^2}} \ . \tag{4.137}$$

In order to integrate eq. (4.131) we go back to real coordinates and choose the orthonormal reper

$$\mathcal{E} = \left\{ N, Y, \frac{\partial_\sigma Y}{\rho}, \frac{\partial_\tau Y}{\sqrt{1+\rho^2}} \right\} \ . \tag{4.138}$$

The linear system eq. (4.131) then reads

$$\partial_a \mathcal{E} = \mathcal{A}_a \mathcal{E} \ , \tag{4.139}$$

with

$$\mathcal{A}_\sigma = \begin{pmatrix} 0 & B_1 \\ B_1^T & 0 \end{pmatrix} \quad , \qquad \mathcal{A}_\tau = \begin{pmatrix} 0 & B_2 \\ B_2^T & 0 \end{pmatrix} \ , \tag{4.140}$$

where B_1 and B_2 are

$$B_1 = \begin{pmatrix} \sqrt{1+\rho^2}\sin 2\phi & \rho\cos 2\phi \\ \rho & 0 \end{pmatrix} \ , \quad B_2 = \begin{pmatrix} \sqrt{1+\rho^2}\cos 2\phi & -\rho\sin 2\phi \\ 0 & \sqrt{1+\rho^2} \end{pmatrix} \ . \tag{4.141}$$

We use the usual $\mathfrak{so}(2,2) = \mathfrak{sl}(2,\mathbb{R}) \oplus \mathfrak{sl}(2,\mathbb{R})$ decomposition with the basis vectors $\{L_0, L_1, L_2\}$ and $\{R_0, R_1, R_2\}$ from eq. (4.66). Calculating the projections of $\mathcal{A}_\sigma$ and $\mathcal{A}_\tau$ on the left and right sub-algebra we find

$$\begin{aligned} \mathcal{A}^L_\sigma &= \begin{pmatrix} 0 \\ +\sqrt{\rho^2+1}\sin\phi\cos\phi \\ \rho\cos^2\phi \end{pmatrix} \ , \quad \mathcal{A}^L_\tau = \begin{pmatrix} 0 \\ \sqrt{\rho^2+1}\sin\phi\cos\phi \\ \rho\cos^2\phi \end{pmatrix} \ , \\ \mathcal{A}^R_\sigma &= \begin{pmatrix} 0 \\ -\sqrt{\rho^2+1}\sin\phi\cos\phi \\ \rho\sin^2\phi \end{pmatrix} \ , \quad \mathcal{A}^R_\tau = \begin{pmatrix} 0 \\ -\sqrt{\rho^2+1}\cos^2\phi \\ \rho\sin\phi\cos\phi \end{pmatrix} \ . \end{aligned} \tag{4.142}$$

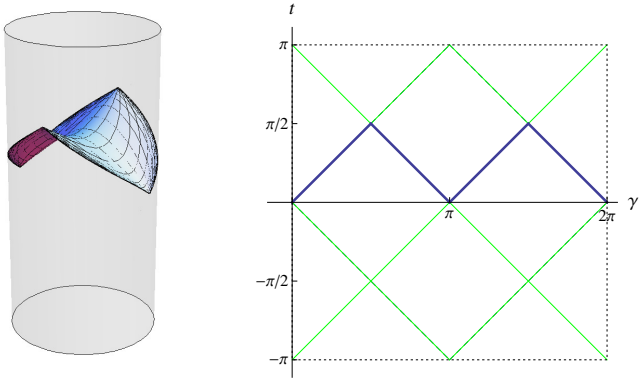

Figure 12: The space-like tetragon solution reproduces for $\theta = \pm\pi/4$ the surface analysed in [8]. Again, further boundaries generated by the quadratic relation are represented by green lines.

We see that with respect to the Killing form (4.70) all vectors are space-like. Thus there are no subclasses for a space-like AdS projection in contrast to the time-like case. To reconstruct the orthonormal reper one has to calculate

$$\mathcal{E} = \exp(\theta_L L_0)\exp(\theta_R R_0)\exp(\eta R_1)\exp(\xi L_1)\exp(-\theta_R R_0)\exp(-\theta_L L_0) \ , \tag{4.143}$$

where again $\exp(\theta_L L_0)\exp(\theta_R R_0)$ can be absorbed by an isometry transformation. So we are interested in the second row of

$$\exp(\eta R_1)\exp(\xi L_1)\exp(-\theta_R R_0)\exp(-\theta_L L_0) \ , \tag{4.144}$$

which is

$$Y = (\cosh\xi_- \sin\theta, \cosh\xi_+ \cos\theta, -\sinh\xi_- \sin\theta, -\sinh\xi_+ \cos\theta) \ , \quad (4.145)$$

where $\theta = \theta_R - \theta_L$ and $\xi_\pm = \eta \pm \xi$. This solution satisfies the quadratic equation

$$(Y^0)^2 - (Y^2)^2 = \cos^2\theta \ . \quad (4.146)$$

Calculating θ explicitly, we find that

$$\cot 2\theta = \frac{\sin 2\phi}{2\rho\sqrt{1+\rho^2}} \ . \quad (4.147)$$

Thus, the mean curvature is given by

$$H = \cot 2\theta \ . \quad (4.148)$$

4.6 Deformations and limits

Here we will show how some classes of solutions are connected. The space-like tetragon has the defining quadric

$$(Y^0)^2 - (Y^2)^2 = \cos^2\theta \ \stackrel{\theta\to 0}{\longrightarrow}\ (Y^0)^2 - (Y^2)^2 = 1 \ , \tag{4.149}$$

which is the defining quadric of the light-like tetragon, see eq. 4.120. The time-like tetragon from section 4.2.2 also has a smooth limit to the light-like tetragon.

$$(Y^0)^2 - (Y^2)^2 = \cosh^2\theta \ . \ \stackrel{\theta\to 0}{\longrightarrow}\ (Y^0)^2 - (Y^2)^2 = 1 \ , \tag{4.150}$$

Figure 13: Adjusting θ one can approach the degenerated AdS projection from the time-like as well as the space-like side. However, the limiting surfaces contain different *leaves* of the degenerated solution.

Isometry transformations in the interior of AdS can be continued to the

conformal boundary, where they act as conformal transformations. Using isometry transformations one can deform the surfaces such that they apparently look like another class of solutions. This is similar to the fact that one can approach a light-like trajectory with an ultra-relativistic massive particle. Below we plot how by isometry transformations the case of spinning string solutions (inside the triangles ACD or BCE in fig. 3) can be deformed into the spinning string solutions that touch the boundary in a single line (this corresponds to the line DC or EC in fig. 3). Also, the tube solution (inside the triangle CDE in fig. 3) can be related to this case.

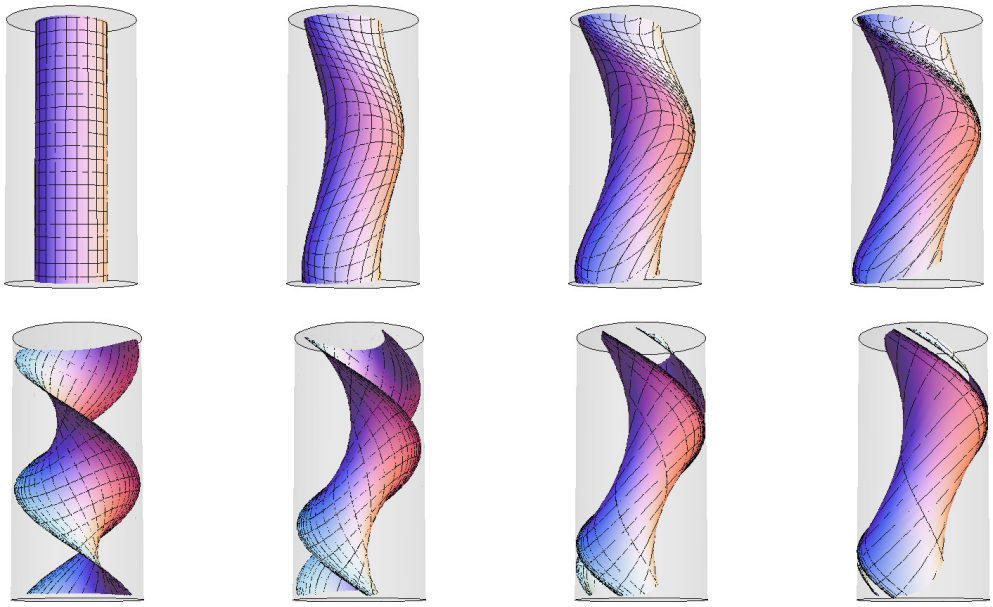

Figure 14: Via boosts one can change the apparent shape of the time-like tube and the time-like two line solution to look similar to a time-like one line surface.

4.7 Regularised area

Here we give the regularised area of surfaces that can be embedded in the finite region of a single Poincaré patch and that have a light-like polygon on the conformal boundary. It can be verified that antipodal points in AdS_3 will also be antipodal in AdS_5, given that the embedding is totally geodesic. Thus solutions that do not fit into a single Poincaré patch of AdS_3 will also not fit into a single Poincaré patch of AdS_5. From all previously discussed cases only two cases fulfil these criteria. The calculation for the surface that has a time-like tetragon in the AdS part is performed explicitly in appendix 8.7. The result reads

$$S_{reg} = \frac{\sqrt{\lambda}}{2\pi} \frac{(\rho^2 + \rho_s^2) \sinh 2\theta}{\rho\sqrt{1-\rho^2}} \; I(r_c) \; , \tag{4.151}$$

with

$$I(r_c) = \frac{1}{4}\left(\log \frac{r_c^2 \sinh^2\theta}{4\pi^2 s}\right)^2 + \frac{1}{4}\left(\log \frac{r_c^2 \cosh^2\theta}{-4\pi^2 t}\right)^2 - \frac{1}{4}\left(\log \frac{s \coth^2\theta}{-t}\right)^2 - \frac{\pi^2}{3} \; , \tag{4.152}$$

where the definition of $\theta(\rho, \phi)$ is given by formula (4.77). For the surface with a space-like tetragon in the AdS part, the calculation of the regularised action is similar and has been performed in [34]. The result is

$$S_{reg} = \frac{\sqrt{\lambda}}{2\pi} \frac{(1 + \rho^2 + \rho_s^2) \sin 2\theta}{\rho\sqrt{1+\rho^2}} \, I(r_c) \; , \tag{4.153}$$

with

$$I(r_c) = \frac{1}{4}\left(\log \frac{r_c^2 \sin^2\theta}{-4\pi^2 s}\right)^2 + \frac{1}{4}\left(\log \frac{r_c^2 \cos^2\theta}{-4\pi^2 t}\right)^2 - \frac{1}{4}\left(\log \frac{s \cot^2\theta}{t}\right)^2 - \frac{\pi^2}{3} \; , \tag{4.154}$$

where $\theta(\rho, \phi)$ is defined by equation (4.147). For $\theta = \pi/4$ this result coincides with the expression given in [8], see eq. (3.5).

4.8 Summary and discussion

This first part contains a complete classification of space-like flat minimal surfaces in $AdS_3 \times S^3$. We have shown that these surfaces form a four parameter family characterised by $(\rho, \phi, \rho_s, \phi_s)$. These parameters uniquely fix a surface in the product space. However, if one is interested in the AdS projection only, this set is redundant. The shape of the AdS projections is defined by the parameter $\theta(\rho, \phi)$. θ also determines the mean curvatures

of the projections. All projections that we calculate have a constant mean curvature. In fact, it has been shown that all flat constant mean curvature surfaces in AdS appear as projections in our classification. Furthermore, all projections (except the one discussed in 4.2.3, which is defined by a linear equation) are given as an intersection of a quadratic relation of the embedding coordinates with the AdS-defining equation. Also the famous tetragon solution in pure AdS in [8] can be found in our classification together with a trivial spherical projection.

In two cases the boundary of the surface is a closed light-like tetragon that can be embedded in a single Poincaré patch. In those cases we gave the regularised action in (4.151) and (4.153). The expressions are related via $\theta \leftrightarrow i\theta$ and $\rho^2 - 1 \leftrightarrow \rho^2$. For the space-like tetragon, one can rewrite $I(r_c)$ in the following way

$$\begin{aligned} I(r_c) =& \frac{1}{4}\left(\log\frac{r_c^2\cos^2\theta}{-4\pi^2 s}\right)^2 + \frac{1}{4}\left(\log\frac{r_c^2\sin^2\theta}{-4\pi^2 t}\right)^2 \\ & - \frac{1}{4}\left(\log\frac{s}{t}\right)^2 - \frac{1}{4}\left(\log\cot^2\theta\right)^2 - \frac{\pi^2}{3}\ . \end{aligned} \tag{4.155}$$

The dependence on the Mandelstam variables (s,t) in the finite part is then exactly what is needed to match with the BDS formula. This means, that the prefactor of the regularised area in (4.153) and (4.151) has to be equal to one. One can check that for the space-like tetragon

$$\min(\sin 2\theta) = \frac{2\rho\sqrt{1+\rho^2}}{1+2\rho^2}\ . \tag{4.156}$$

This implies that the minimal value of the prefactor is reached for $\rho \to \infty$ and $\rho_s \to 0$. This implies $\theta \to \frac{\pi}{4}$ and the result coincides with the tetragon surface given in [8]. The situation for the time-like tetragon is different. Inside the relevant region in the parameter space (inside the triangle ABC in fig. 3)

$$\sinh 2\theta(\rho,\phi) \geq \sinh 2\theta(\rho,\pi/4) = \frac{2\rho\sqrt{1-\rho^2}}{2\rho^2-1}\ . \tag{4.157}$$

Thus the prefactor is > 2 for $\rho^2 \in (1/2, 1)$. The lower bound is reached for $\rho^2 \to 1$. However, this corresponds to $\theta \to 0$ which yields additional divergences in eq. (4.152). Thus, the role of these new classes of minimal surfaces in the AdS/CFT correspondence is not yet understood.

Part II
Weak coupling

We are considering light-light polygonal Wilson-loops in $\mathcal{N} = 4$ sYM theory. Let us denote by

$$\mathcal{U}(\mathcal{C}) := \frac{1}{N} \text{ tr } \mathcal{P} \text{ exp}\left(ig \int_{\mathcal{C}} A^{\mu} \mathrm{d}x_{\mu}\right) \tag{4.158}$$

the parallel transport. The Wilson-loop is defined by

$$\mathcal{W} \ := \ \langle 0 \,|\, \mathcal{U}(\mathcal{C}) \,|\, 0 \rangle \ . \tag{4.159}$$

Here, A^{μ} is the gauge field and N the rank of the gauge group SU(N). The contour $\mathcal{C}$ is a light-like polygon. We are interested in the planar limit $N \to \infty$ but keeping $a := \frac{g^2 N}{8\pi^2}$ finite.

5 BDS Ansatz and self-crossing Wilson loops

Up to an additional remainder function, light-like polygonal Wilson loops are given up to all loops by the BDS Ansatz [13, 12, 14] which is a consequence of the non-abelian exponentiation theorem. This Ansatz also solves the conformal Ward identities. However, starting at six cusps, the BDS Ansatz is modified by a remainder function $\mathcal{R}_n$. The remainder function, as it is usually used, depends on cross ratios only and its perturbative expansion starts at order $\mathcal{O}(a^2)$. Due to kinematical restrictions the closed, light-like tetra- and pentagons have no free cross ratios. Hence, remainder functions become important for Wilson loops with more than five cusps. The BDS terms are given by

$$[\text{BDS}]_n \ = \ \sum_{l=1}^{\infty} a^l \big(f^{(l)}(\epsilon) \ w_n(l\epsilon) \ + \ C_n^{(l)} \big) \ . \tag{5.1}$$

Here,

$$w_n(\epsilon) \ = \ -\frac{1}{2} \sum_{k=1}^{n} \frac{1}{\epsilon^2} \ (-\mu^2 s_{k-1,k+1} + i\varepsilon)^{\epsilon} \ + \ F_n(\mu^2, \epsilon, s) \ . \tag{5.2}$$

is the one-loop contribution of the Wilson loop, with F_n being the one-loop finite terms. Further, the $C^{(l)}$ are numbers and $f^{(l)}(\epsilon) = f_0^{(l)} + \epsilon f_1^{(l)} + \epsilon^2 f_2^{(l)}$, which is related via

$$f_0^{(l)} \ = \ \frac{\Gamma_{\text{cusp}}^{(l)}}{2} \ , \quad f_1^{(l)} = \frac{l \ \Gamma^{(l)}}{2} \ . \tag{5.3}$$

The cusp anomalous dimension has the expansion

$$\Gamma_{\text{cusp}} = 2a - \frac{\pi^2}{3}a^2 + \mathcal{O}(a^3) \ . \tag{5.4}$$

The so-called collinear anomalous dimension reads

$$\Gamma = -7\zeta_3 a^2 + \mathcal{O}(a^3) \ . \tag{5.5}$$

For our purpose we will define the remainder function to be

$$\mathcal{R}_n := \log\langle \mathcal{W}(\mathcal{C}_n)\rangle - [\text{BDS}]_n \ . \tag{5.6}$$

For a general (non-self-crossing) Wilson loop, this definition coincides with the usual one when setting $\epsilon \to 0$. However, considering self-crossing Wilson loops, this remainder function $\mathcal{R}(\mu^2, \epsilon, \{s\})$ has poles in ϵ and depends on the Mandelstam variables. Spelling out the BDS Ansatz eqns. (5.1),(5.6) we get up to two loops [26]

$$\begin{aligned}\log \mathcal{W} = &-\frac{1}{4}\sum_{l=1,2} a^l \left(\frac{\Gamma^{(l)}_{\text{cusp}}}{(l\epsilon)^2} + \frac{\Gamma^{(l)}}{l\epsilon}\right)\sum_k (-\mu^2 s_{k-1,k+1})^{l\epsilon} \\ &+ a\ F_n(\mu^2,\epsilon,s) - \frac{a^2 n}{8} f_2^{(2)} \\ &+ a^2\Big(\frac{\Gamma^{(2)}_{\text{cusp}}}{2} F_n(\mu^2, 2\epsilon, s) + \epsilon\Gamma^{(2)} F_n(\mu^2, 2\epsilon, s) + C^{(2)} + \mathcal{R}_n^{(2)}(\mu^2,\epsilon,s)\Big) + \mathcal{O}(\epsilon) \ .\end{aligned} \tag{5.7}$$

The term $\epsilon\Gamma^{(2)}F_n$ has been kept, since in the crossing configuration under discussion F_n, develops a pole in ϵ.

5.1 Self-crossing Wilson loops

Self-crossing Wilson loops have several special properties. Starting from a generic, non-self-crossing contour, in the self-crossing-limit the Wilson loop becomes more divergent. Looking at the BDS structure (5.1),(5.6) these new divergences have two sources. First, the one-loop finite part $F_n(\mu^2, \epsilon, s)$ becomes divergent as the self-crossing limit leads to new cusps with new one-loop cusp divergences. Furthermore, the remainder function $\mathcal{R}_n$ can be divergent, as well. The divergences of $F_n(\mu^2, \epsilon, s)$ can easily be calculated.
The other option is to look at self-crossing Wilson-loops without considering the limit from a generic contour. Then (for a simple crossing), we face operator mixing between two different Wilson loops, see figure 15, for example.

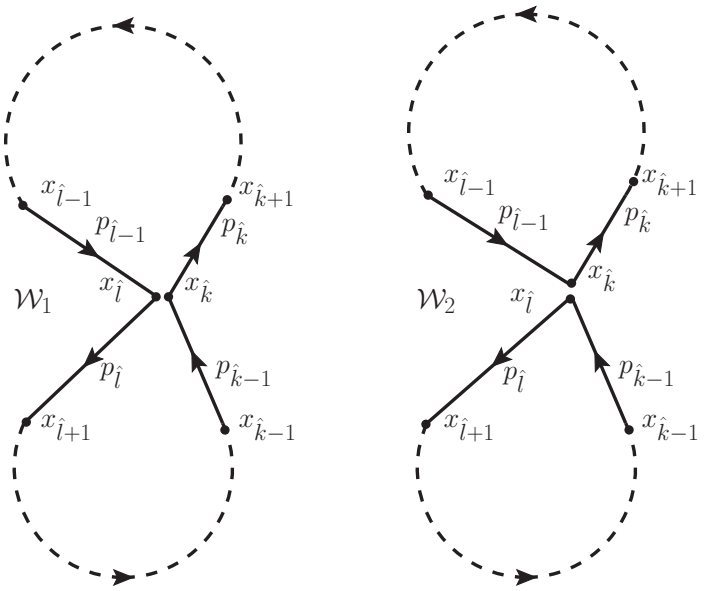

Figure 15: The crossing situation for $x_{\hat{k}} = x_{\hat{l}}$. Both Wilson loops mix under renormalisation. The dashed lines correspond to some further arbitrary light-like polygonal segments of the Wilson loop.

It was shown in [41, 42, 43, 44, 45] in QCD that self-crossing Wilson loops can be renormalised multiplicatively using a $\mathcal{Z}$ matrix.

$$\mathcal{W}_1 := \langle \mathcal{U}(\mathcal{C}) \rangle \ , \quad \mathcal{W}_2 := \langle \mathcal{U}(\mathcal{C}^{\text{upper}}) \mathcal{U}(\mathcal{C}^{\text{lower}}) \rangle \tag{5.8}$$

are the two mixing Wilson loop operators. $\mathcal{C}^{\text{upper}}$ and $\mathcal{C}^{\text{lower}}$ are the two light-like polygonal sub-contours that start and end at the crossing point. We denote the vertices of the light-like polygon by x_i and, because of the correspondence to scattering amplitudes, we call $p_i = (x_{i+1} - x_i)$ a momentum. We are interested in the planar limit $N \to \infty$, but keeping $a = \frac{g^2 N}{8\pi^2}$ finite. In this limit

$$\mathcal{W}_2 \overset{N\to\infty}{=} \langle \mathcal{U}(\mathcal{C}^{\text{upper}}) \rangle \langle \mathcal{U}(\mathcal{C}^{\text{lower}}) \rangle \ . \tag{5.9}$$

We have

$$\mathcal{W}_a \ = \ \mathcal{Z}_{ab} \, \mathcal{W}_b^{\text{ren}} \quad , \qquad a, b \in \{1, 2\} \ . \tag{5.10}$$

In the planar limit under discussion the $\mathcal{Z}$ matrix has the form

$$\mathcal{Z} \overset{N\to\infty}{=} \begin{pmatrix} \mathcal{Z}_{11} & \mathcal{Z}_{12} \\ 0 & \mathcal{Z}_{22} \end{pmatrix} \ , \tag{5.11}$$

which implies a similar structure for the Γ matrix (see appendix 8.9). Expanding (5.10) in a we find for the logarithms of the Wilson loops within minimally subtracted dimensional regularisation[5]

$$\begin{aligned}
\log \mathcal{W}_1^{\mathrm{ren}(1)} &= \mathrm{MS}\Big[\log \mathcal{W}_1^{(1)}\Big] = \mathcal{W}_1^{\mathrm{ren}(1)} \ , \\
\log \mathcal{W}_1^{\mathrm{ren}(2)} &= \mathrm{MS}\Big[\log \mathcal{W}_1^{(2)} + \mathcal{Z}_{12}^{(1)}\left(\mathcal{W}_1^{\mathrm{ren}(1)} - \mathcal{W}_2^{\mathrm{ren}(1)}\right)\Big] \ , \\
\log \mathcal{W}_1^{\mathrm{ren}(3)} &= \mathrm{MS}\Big[\log \mathcal{W}_1^{(3)} \ - \ T_1 \ - \ T_2\Big] \ ,
\end{aligned} \tag{5.12}$$

with $\mathrm{MS}[\ .\ ]$ denoting minimal subtraction and

$$T_1 := \mathcal{Z}_{12}^{(1)}\left(\frac{1}{2}\left(\mathcal{W}_1^{\mathrm{ren}(1)} - \mathcal{W}_2^{\mathrm{ren}(1)}\right)^2 - \log \mathcal{W}_1^{\mathrm{ren}(2)} + \log \mathcal{W}_2^{\mathrm{ren}(2)}\right) \ , \tag{5.13}$$

$$T_2 := \left(\left(\mathcal{Z}_{12}^{(1)}\right)^2 + \mathcal{Z}_{12}^{(1)}\mathcal{Z}_{11}^{(1)} - \mathcal{Z}_{12}^{(2)}\right)\left(\mathcal{W}_1^{\mathrm{ren}(1)} - \mathcal{W}_2^{\mathrm{ren}(1)}\right) \ . \tag{5.14}$$

In contrast, the expressions for $\mathcal{W}_2$ are simpler, due to the triangular form of the $\mathcal{Z}$-matrix in (5.11)

$$\log \mathcal{W}_2^{\mathrm{ren}(l)} \ = \ \mathrm{MS}\Big[\ \log \mathcal{W}_2^{(l)}\ \Big] \ . \tag{5.15}$$

The expansion of (5.10) up to $\mathcal{O}(a^4)$ is a bit lengthy and we postpone it to section 6.3. The renormalisation group equation (RGE) here is

$$\mu\frac{\mathrm{d}}{\mathrm{d}\mu}\ \mathcal{W}_a^{\mathrm{ren}} \ = \ - \ \Gamma_{ab}\ \mathcal{W}_b^{\mathrm{ren}} \ , \ a,b \in \{1,2\} \ , \tag{5.16}$$

where

$$\Gamma_{ab} := \left(\mathcal{Z}^{-1}\mu\frac{\mathrm{d}}{\mathrm{d}\mu}\mathcal{Z}\right)_{ab}|_{g_{\mathrm{bare\ fixed}}} \tag{5.17}$$

is the anomalous dimension matrix. In (5.16), we take the total derivative $\mu\frac{\mathrm{d}}{\mathrm{d}\mu}$ because we want to use this equation for ϵ non-zero, where the β-function does not vanish. Equation (5.16) implies

$$\mu\frac{\mathrm{d}}{\mathrm{d}\mu}\ \log \mathcal{W}_1^{\mathrm{ren}} \ = \ - \ \Gamma_{12}\ \frac{\mathcal{W}_2^{\mathrm{ren}}}{\mathcal{W}_1^{\mathrm{ren}}} \ - \ \Gamma_{11} \ . \tag{5.18}$$

for $\mathcal{W}_1$. Our goal is to use the expressions (5.12) order by order and plug them into (5.18) to find the μ dependence of $\mathrm{MS}[\ \mathcal{R}_n\ ]$. In order to achieve

[5]We are using a slightly sloppy notation here. By $\log \mathcal{W}_i^{\mathrm{ren}(l)}$ we denote the l-loop contribution of the logarithm of the renormalised Wilson loop, meaning $\log \mathcal{W}_i^{\mathrm{ren}(l)} = \left(\log\left(\mathcal{W}_i^{\mathrm{ren}}\right)\right)^{(l)}$. These coefficients naturally appear in the BDS Ansatz formula.

this, we have to know the matrices $\mathcal{Z}$ and Γ. We will use an Ansatz for Γ and consider (5.17) as a differential equation in μ for $\mathcal{Z}$. Spelling out (5.17) for the components, we find

$$\begin{aligned} \mu\frac{\mathrm{d}}{\mathrm{d}\mu}\log\mathcal{Z}_{11} &= \Gamma_{11}\ , \qquad & \mu\frac{\mathrm{d}}{\mathrm{d}\mu}\mathcal{Z}_{12} &= \mathcal{Z}_{11}\Gamma_{12}+\mathcal{Z}_{12}\Gamma_{22}\ , \\ \mu\frac{\mathrm{d}}{\mathrm{d}\mu}\log\mathcal{Z}_{22} &= \Gamma_{22}\ . \end{aligned} \tag{5.19}$$

Now we have to consider several types of crossing. In principle, a simple crossing may occur in three variants. The crossing point can be between two edges, at two vertices, or between an edge and a vertex. In the next section, we will discuss a self-crossing Wilson loop with a crossing between two edges. The section includes the discussions in [26] for two loops, our work in [28] for three loops and further work at four loops. Then, we give a detailed discussion on self-crossing Wilson loops with a crossing at two vertices, and extend our work from [27] with a calculation at three and four loops.

6 Crossing between two edges

For clarification we depict this situation in figure 16 and introduce some notation. We consider arbitrary light-like n-gons with a crossing between two edges, which we call p and q. As all momenta are considered to be real, n has to be greater or equal to six. x and y are two dimensionless parameters between 0 and 1 that fix the position of the crossing on the edges. The predecessor of p is called p_- and the successor p_+ and similarly for q.

The anomalous dimension of a Wilson loop for a self-crossing null polygon is given [20, 45, 26] via

$$\Gamma = \begin{pmatrix} 1 & 0 \\ 0 & 1 \end{pmatrix} \frac{\Gamma_{\text{cusp}}(a)}{2} \sum_{k \in \text{cusps}} \log\left(-s_k \mu^2\right) + \begin{pmatrix} A & \gamma_{12}(a) \\ 0 & B \end{pmatrix} , \tag{6.1}$$

where

$$\begin{aligned} A =& \frac{\Gamma_{\text{cusp}}(a)}{2} \left(\log(-2pp_-\mu^2) + \log(-2pp_+\mu^2) + \log(-2qq_-\mu^2) + \log(-2qq_+\mu^2)\right) , \\ B =& \frac{\Gamma_{\text{cusp}}(a)}{2} \left(\log(-2pp_-x\mu^2) + \log(-2pp_+(1-x)\mu^2) + \log(-2qq_-(1-y)\mu^2)\right. \\ & \left. + \log(-2qq_+y\mu^2)\right) + \gamma_{22}(a) \left(\log(-sxy\mu^2) + \log(-s(1-x)(1-y)\mu^2)\right) , \end{aligned}$$

with $a = \frac{g^2 N}{8\pi^2}$ and $s = 2pq$. By $\sum_{k \in \text{cusps}}$ we denote all cusps that are *not* adjacent to the crossing and by $s_k = (x_{k-1} - x_{k+1})^2$ the Mandelstam variables at the cusps.

All entries in the anomalous dimension matrix that are proportional to Γ_{cusp} originate from UV divergences that are related to cusps. The cusps adjacent to the crossing contribute in a different manner to $\mathcal{W}_1$ and $\mathcal{W}_2$. For $\mathcal{W}_1$ the full momenta p and q are relevant and for $\mathcal{W}_2$ only fractions thereof. Therefore, also the cusp terms in the anomalous dimension matrix are *not* a multiple of the unit matrix. In the anomalous dimension matrix γ_{12} and γ_{22} are functions of the coupling only. The one-loop results in planar limit are

$$\gamma_{12}^{(1)} = \pm \text{ sgn}(pq)\ 2\pi i \ , \quad \gamma_{22}^{(1)} = 1 \ , \quad \Gamma_{\text{cusp}}^{(1)} = 2 \ . \tag{6.2}$$

It has been argued in [46, 26] that the $i\varepsilon$ prescription of the gluon propagator for the duality between Wilson loops and scattering amplitudes has to be flipped compared to the standard position space propagator. This amounts in a change of the sign of $\gamma_{12}^{(1)}$ compared to [45]. The sign of $\gamma_{12}^{(1)}$ plays an important role for the analytic continuations discussed in section 6.4. A one-loop calculation for the anomalous dimension matrix is available in appendix 8.9.

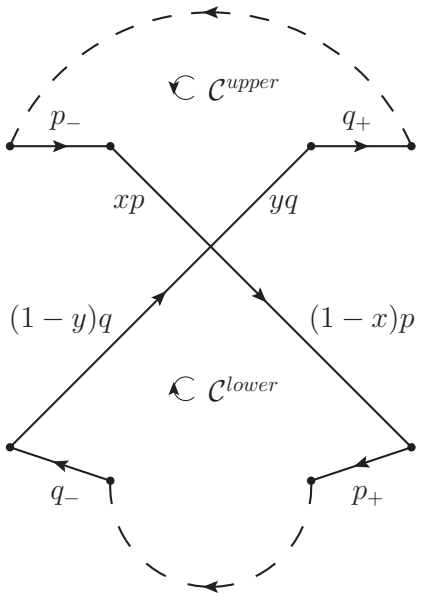

Figure 16: *A self-crossing Wilson loop with crossing edges p and q. The dashed lines represent any light-like continuation. The dimensionless parameters $x, y \in (0,1)$ define where the crossing is located exactly.*

We will now solve the differential equation (5.19) for the anomalous dimension matrix (6.1). We solve this as an expansion in powers of a, i.e. $\Gamma = \sum_l a^l \Gamma^{(l)}$ and similar for $\mathcal{Z}$. Keeping in mind that the μ derivative has to be taken at fixed bare coupling and that $a = a_{\text{bare}}\mu^{-2\epsilon}$, the first two equations give for a n-gon

$$\begin{aligned} \mathcal{Z}_{11}^{(0)} &= 1 \ , \qquad \mathcal{Z}_{11}^{(1)} = -\frac{n\Gamma_{\text{cusp}}^{(1)}}{4\epsilon^2} - \frac{\Gamma_{11}^{(1)}}{2\epsilon} \ , \\ \mathcal{Z}_{22}^{(0)} &= 1 \ , \qquad \mathcal{Z}_{22}^{(1)} = -\frac{n\Gamma_{\text{cusp}}^{(1)} + 4\gamma_{22}^{(1)}}{4\epsilon^2} - \frac{\Gamma_{22}^{(1)}}{2\epsilon} \ . \end{aligned} \tag{6.3}$$

Now we solve (5.19) for $\mathcal{Z}_{12}$. A priori it is clear that $\mathcal{Z}_{12}^{(0)} = 0$. At order $\mathcal{O}(a)$ we find

$$\Gamma_{12}^{(1)} a = \mu \frac{\mathrm{d}}{\mathrm{d}\mu}\left(\mathcal{Z}_{12}^{(1)} a\right) \quad \Longrightarrow \quad \mathcal{Z}_{12}^{(1)} = -\frac{\gamma_{12}^{(1)}}{2\epsilon} \ . \tag{6.4}$$

At order $\mathcal{O}(a^2)$ eq.(5.19) means

$$a^2\left(\Gamma_{12}^{(2)} + \mathcal{Z}_{11}^{(1)}\Gamma_{12}^{(1)} + \mathcal{Z}_{12}^{(1)}\Gamma_{22}^{(1)}\right) = \mu \frac{\mathrm{d}}{\mathrm{d}\mu}\left(\mathcal{Z}_{12}^{(2)} a^2\right) \ . \tag{6.5}$$

Integration yields

$$\mathcal{Z}_{12}^{(2)} = \frac{(n\Gamma_{\text{cusp}}^{(1)} + \gamma_{22}^{(1)})\gamma_{12}^{(1)}}{8\epsilon^3} + \frac{\gamma_{12}^{(1)}\left(\Gamma_{11}^{(1)} + \Gamma_{22}^{(1)}\right)}{8\epsilon^2} - \frac{\gamma_{12}^{(2)}}{4\epsilon} \ . \tag{6.6}$$

Note, that the Ansatz for the crossing anomalous dimension (6.1) leads to $\mathcal{Z}$-factors that contain pure pole terms, as it should be within minimal subtraction. Now we have prepared all components to calculate the leading divergences of the remainder for a self-crossing between two edges up to $\mathcal{O}(a^3)$. The $\mathcal{Z}$-factors that are relevant at four loops will be presented further on for reasons of readability, as they are more complicated.

For convenience, we introduce an abbreviation here

$$\mathcal{X} \ := (1-x)\ x\ (1-y)\ y \ . \tag{6.7}$$

6.1 On 2-loop divergences of the remainder

We start to analyse the integrated version of equation (5.18) at two loops. Together with (5.12) we find

$$\begin{aligned} \text{MS}\Big[[\text{BDS}]^{(2)} + \mathcal{R}^{(2)} + \mathcal{Z}_{12}^{(1)}\left(\mathcal{W}_1^{\text{ren}(1)} - \mathcal{W}_2^{\text{ren}(1)}\right)\Big] = \\ - \int \left(\left(\Gamma_{12}\ \frac{\mathcal{W}_2^{\text{ren}}}{\mathcal{W}_1^{\text{ren}}}\right)^{(2)} + \Gamma_{11}^{(2)}\right)\frac{\mathrm{d}\mu}{\mu} \ . \end{aligned} \tag{6.8}$$

Let us start by evaluating $\left(\mathcal{W}_1^{\text{ren}(1)} - \mathcal{W}_2^{\text{ren}(1)}\right)$. This term has to be evaluated at $\mathcal{O}(\epsilon)$ due to the pole of the $\mathcal{Z}$ factor in (6.4). For every cusp we get a term $-\frac{1}{2\epsilon^2}\left(-\mu^2 s_{\text{cusp}} \pm i\varepsilon\right)^\epsilon$ at one loop. Minimally subtracting the poles one ends up with

$$\begin{aligned} \text{MS}\Big[\frac{-1}{2\epsilon^2}\left(-\mu^2 s_{\text{cusp}} \pm i\varepsilon\right)^\epsilon\Big] = -\frac{1}{4}\log^2\left(-\mu^2 s_{\text{cusp}} \pm i\varepsilon\right) - \frac{\epsilon}{12}\log^3\left(-\mu^2 s_{\text{cusp}} \pm i\varepsilon\right) \\ - \frac{\epsilon^2}{48}\log^4\left(-\mu^2 s_{\text{cusp}} \pm i\varepsilon\right) + \mathcal{O}(\epsilon^3) \ . \end{aligned} \tag{6.9}$$

Collecting all one-loop cusp contributions and using the factorization of $\mathcal{W}_2$ in the 't Hooft limit one gets

$$\begin{aligned} &\left(\mathcal{W}_1^{\text{ren}(1)} - \mathcal{W}_2^{\text{ren}(1)}\right) = \text{MS}\Big[\frac{1}{2\epsilon^2}\Big(\left(s\mu^2 x(1-y)\right)^\epsilon + \left(s\mu^2 y(1-x)\right)^\epsilon + \left(-2p\cdot p_-\mu^2 x\right)^\epsilon \\ &+ \left(-2p\cdot p_+\mu^2(1-x)\right)^\epsilon + \left(-2q\cdot q_-\mu^2(1-y)\right)^\epsilon + \left(-2q\cdot q_+\mu^2 y\right)^\epsilon \\ &- \left(-2p\cdot p_-\mu^2\right)^\epsilon - \left(-2p\cdot p_+\mu^2\right)^\epsilon - \left(-2q\cdot q_-\mu^2\right)^\epsilon - \left(-2q\cdot q_+\mu^2\right)^\epsilon\Big)\Big] \ . \end{aligned} \tag{6.10}$$

Above we have suppressed the $i\varepsilon$-prescription. It is the same in all terms. Note the absence of the minus sign in the basis of the first two ϵ-powers on the r.h.s.. This is due to their different situation concerning the direction of the arrows in fig.16. Further on, this fact will be crucial for the generation of different imaginary parts, depending on whether $s = 2pq$ is negative or positive.

The divergent terms contained in the expression for $\left(\mathcal{W}_1^{\text{ren}(1)} - \mathcal{W}_2^{\text{ren}(1)}\right)$ are due to divergences of the BDS structure, present already in a generic configuration, as well as divergences in the one loop "finite" part $F(\mu^2, \epsilon, \{s\})$, which becomes divergent in the self-crossing limit. Let us now introduce a shorthand notation for the ϵ-expansion of eq. (6.10)

$$\left(\mathcal{W}_1^{\text{ren}(1)} - \mathcal{W}_2^{\text{ren}(1)}\right) \approxeq: C_{[0]}^{(1)} + C_{[1]}^{(1)}\epsilon + C_{[2]}^{(1)}\epsilon^2 + \dots \ . \tag{6.11}$$

For the $C_{[k]}^{(1)}$, we find [6]

$$C_{[k]}^{(1)} = \frac{1}{(k+2)!}\left(\log^{(k+2)}\mu^2 + (k+2)\log\left(s\mathcal{X} \pm i\varepsilon\right)\log^{(k+1)}\mu^2\right) + \mathcal{O}(\log^k \mu^2) \ , \tag{6.12}$$

using the abbreviation from (6.7). Then (6.11) is an equation just up to sub-sub-leading terms in $\log\mu^2$ at every order in ϵ. This simplification can be done, as we are only interested in leading and next-leading divergences of the remainder function.
Thus, we find

$$\mathcal{Z}_{12}^{(1)}\left(\mathcal{W}_1^{\text{ren}(1)} - \mathcal{W}_2^{\text{ren}(1)}\right) = -\frac{\gamma_{12}^{(1)}}{2}C_{[1]}^{(1)} \ , \tag{6.13}$$

again, only up to next-leading terms in $\log\mu^2$.

The next parts to calculate are the contributions from the BDS Ansatz. It is obvious that the BDS terms only contribute with $\mathcal{O}(\log^2\mu^2)$ at $\mathcal{O}(\epsilon^0)$ at all loop orders. Anticipating that the two-loop divergences for the remainder function will be $\mathcal{O}\left(\frac{1}{\epsilon^3}\right)$, the contributions of the BDS terms are only sub-leading here. For higher loop calculations they will be completely negligible.

$$\text{MS}\Big[[\text{BDS}]^{(2)}\Big] = -\ \frac{n\ \Gamma_{\text{cusp}}^{(2)}}{8}\log^2\mu^2\ +\ \mathcal{O}(\log\mu^2) \ . \tag{6.14}$$

[6] We are only interested in the μ-behaviour of these expressions. To handle logarithms of dimensionless quantities in the following expressions one should introduce a new scale $\tilde{\mu}$ and write $\log\left(-s\mu^2\right) = \log\left(-s\tilde{\mu}^2\right) + \log\frac{\mu^2}{\tilde{\mu}^2}$. We suppress this negligibility here since $\tilde{\mu}$ drops out in the end.

Expanding the r.h.s.. of equation (6.8) we find that the integrand is given by

$$\left(\left(\Gamma_{12}\,\frac{\mathcal{W}_2^{\rm ren}}{\mathcal{W}_1^{\rm ren}}\right)^{(2)}+\Gamma_{11}^{(2)}\right)=\left(\Gamma_{12}^{(1)}\,\left(\frac{\mathcal{W}_2^{\rm ren}}{\mathcal{W}_1^{\rm ren}}\right)^{(1)}+\Gamma_{11}^{(2)}\right)\,. \tag{6.15}$$

As we will perform a $\mathrm{d}\log\mu$ integration, these terms have to be known at $\mathcal{O}(\log\mu^2)$. We find

$$\Gamma_{11}^{(2)}=\frac{n\;\Gamma_{\rm cusp}^{(2)}}{2}\log\mu^2\;, \tag{6.16}$$

which will cancel the n-dependent contribution from the BDS terms after integration. Furthermore, we have

$$\left(\frac{\mathcal{W}_2^{\rm ren}}{\mathcal{W}_1^{\rm ren}}\right)^{(1)}=-\left(\mathcal{W}_1^{{\rm ren}(1)}-\mathcal{W}_2^{{\rm ren}(1)}\right)\approx -C_{[0]}^{(1)}\;. \tag{6.17}$$

Performing the $\mathrm{d}\log\mu$ integration we find

$$\begin{aligned}&-\int\left(\left(\Gamma_{12}\,\frac{\mathcal{W}_2^{\rm ren}}{\mathcal{W}_1^{\rm ren}}\right)^{(2)}+\Gamma_{11}^{(2)}\right)\frac{\mathrm{d}\mu}{\mu} \\ &=\frac{\Gamma_{12}^{(1)}\;\log^3\mu^2}{12}+\left(\frac{\Gamma_{12}^{(1)}\;\log\left(s\;\mathcal{X}\pm i\varepsilon\right)}{4}-\frac{n\;\Gamma_{\rm cusp}^{(2)}}{8}\right)\log^2\mu^2\;.\end{aligned} \tag{6.18}$$

Now we may put everything together to calculate

$$\begin{aligned}\mathrm{MS}\Big[\mathcal{R}^{(2)}\Big]&=\frac{\Gamma_{12}^{(1)}\;\log^3\mu^2}{12}+\frac{\Gamma_{12}^{(1)}\;\log\left(s\;\mathcal{X}\pm i\varepsilon\right)}{4}\log^2\mu^2+\frac{\Gamma_{12}^{(1)}C_{[1]}^{(1)}}{2}\\ &=\frac{\Gamma_{12}^{(1)}\;\log^3\mu^2}{6}+\frac{\Gamma_{12}^{(1)}\;\log\left(s\;\mathcal{X}\pm i\varepsilon\right)}{2}\log^2\mu^2\;.\end{aligned} \tag{6.19}$$

Recalling that $\Gamma_{12}^{(1)}=\gamma_{12}^{(1)}=\pm\,\mathrm{sgn}(pq)\;2\pi i$, we have

$$\mathrm{MS}\Big[\mathcal{R}^{(2)}\Big]=\pm\,\mathrm{sgn}(pq)\;\pi i\left(\frac{\log^3\mu^2}{3}+\log\left(s\;\mathcal{X}\pm i\varepsilon\right)\log^2\mu^2\right)\;. \tag{6.20}$$

Now, we want to reconstruct the *bare* remainder function. We know that the remainder function has an expansion in $a_{\rm bare}=a\mu^{2\epsilon}$. The terms that we have just calculated are remnants of

$$\begin{aligned}&\mathrm{MS}\Big[\;\frac{1}{\epsilon^3}\;\left(A+B\;\epsilon\right)\;\mu^{4\epsilon}\Big]\\ &=\frac{A}{\epsilon^3}+\frac{B+2\;A\;\log\mu^2}{\epsilon^2}+\cdots+\frac{4}{3}A\;\log^3\mu^2+2\;B\;\log^2\mu^2+\ldots\;.\end{aligned} \tag{6.21}$$

Comparing the coefficients, we find for the remainder

$$\mathcal{R}^{(2)} = \frac{\pm\,\mathrm{sgn}(pq)\;\pi i}{4}\left(\frac{1}{\epsilon^3} + \frac{2\log\left(s\;\mathcal{X}\;\mu^2 \pm i\varepsilon\right)}{\epsilon^2}\right)\;. \tag{6.22}$$

6.2 On 3-loop divergences of the remainder

Evaluating (5.18) at three loops and using the abbreviations (5.13) and (5.14), we end up with

$$\mathrm{MS}\Big[[\mathrm{BDS}]^{(3)} + \mathcal{R}^{(3)}(\mu,\epsilon,p_i) - T_1 - T_2\Big] = \int\Big(-T_3 - \Gamma_{11}^{(3)}\Big)\;\frac{\mathrm{d}\mu}{\mu}\;, \tag{6.23}$$

where

$$T_1 := \mathcal{Z}_{12}^{(1)}\left(\frac{1}{2}\left(\mathcal{W}_1^{\mathrm{ren}(1)} - \mathcal{W}_2^{\mathrm{ren}(1)}\right)^2 - \log\mathcal{W}_1^{\mathrm{ren}(2)} + \log\mathcal{W}_2^{\mathrm{ren}(2)}\right)\;, \tag{6.24}$$

$$T_2 := \left(\left(\mathcal{Z}_{12}^{(1)}\right)^2 + \mathcal{Z}_{12}^{(1)}\,\mathcal{Z}_{11}^{(1)} - \mathcal{Z}_{12}^{(2)}\right)\left(\mathcal{W}_1^{\mathrm{ren}(1)} - \mathcal{W}_2^{\mathrm{ren}(1)}\right) \tag{6.25}$$

and

$$T_3 := \left(\Gamma_{12}\;\frac{\mathcal{W}_2^{\mathrm{ren}}}{\mathcal{W}_1^{\mathrm{ren}}}\right)^{(3)}\;. \tag{6.26}$$

As the leading terms at three loops in a $\log\mu^2$ expansion are $\mathcal{O}(\log^5\mu^2)$, we discard all terms that are $\mathcal{O}(\log^3\mu^2)$ or less. This includes all terms $[\mathrm{BDS}]^{(3)}$ coming from the BDS structure. Therefore, to get the interesting piece of $\mathrm{MS}[\mathcal{R}^{(3)}]$, we only need to calculate the terms T_1 to T_3. Let us discuss them one after the other.

Calculating term T_1

Recalling the notations (6.7) and (6.11),

$$\frac{1}{2}\left(\mathcal{W}_1^{\mathrm{ren}(1)} - \mathcal{W}_2^{\mathrm{ren}(1)}\right)^2\Big|_{\mathcal{O}(\epsilon)} = \epsilon\left(C_{[0]}^{(1)}\;C_{[1]}^{(1)}\right)\;. \tag{6.27}$$

Now, using (6.24), let us turn to

$$\begin{aligned}\log\mathcal{W}_1^{\mathrm{ren}(2)} - \log\mathcal{W}_2^{\mathrm{ren}(2)} =& \mathrm{MS}\Big[[\mathrm{BDS}]^{(2)} + \mathcal{R}^{(2)} + \mathcal{Z}_{12}^{(1)}\left(\mathcal{W}_1^{\mathrm{ren}(1)} - \mathcal{W}_2^{\mathrm{ren}(1)}\right)\Big]\\ &- \mathrm{MS}\Big[[\mathrm{BDS}]^{(2)}_{\mathrm{upper}} + [\mathrm{BDS}]^{(2)}_{\mathrm{lower}}\Big] - \mathcal{R}^{(2)}_{\mathrm{upper}} - \mathcal{R}^{(2)}_{\mathrm{lower}}\;.\end{aligned} \tag{6.28}$$

Here some comments are in order. The remainder functions for the upper and lower contours contributing to $\mathcal{W}_2$ in the 't Hooft limit, see (5.9), do not become divergent in the self-crossing case. Thus they drop their μ dependence as $\epsilon \to 0$. For T_1 we need (6.28) at $\mathcal{O}(\epsilon)$. All BDS terms in (6.28) will only contribute at $\mathcal{O}(\log^3 \mu^2)$ at $\mathcal{O}(\epsilon)$. Thus we are left with $\mathrm{MS}[\mathcal{R}^{(2)} + \mathcal{Z}_{12}^{(1)}(\mathcal{W}_1^{\mathrm{ren}(1)} - \mathcal{W}_2^{\mathrm{ren}(1)})]$. For the two-loop remainder function we recall the result from the previous section to obtain $\mathcal{R}^{(2)} = \frac{\gamma_{12}^{(1)}}{8\epsilon^3}(\mu^2)^{2\epsilon}$. It contributes with $\mathcal{O}(\log^4 \mu^2)$ at $\mathcal{O}(\epsilon)$.

Similarly to the one loop case we introduce a short-hand notation

$$\left(\log \mathcal{W}_1^{\mathrm{ren}(2)} - \log \mathcal{W}_2^{\mathrm{ren}(2)}\right) \approxeq: C_{[0]}^{(2)} + C_{[1]}^{(2)}\ \epsilon + C_{[2]}^{(2)}\ \epsilon^2 + \dots \tag{6.29}$$

where the $C_{[i]}^{(2)}$ again contain the relevant $\log^n \mu^2$ terms at each order in ϵ. The $C_{[i]}^{(2)}$ are given by

$$C_{[i]}^{(2)} = \gamma_{12}^{(1)} \left(\frac{(2)^i}{(i+3)!} \log^{(i+3)} \mu^2 - \frac{C_{[i+1]}^{(1)}}{2} \right) \tag{6.30}$$

Combining this with (6.4),(5.13), (6.11) and(6.27) we find

$$\begin{aligned} T_1 &= \frac{\gamma_{12}^{(1)}}{2} \left(C_{[1]}^{(2)} - C_{[0]}^{(1)} C_{[1]}^{(1)} \right) \\ &= \frac{\gamma_{12}^{(1)}}{96} \left(3\gamma_{12}^{(1)} - 4 \log \mu^2 - 20 \log \left(s\ \mathcal{X} \pm i\varepsilon \right) \right) \log^4 \mu^2 \ . \end{aligned} \tag{6.31}$$

Calculating term T_2

At first we calculate the combination of $\mathcal{Z}$-factors in (5.14)

$$\left(\mathcal{Z}_{12}^{(1)}\right)^2 + \mathcal{Z}_{12}^{(1)} \mathcal{Z}_{11}^{(1)} - \mathcal{Z}_{12}^{(2)} = \frac{\gamma_{12}^{(1)}}{4\epsilon^2} \left(\gamma_{12}^{(1)} - \log \left(-\mu^2 s \mathcal{X} \pm i\varepsilon \right) \right) + \frac{\gamma_{12}^{(2)}}{4\epsilon} - \frac{\gamma_{12}^{(1)}}{8\epsilon^3} \ . \tag{6.32}$$

Thus it is obvious that one has to expand $\left(\mathcal{W}_1^{\mathrm{ren}(1)} - \mathcal{W}_2^{\mathrm{ren}(1)}\right)$ up to $\mathcal{O}(\epsilon^3)$. The final result for T_2 is

$$T_2 = -\frac{\gamma_{12}^{(1)}}{8}\ C_{[3]}^{(1)}\ + \frac{\gamma_{12}^{(1)}}{4} \left(\gamma_{12}^{(1)} - \log \left(-\mu^2 s \mathcal{X} \pm i\varepsilon \right) \right)\ C_{[2]}^{(1)}\ +\ \mathcal{O}(\log^3 \mu^2) \tag{6.33}$$

$$= -\frac{\gamma_{12}^{(1)}}{960} \left(-10\gamma_{12}^{(1)} + 11 \log \mu^2 + 10 \log \left(-s\ \mathcal{X} \pm i\varepsilon \right) + 45 \log \left(s\ \mathcal{X} \pm i\varepsilon \right) \right) \log^4 \mu^2 \ .$$

Calculating term T_3

Here we have to keep terms including $\mathcal{O}(\log^3 \mu^2)$, since T_3 is integrated in (6.23). From (6.26), we get

$$T_3 \;=\; \Gamma_{12}^{(1)} \Big(\frac{\mathcal{W}_2^{\rm ren}}{\mathcal{W}_1^{\rm ren}}\Big)^{(2)} + \Gamma_{12}^{(2)} \Big(\frac{\mathcal{W}_2^{\rm ren}}{\mathcal{W}_1^{\rm ren}}\Big)^{(1)} + \;\Gamma_{12}^{(3)} \;. \tag{6.34}$$

Note that the contributions coming from $\Gamma_{11}^{(3)}$ are sub-sub-leading. Due to the structure of the crossing anomalous dimension matrix in (6.1) we know that the $\Gamma_{12}^{(k)}$ are independent of μ. Furthermore, since $\mathcal{W}_1^{\rm ren(1)}$ and $\mathcal{W}_2^{\rm ren(1)}$ contain at most $\mathcal{O}(\log^2 \mu^2)$ terms, we have to keep track of the first term in (6.34) only. Then for

$$\left(\frac{\mathcal{W}_2^{\rm ren}}{\mathcal{W}_1^{\rm ren}}\right)^{(2)} = \log \mathcal{W}_2^{\rm ren(2)} - \log \mathcal{W}_1^{\rm ren(2)} + \frac{1}{2}\left(\mathcal{W}_1^{\rm ren(1)} - \mathcal{W}_2^{\rm ren(1)}\right)^2 \tag{6.35}$$

similar arguments as above allow to neglect all BDS terms. Thus we can continue with

$$\left(\frac{\mathcal{W}_2^{\rm ren}}{\mathcal{W}_1^{\rm ren}}\right)^{(2)} = -C_{[0]}^{(2)} + \frac{\left(C_{[0]}^{(1)}\right)^2}{2} \;.$$

Together with (6.11)and (6.30) eventually we get

$$\begin{aligned} T_3 &= \frac{\gamma_{12}^{(1)}}{2}\left(\left(C_{[0]}^{(1)}\right)^2 - C_{[0]}^{(2)}\right) \\ &= -\frac{\gamma_{12}^{(1)}}{24}\Big(2\gamma_{12}^{(1)} - 3\log\mu^2 - 12\log\left(s\;\mathcal{X} \pm i\varepsilon\right)\Big)\log^3\mu^2 \;. \end{aligned} \tag{6.36}$$

Then the integral $-\int \frac{T_3}{\mu}\mathrm{d}\mu$ reads

$$-\int \frac{T_3}{\mu}\mathrm{d}\mu = \frac{\gamma_{12}^{(1)}}{480}\Big(5\gamma_{12}^{(1)} - 6\log\mu^2 - 30\log\left(s\mathcal{X} \pm i\varepsilon\right)\Big)\log^4\mu^2 \;. \tag{6.37}$$

Combining the three terms that we calculated we arrive at

$$\begin{aligned} \mathrm{MS}\Big[\mathcal{R}^{(3)}\Big] =& -\frac{21\;\gamma_{12}^{(1)}}{320}\log^5\mu^2 \\ &+ \frac{\gamma_{12}^{(1)}}{192}\Big(10\gamma_{12}^{(1)} - 2\log\left(-s\;\mathcal{X} \pm i\varepsilon\right) - 61\log\left(s\;\mathcal{X} \pm i\varepsilon\right)\Big)\log^4\mu^2 \;. \end{aligned} \tag{6.38}$$

We know that for $\epsilon \neq 0$ the remainder $\mathcal{R}(\mu, \epsilon, \{s\})$ depends on μ via $a_{\rm bare} = a\mu^{2\epsilon}$ only. Thus, the source for the $\log^5 \mu^2$ and $\log^4 \mu^2$ term has to be a term like

$$(A + \epsilon B)\, \frac{(\mu^2)^{3\epsilon}}{\epsilon^5} = \frac{A}{\epsilon^5} + \frac{B + 3A \log \mu^2}{\epsilon^4} + \cdots + \frac{27}{8} B \log^4 \mu^2 + \frac{81}{40} A \log^5 \mu^2 \; . \tag{6.39}$$

This way one can reconstruct the leading divergences of $\mathcal{R}^{(3)}$.

$$\mathcal{R} = -\frac{7}{216} \frac{\gamma_{12}^{(1)}}{\epsilon^5} + \frac{\gamma_{12}^{(1)}}{\epsilon^4} \left(\frac{5}{324} \gamma_{12}^{(1)} - \frac{1}{648} \left(2 \log \left(-s\ \mathcal{X} \mu^2 \pm i\varepsilon \right) + 61 \log \left(s\ \mathcal{X} \mu^2 \pm i\varepsilon \right) \right) \right) \tag{6.40}$$

We also take into account that the factor with the two s-dependent logarithms in the second line of (6.40) generates different imaginary parts, depending on the sign of $s = 2pq$.

6.3 On 4-loop divergences of the remainder

In order to evaluate the renormalisation group equation (5.18) at order $\mathcal{O}(a^4)$ we need $\log \mathcal{W}_1^{\rm ren(4)}$ which is defined by (5.10). The expansion yields

$$\begin{aligned}
&\log \mathcal{W}_1^{\rm ren(4)} = \\
&{\rm MS}\Big[\log \mathcal{W}_1^{(4)} - \left(\mathcal{W}_1^{\rm ren(1)} - \mathcal{W}_2^{\rm ren(1)} \right) \left((\mathcal{Z}_{11}^{(1)})^2 \mathcal{Z}_{12}^{(1)} - \mathcal{Z}_{11}^{(2)} \mathcal{Z}_{12}^{(1)} + 2 \mathcal{Z}_{11}^{(1)} (\mathcal{Z}_{12}^{(1)})^2 \right. \\
&\left. + (\mathcal{Z}_{12}^{(1)})^3 - \mathcal{Z}_{11}^{(1)} \mathcal{Z}_{12}^{(2)} - 2 \mathcal{Z}_{12}^{(1)} \mathcal{Z}_{12}^{(2)} + \mathcal{Z}_{12}^{(3)} \right) \\
&- \left(\log \mathcal{W}_1^{\rm ren(3)} - \log \mathcal{W}_2^{\rm ren(3)} \right) \mathcal{Z}_{12}^{(1)} \\
&+ \left(\mathcal{Z}_{11}^{(1)} \mathcal{Z}_{12}^{(1)} + (\mathcal{Z}_{12}^{(1)})^2 - \mathcal{Z}_{12}^{(2)} \right) \left(\log \mathcal{W}_1^{\rm ren(2)} - \log \mathcal{W}_2^{\rm ren(2)} \right) \\
&+ \left(\mathcal{W}_1^{\rm ren(1)} - \mathcal{W}_2^{\rm ren(1)} \right) \left(\log \mathcal{W}_1^{\rm ren(2)} - \log \mathcal{W}_2^{\rm ren(2)} \right) \mathcal{Z}_{12}^{(1)} \\
&- \frac{1}{2} \left(\mathcal{W}_1^{\rm ren(1)} - \mathcal{W}_2^{\rm ren(1)} \right)^2 \left(\mathcal{Z}_{11}^{(1)} \mathcal{Z}_{12}^{(1)} + 2 (\mathcal{Z}_{12}^{(1)})^2 - \mathcal{Z}_{12}^{(2)} \right) - \frac{1}{6} \left(\mathcal{W}_1^{\rm ren(1)} - \mathcal{W}_2^{\rm ren(1)} \right)^3 \mathcal{Z}_{12}^{(1)} \Big] \; .
\end{aligned} \tag{6.41}$$

This expansion is also valid for the crossing at two vertices (octagon). The re normalisation group equation to examine at four loops reads

$$\log \mathcal{W}_1^{\rm ren(4)} \;=\; -\int \frac{{\rm d}\mu}{\mu} \left(\Gamma_{12}\, \frac{\mathcal{W}_2^{\rm ren}}{\mathcal{W}_1^{\rm ren}} \;-\; \Gamma_{11} \right)^{(4)} \; . \tag{6.42}$$

Only being interested in leading and sub-leading contributions ($\mathcal{O}(\log^6 \mu^2)$ and $\mathcal{O}(\log^7 \mu^2)$) for the remainder function the r.h.s.. of (6.42) reads

$$-\int \frac{{\rm d}\mu}{\mu} \left(\Gamma_{12}\, \frac{\mathcal{W}_2^{\rm ren}}{\mathcal{W}_1^{\rm ren}} \;-\; \Gamma_{11} \right)^{(4)} = \; -\; \gamma_{12}^{(1)} \int \frac{{\rm d}\mu}{\mu} \left(\frac{\mathcal{W}_2^{\rm ren}}{\mathcal{W}_1^{\rm ren}} \right)^{(3)} \; . \tag{6.43}$$

By expansion one can verify that

$$\begin{aligned}\left(\frac{\mathcal{W}_2^{\text{ren}}}{\mathcal{W}_1^{\text{ren}}}\right)^{(3)} &= -\left(\log \mathcal{W}_1^{\text{ren}(3)} - \log \mathcal{W}_2^{\text{ren}(3)}\right) \\ &\quad + \left(\log \mathcal{W}_1^{\text{ren}(2)} - \log \mathcal{W}_2^{\text{ren}(2)}\right)\left(\mathcal{W}_1^{\text{ren}(1)} - \mathcal{W}_2^{\text{ren}(1)}\right) \\ &\quad -\frac{1}{6}\left(\mathcal{W}_1^{\text{ren}(1)} - \mathcal{W}_2^{\text{ren}(1)}\right)^3 \ .\end{aligned} \tag{6.44}$$

We see from eq. (6.41) that we have to compute far more complicated combinations of $\mathcal{Z}$ factors. Furthermore, we now need $\mathcal{Z}_{11}^{(2)}$ and $\mathcal{Z}_{12}^{(3)}$ which we compute by solving the differential equation (5.19) with (6.1). We find

$$\mathcal{Z}_{11}^{(2)} = \frac{n^2(\Gamma_{\text{cusp}}^{(1)})^2}{32\epsilon^4} + \frac{n\Gamma_{\text{cusp}}^{(1)}\Gamma_{11}^{(1)}}{8\epsilon^3} + \frac{2(\Gamma_{11}^{(1)})^2 - n\Gamma_{\text{cusp}}^{(2)}}{16\epsilon^2} - \frac{\Gamma_{11}^{(2)}}{4\epsilon} \ . \tag{6.45}$$

Expanding (5.19) at three loops we find

$$\mu\frac{\mathrm{d}}{\mathrm{d}\mu}\left(\mathcal{Z}_{12}^{(3)}a^3\right) = \left(\Gamma_{12}^{(3)} + \mathcal{Z}_{11}^{(1)}\Gamma_{12}^{(2)} + \mathcal{Z}_{11}^{(2)}\Gamma_{12}^{(1)} + \mathcal{Z}_{12}^{(1)}\Gamma_{22}^{(2)} + \mathcal{Z}_{12}^{(2)}\Gamma_{22}^{(1)}\right)a^3 \ , \tag{6.46}$$

still remembering the μ dependence of $a(\mu) = a_{\text{bare}}\mu^{-2\epsilon}$. Now we need to integrate (6.46).

$$\begin{aligned}\mathcal{Z}_{12}^{(3)} =& -\frac{\gamma_{12}^{(1)}\left(56\ (\gamma_{22}^{(1)})^2 + 54\ n\ \gamma_{22}^{(1)}\Gamma_{\text{cusp}}^{(1)} + 27\ n^2(\Gamma_{\text{cusp}}^{(1)})^2\right)}{1728\ \epsilon^5} \\ &- \frac{\gamma_{12}^{(1)}\left(4\ \Gamma_{11}^{(1)}\gamma_{22}^{(1)} + 14\ \Gamma_{22}^{(1)}\gamma_{22}^{(1)} + 9\ n\ \Gamma_{11}^{(1)}\Gamma_{\text{cusp}}^{(1)} + 9\ n\ \Gamma_{22}^{(1)}\Gamma_{\text{cusp}}^{(1)}\right)}{288\ \epsilon^4} \\ &+ \frac{1}{288\ \epsilon^3}\Big(8\ \gamma_{12}^{(2)}\gamma_{22}^{(1)} + 16\ \gamma_{12}^{(1)}\gamma_{22}^{(2)} + 18\ n\gamma_{12}^{(2)}\Gamma_{\text{cusp}}^{(1)} + 9\ n\ \gamma_{12}^{(1)}\Gamma_{\text{cusp}}^{(2)} \\ &\qquad - 6\ (\Gamma_{11}^{(1)})^2\ \gamma_{12}^{(1)} - 6\ \Gamma_{11}^{(1)}\Gamma_{22}^{(1)}\gamma_{12}^{(1)} - 6\ (\Gamma_{22}^{(1)})^2\gamma_{12}^{(1)}\Big) \\ &+ \frac{\Gamma_{11}^{(2)}\gamma_{12}^{(1)} + 2\ \Gamma_{11}^{(1)}\gamma_{12}^{(2)} + \gamma_{12}^{(2)}\Gamma_{22}^{(1)} + 2\ \gamma_{12}^{(1)}\Gamma_{22}^{(2)}}{24\ \epsilon^2} - \frac{\gamma_{12}^{(3)}}{6\ \epsilon}\end{aligned} \tag{6.47}$$

We will examine equation (6.41) term by term.

first two lines of (6.41)

Using these expressions we calculate the lengthy combination of $\mathcal{Z}$ factors in (6.41). However, we are not interested in the complete expression. We expect

that the leading $\log(\mu^2)$ behaviour of $\mathrm{MS}\Big[\mathcal{R}^{(4)}(\mu^2,\epsilon,\{s\})\Big]$ is $\mathcal{O}(\log^7(\mu^2))$. So the relevant (leading and next-leading) terms in the combination of $\mathcal{Z}$ factors are those whose pole order in ϵ *plus* their order in $\log\mu^2$ are greater or equal to four, provided that we are only interested in next-leading corrections for the remainder function. Recalling that

$$\gamma_{22}^{(1)} = 1 \quad , \qquad \Gamma_{\text{cusp}}^{(1)} = 2 \tag{6.48}$$

we find

$$\begin{aligned}(\mathcal{Z}\text{- terms}) = &-\frac{7\ \gamma_{12}^{(1)}}{216\ \epsilon^5} + \frac{\gamma_{12}^{(1)}\left(9\ \gamma_{12}^{(1)} - 7\ \log\left(-s\mathcal{X}\mu^2\right)\right)}{72\ \epsilon^4} \\ &+ \frac{\gamma_{12}^{(1)}\left(3\ \gamma_{12}^{(1)} - 2\log\left(-s\mathcal{X}\right)\right)\log\left(\mu^2\right)}{12\ \epsilon^3} - \frac{\gamma_{12}^{(1)}\log^2\left(\mu^2\right)}{12\ \epsilon^3}\ ,\end{aligned} \tag{6.49}$$

using the abbreviation (6.7). This is a remarkable simplification. As it should be, the relevant combination of $\mathcal{Z}$-factors only depends on crossing data - thus the dependence on the total number of cusps and the other cusp Mandelstam variables cancels out. We are now prepared to calculate the second term in the r.h.s.. of (6.41).

$$\begin{aligned}&\mathrm{MS}\Big[-\left(\mathcal{W}_1^{\text{ren}(1)} - \mathcal{W}_2^{\text{ren}(1)}\right)(\mathcal{Z}\text{- terms})\Big] = \\ &\quad\frac{7\ \gamma_{12}^{(1)}}{216}C_{[5]}^{(1)} - \frac{\gamma_{12}^{(1)}\left(9\ \gamma_{12}^{(1)} - 7\ \log\left(-s\mathcal{X}\mu^2\right)\right)}{72}C_{[4]}^{(1)} \\ &\quad - \frac{\gamma_{12}^{(1)}\left(3\ \gamma_{12}^{(1)} - 2\log\left(-s\mathcal{X}\right)\right)\log\left(\mu^2\right)}{12}C_{[3]}^{(1)} + \frac{\gamma_{12}^{(1)}\log^2\left(\mu^2\right)}{12}C_{[3]}^{(1)} + \mathcal{O}(\log^5\mu^2)\end{aligned} \tag{6.50}$$

Inserting the abbreviations and keeping relevant terms only we arrive at

$$\begin{aligned}&\mathrm{MS}\Big[-\left(\mathcal{W}_1^{\text{ren}(1)} - \mathcal{W}_2^{\text{ren}(1)}\right)(\mathcal{Z}\text{- terms})\Big] = \\ &\quad\frac{\gamma_{12}^{(1)}\log^6\mu^2\left(-351\gamma_{12}^{(1)} + 130\log\mu^2 + 237\log\left(-s\ \mathcal{X}\right) + 673\log\left(s\ \mathcal{X}\right)\right)}{155520}\end{aligned} \tag{6.51}$$

third line of (6.41)

The next part to calculate is $\left(\log\mathcal{W}_1^{\text{ren}(3)} - \log\mathcal{W}_2^{\text{ren}(3)}\right)$. Using equation (5.12) we find

$$\begin{aligned}\left(\log\mathcal{W}_1^{\text{ren}(3)} - \log\mathcal{W}_2^{\text{ren}(3)}\right) = \Big(\mathrm{MS}\Big[&[\mathrm{BDS}]^{(3)} + \mathcal{R}^{(3)} - T_1 - T_2 \\ &- [\mathrm{BDS}]_{\text{upper}}^{(3)} - \mathcal{R}_{\text{upper}}^{(3)} - [\mathrm{BDS}]_{\text{lower}}^{(3)} - \mathcal{R}_{\text{lower}}^{(3)}\Big]\Big)\ .\end{aligned} \tag{6.52}$$

We will only be interested in the relevant (leading and next- leading) terms. As this expression is multiplied with $\mathcal{Z}_{12}^{(1)}$, we are interested in the $\mathcal{O}(\epsilon)$ terms that are at least $\mathcal{O}(\log^6 \mu^2)$. All BDS terms can be neglected as they only contribute $\mathcal{O}(\log^3 \mu^2)$ at $\mathcal{O}(\epsilon)$. The remainder functions of the upper and lower part of the contour are also not divergent in the self-crossing case and thus do not contribute here. We are left with

$$\left(\log \mathcal{W}_1^{\text{ren}(3)} - \log \mathcal{W}_2^{\text{ren}(3)}\right) = \left(\text{MS}\Big[\mathcal{R}^{(3)} - T_1 - T_2\Big]\right) \ . \tag{6.53}$$

Using our three-loop result the leading contribution of the remainder function is $\mathcal{R}^{(3)} = -\frac{7\ \gamma_{12}^{(1)}(\mu^{2\epsilon})^3}{216\ \epsilon^5}$. At $\mathcal{O}(\epsilon)$ this means $\mathcal{R} = -\frac{21\gamma_{12}^{(1)}\epsilon}{640}\log^6 \mu^2$. Putting it together we find

$$-\text{MS}\Big[\left(\log \mathcal{W}_1^{\text{ren}(3)} - \log \mathcal{W}_2^{\text{ren}(3)}\right)\mathcal{Z}_{12}^{(1)}\Big] = -\frac{19\left(\gamma_{12}^{(1)}\right)^2}{2880}\log^6 \mu^2 \ . \tag{6.54}$$

fourth line of (6.41)

The next combination of $\mathcal{Z}$ factors is already known from the three loop calculation

$$\left(\mathcal{Z}_{12}^{(1)}\right)^2 + \mathcal{Z}_{12}^{(1)}\mathcal{Z}_{11}^{(1)} - \mathcal{Z}_{12}^{(2)} = \frac{\gamma_{12}^{(1)}}{4\epsilon^2}\left(\gamma_{12}^{(1)} - \log\left(-\mu^2 s\mathcal{X}\right)\right) + \frac{\gamma_{12}^{(2)}}{4\epsilon} - \frac{\gamma_{12}^{(1)}}{8\epsilon^3} \ . \tag{6.55}$$

Again, we are only interested in the leading term

$$\left(\mathcal{Z}_{12}^{(1)}\right)^2 + \mathcal{Z}_{12}^{(1)}\mathcal{Z}_{11}^{(1)} - \mathcal{Z}_{12}^{(2)} = -\frac{\gamma_{12}^{(1)}}{4\epsilon^2}\log\left(\mu^2\right) - \frac{\gamma_{12}^{(1)}}{8\epsilon^3} \ . \tag{6.56}$$

Apparently, we need $\left(\log \mathcal{W}_1^{\text{ren}(2)} - \log \mathcal{W}_2^{\text{ren}(2)}\right)$ at order $\mathcal{O}(\epsilon^2)$ and $\mathcal{O}(\epsilon^3)$. We use the short-hand notation for the relevant terms from eq. (6.30).

$$\left(\log \mathcal{W}_1^{\text{ren}(2)} - \log \mathcal{W}_2^{\text{ren}(2)}\right) = C_{[0]}^{(2)} + \epsilon C_{[1]}^{(2)} + \epsilon^2 C_{[2]}^{(2)} + \epsilon^3 C_{[3]}^{(2)} + \dots \ . \tag{6.57}$$

Putting it together we find

$$\begin{aligned}&\text{MS}\Big[\left(\mathcal{Z}_{11}^{(1)}\mathcal{Z}_{12}^{(1)} + (\mathcal{Z}_{12}^{(1)})^2 - \mathcal{Z}_{12}^{(2)}\right)\left(\log \mathcal{W}_1^{\text{ren}(2)} - \log \mathcal{W}_2^{\text{ren}(2)}\right)\Big] = \\ &-\frac{11}{1280}\left(\gamma_{12}^{(1)}\right)^2\log^6 \mu^2\end{aligned} \tag{6.58}$$

fifth line of (6.41)

All parts have been calculated earlier. Thus we just give the result.

$$\mathrm{MS}\Big[\left(\mathcal{W}_1^{\mathrm{ren}(1)}-\mathcal{W}_2^{\mathrm{ren}(1)}\right)\left(\log\mathcal{W}_1^{\mathrm{ren}(2)}-\log\mathcal{W}_2^{\mathrm{ren}(2)}\right)\mathcal{Z}_{12}^{(1)}\Big]= -\frac{13}{576}\left(\gamma_{12}^{(1)}\right)^2\log^6\mu^2. \tag{6.59}$$

last line of (6.41)

In the last line all parts but the new combination of $\mathcal{Z}$-factors are already known. The new combination reads

$$\begin{aligned}\left(\mathcal{Z}_{11}^{(1)}\mathcal{Z}_{12}^{(1)}+2(\mathcal{Z}_{12}^{(1)})^2-\mathcal{Z}_{12}^{(2)}\right)&=-\frac{\gamma_{12}^{(1)}}{8\epsilon^3}+\frac{\gamma_{12}^{(2)}}{4\epsilon}+\frac{\gamma_{12}^{(1)}\left(2\gamma_{12}^{(1)}-\log\left(-s\ \mathcal{X}\ \mu^2\right)\right)}{4\epsilon^2}\\&\approx-\frac{\gamma_{12}^{(1)}}{8\epsilon^3}+\frac{\gamma_{12}^{(1)}\left(2\gamma_{12}^{(1)}-\log\left(-s\ \mathcal{X}\ \mu^2\right)\right)}{4\epsilon^2}\ ,\end{aligned} \tag{6.60}$$

dropping irrelevant terms. The result is

$$\begin{aligned}&\mathrm{MS}\Big[-\frac{1}{2}\left(\mathcal{W}_1^{\mathrm{ren}(1)}-\mathcal{W}_2^{\mathrm{ren}(1)}\right)^2\left(\mathcal{Z}_{11}^{(1)}\mathcal{Z}_{12}^{(1)}+2(\mathcal{Z}_{12}^{(1)})^2-\mathcal{Z}_{12}^{(2)}\right)\\&\qquad-\frac{1}{6}\left(\mathcal{W}_1^{\mathrm{ren}(1)}-\mathcal{W}_2^{\mathrm{ren}(1)}\right)^3\mathcal{Z}_{12}^{(1)}\Big]\\&=\frac{\gamma_{12}^{(1)}\left(-50\gamma_{12}^{(1)}+59\log\mu^2+25\log(-\ s\ \mathcal{X})+388\log(s\ \mathcal{X})\right)}{2880}\log^6\mu^2\ .\end{aligned} \tag{6.61}$$

r.h.s.. of the RGE

We have to calculate

$$-\int\frac{\mathrm{d}\mu}{\mu}\left(\Gamma_{12}\ \frac{\mathcal{W}_2^{\mathrm{ren}}}{\mathcal{W}_1^{\mathrm{ren}}}\ -\ \Gamma_{11}\right)^{(4)}=\ -\ \gamma_{12}^{(1)}\int\frac{\mathrm{d}\mu}{\mu}\left(\frac{\mathcal{W}_2^{\mathrm{ren}}}{\mathcal{W}_1^{\mathrm{ren}}}\right)^{(3)}\ , \tag{6.62}$$

with

$$\begin{aligned}\left(\frac{\mathcal{W}_2^{\mathrm{ren}}}{\mathcal{W}_1^{\mathrm{ren}}}\right)^{(3)}&=-\left(\log\mathcal{W}_1^{\mathrm{ren}(3)}-\log\mathcal{W}_2^{\mathrm{ren}(3)}\right)\\&\quad+\left(\log\mathcal{W}_1^{\mathrm{ren}(2)}-\log\mathcal{W}_2^{\mathrm{ren}(2)}\right)\left(\mathcal{W}_1^{\mathrm{ren}(1)}-\mathcal{W}_2^{\mathrm{ren}(1)}\right)\\&\quad-\frac{1}{6}\left(\mathcal{W}_1^{\mathrm{ren}(1)}-\mathcal{W}_2^{\mathrm{ren}(1)}\right)^3\ .\end{aligned} \tag{6.63}$$

Using

$$\begin{aligned}&\left(\log \mathcal{W}_1^{\text{ren}(3)} - \log \mathcal{W}_2^{\text{ren}(3)}\right) \approx \\ &\text{MS}\Big[\mathcal{R}^{(3)} - \mathcal{Z}_{12}^{(1)}\left(\frac{1}{2}\left(\mathcal{W}_1^{\text{ren}(1)} - \mathcal{W}_2^{\text{ren}(1)}\right)^2 - \left(\mathcal{W}_1^{\text{ren}(2)} - \mathcal{W}_2^{\text{ren}(2)}\right)\right) \\ &- \left(\mathcal{Z}_{11}^{(1)}\mathcal{Z}_{12}^{(1)} + (\mathcal{Z}_{12}^{(1)})^2 - \mathcal{Z}_{12}^{(2)}\right)\left(\mathcal{W}_1^{\text{ren}(1)} - \mathcal{W}_2^{\text{ren}(1)}\right)\Big] ,\end{aligned} \tag{6.64}$$

we are prepared to calculate

$$\left(\frac{\mathcal{W}_2^{\text{ren}}}{\mathcal{W}_1^{\text{ren}}}\right)^{(3)} = \frac{1}{240}\left(13\gamma_{12}^{(1)} - 5\log\mu^2 - 30\log(s\ \mathcal{X})\right)\log^5\mu^2 \ . \tag{6.65}$$

Performing the integration we finally find

$$\begin{aligned}&-\gamma_{12}^{(1)}\int\frac{\mathrm{d}\mu}{\mu}\left(\frac{\mathcal{W}_2^{\text{ren}}}{\mathcal{W}_1^{\text{ren}}}\right)^{(3)} = \\ &-\frac{\gamma_{12}^{(1)}\left(91\gamma_{12}^{(1)} - 30\log(\mu^2) - 210\log(s\ \mathcal{X})\right)}{20160}\log^6\mu^2 \ .\end{aligned} \tag{6.66}$$

Now we add all the ingredients to give MS$[\mathcal{R}^{(4)}]$.

$$\begin{aligned}\text{MS}\Big[\mathcal{R}^{(4)}\Big] =& -\frac{2699}{136080}\gamma_{12}^{(1)}\log^7\mu^2 \\ &+\frac{\gamma_{12}^{(1)}\left(16443\gamma_{12}^{(1)} - 3174\log(-s\ \mathcal{X}) - 40010\log(s\ \mathcal{X})\right)}{311040}\log^6\mu^2 \ .\end{aligned} \tag{6.67}$$

Similar to our previous reasoning, we expand $(A + B\epsilon)(\mu^2)^{4\epsilon}\frac{1}{\epsilon^7}$ and fit the coefficients A and B to eq. (6.67). Thus we can construct the leading and sub-leading divergences of the 4-loop remainder function in dimensional regularisation for a self-crossing at two legs.

$$\begin{aligned}\mathcal{R}^{(4)} =& -\frac{2699}{442368\ \epsilon^7}\gamma_{12}^{(1)} \\ &+\frac{\gamma_{12}^{(1)}\left(16443\gamma_{12}^{(1)} - 3174\log(-s\ \mathcal{X}\mu^2) - 40010\log(s\ \mathcal{X}\mu^2)\right)}{1769472\ \epsilon^6}\end{aligned} \tag{6.68}$$

6.4 Implications for $\mathcal{R}_6$

The renormalisation group equation technique leads to expressions for the divergences of the remainder function of self-crossing Wilson loops which are realised as poles in ϵ and are not conformally invariant. However, we are looking for a conformally invariant expression which goes "unregularised to infinity once we choose the cross ratios in a way that corresponds to a self-crossing Wilson loop. From now on we focus on a self-crossing hexagon with p and q as the crossing momenta. We still use the fractions x and y according to fig. 16.

A generic closed light-like hexagon in four dimensions is characterised by the three conformal invariants [7]

$$u_1 := \frac{x_{13}^2\, x_{46}^2}{x_{14}^2\, x_{36}^2} \ , \quad u_2 := \frac{x_{15}^2\, x_{24}^2}{x_{14}^2\, x_{25}^2} \ , \quad u_3 := \frac{x_{35}^2\, x_{26}^2}{x_{25}^2\, x_{36}^2} \ , \tag{6.69}$$

where $x_{ij}^2 = (x_i - x_j)^2$. An explicit calculation that can be found in [26] shows that for a self-crossing hexagon in four dimensions, one cross-ratio equals one (we follow the the choice of [26] and choose $u_2 = 1$ here) and the remaining two are equal, so $u_1 = u_3 = u$.

Thinking about a non self-crossing contour approaching the self-crossing case we introduce the vector z to be the vector between the marked points on the edges p and q. The marks are defined by x and y, according to fig. 16. Then one can show that

$$u_2 - 1 \ = \ \frac{2pq\ z^2 - 4(qz)(pz)}{(-2y(1-x)pq + \mathcal{O}(z))(-2x(1-y)pq + \mathcal{O}(z))} \ . \tag{6.70}$$

Writing the arbitrary vector z as $z = \alpha p + \beta q + z_\perp$ with $pz_\perp = qz_\perp = 0$, $z_\perp^2 \leq 0$, the numerator of (6.70) turns out to be equal to $2pq\ z_\perp^2$. This implies that for $pq < 0$ ($pq > 0$) the approach to a self-crossing situation is possible only with $u_2 \to 1$ from above (below). For $pq < 0$ we get from (6.70)

$$\log\Big(\frac{1}{-z_\perp^2\mu^2}\Big) \ = \ -\log(u_2 - 1) \ - \ \log\big(-2pq\mu^2\mathcal{X}\big) \ + \ \mathcal{O}(z^2) \ . \tag{6.71}$$

For $pq > 0$ it is more convenient to use instead

$$\log\Big(\frac{1}{-z_\perp^2\mu^2}\Big) \ = \ -\log(1 - u_2) \ - \ \log\big(2pq\mu^2\mathcal{X}\big) \ + \ \mathcal{O}(z^2) \ . \tag{6.72}$$

[7] We emphasise that one cannot construct a light-like polygon in $\mathbb{R}^{(1,3)}$ for *every* three-tupel of real numbers such that the cross-ratios equal those numbers. Also, several Wilson loops that are not conformally equivalent may have the same set of cross-ratios.

Then all terms in (6.71) and (6.72) are real. While in the limit under consideration in both equations the l.h.s and the first term of the r.h.s. diverge, the second r.h.s. term stays finite. Now one expects a correspondence between the divergences of the remainder function in dimensional regularisation and in the geometric "point splitting" regularisation.

6.4.1 Expectations for $R_6^{(2)}$

For the self-crossing Hexagon at two loops we calculated the divergences of the remainder function in eq. (6.22). Using the translation rule between dimensional and "point splitting" regularisation that we motivate in appendix 8.11 we find that $1/\epsilon^3 \;\Leftrightarrow\; 2/3\;\log^3\left(\frac{1}{-z_\perp^2\mu^2}\right)$ and $1/\epsilon^2 \;\Leftrightarrow\; \log^2\left(\frac{1}{-z_\perp^2\mu^2}\right)$. Together with $\gamma_{12}^{(1)} = \pm\,\text{sign}\,(pq)\;2\pi i$ we find for

case 1: $pq < 0$

$$\mathcal{R}_6^{(2)} = -\frac{\pm\pi i}{4}\left(\frac{1}{\epsilon^3} + \frac{2\log\left(s\;\mathcal{X}\;\mu^2 \pm i\varepsilon\right)}{\epsilon^2}\right) + \mathcal{O}(\epsilon^{-1})\;, \tag{6.73}$$

and consequently

$$\mathcal{R}_6^{(2)} = \pm\frac{i\pi}{6}\log^3\left(u_2-1\right) + \frac{\pi^2}{2}\log^2\left(u_2-1\right) + \mathcal{O}\left(\log(u_2-1)\right)\;. \tag{6.74}$$

case 1: $pq > 0$

$$\mathcal{R}_6^{(2)} = \frac{\pm\pi i}{4}\left(\frac{1}{\epsilon^3} + \frac{2\log\left(s\;\mathcal{X}\;\mu^2 \pm i\varepsilon\right)}{\epsilon^2}\right) + \mathcal{O}(\epsilon^{-1})\;, \tag{6.75}$$

and thus

$$\mathcal{R}_6^{(2)} = \mp\frac{i\pi}{6}\log^3\left(1-u_2\right) + \mathcal{O}\left(\log(1-u_2)\right)\;. \tag{6.76}$$

6.4.2 Expectations for $R_6^{(3)}$

The divergences of the remainder function of the self-crossing hexagon at three loops are given by eq. (6.40). At three loops the translation rule in the appendix 8.11 gives the correspondence $1/\epsilon^5 \;\Leftrightarrow\; 9/20\;\log^5\left(\frac{1}{-z_\perp^2\mu^2}\right)$ and $1/\epsilon^4 \;\Leftrightarrow\; 3/4\;\log^4\left(\frac{1}{-z_\perp^2\mu^2}\right)$. This means for

case 1: $pq < 0$

$$\mathcal{R}^{(3)} = \pm\frac{7}{108}\pi i\,\left(\epsilon^{-5} + 3\log(-2pq\mu^2\mathcal{X})\,\epsilon^{-4}\right) - \frac{\pi^2}{4}\,\epsilon^{-4} + \mathcal{O}(\epsilon^{-3})\,, \quad (6.77)$$

and consequently

$$\mathcal{R}_6^{(3)}(\{u\}) = \mp\frac{7}{240}\pi i\log^5(u_2{-}1) - \frac{3}{16}\pi^2\log^4(u_2{-}1) + \mathcal{O}(\log^3(u_2{-}1))\,. \quad (6.78)$$

case 1: $pq > 0$

$$\mathcal{R}^{(3)} = \mp\frac{7}{108}\pi i\,\left(\epsilon^{-5} + 3\log(2pq\mu^2\mathcal{X})\,\epsilon^{-4}\right) - \frac{\pi^2}{18}\,\epsilon^{-4} + \mathcal{O}(\epsilon^{-3})\,, \quad (6.79)$$

and consequently

$$\mathcal{R}_6^{(3)}(\{u\}) = \pm\frac{7}{240}\pi i\log^5(1{-}u_2) - \frac{1}{24}\pi^2\log^4(1{-}u_2) + \mathcal{O}(\log^3(1{-}u_2))\,. \quad (6.80)$$

6.4.3 Expectations for $R_6^{(4)}$ and beyond

Calculating at higher loop orders, we expect the following general structure of the divergences in dimensional regularisation

$$\mathcal{R}^{(l)} = \frac{A\,\pi i}{\epsilon^{2l-1}} + \frac{B\,\pi i\log|s\mu^2\mathcal{X}| + C\,\pi^2}{\epsilon^{2l-2}} + \mathcal{O}(\epsilon^{-(2l-3)})\,, \quad (6.81)$$

where A, B and C are just numbers. The $\frac{1}{\epsilon^{2l-1}}$ pole is related to a branch cut of a $\mathrm{Li}_{2l}(1-1/u_2)$ term in the remainder function (which will be clarified in the next section). Thus, the coefficient of the leading pole is automatically conformally invariant. The sub-leading pole generally has a conformally invariant (C) and a non-conformally invariant part (B). If by any translation between dimensional and geometric regularisation the generated sub-leading non-conformal terms should cancel, only terms proportional to $\log|s\mu^2\mathcal{X}|$ may enter the above equation, due to eq. (6.71) and (6.72). These arguments fix the structure of the leading and sub-leading poles of the remainder function to the expression eq. (6.81). Although the prefactors are a little complicated, the four-loop result eq. (6.68) has this structure (which of course also holds for the lower loop results eqns. (6.22) and (6.40)). We emphasise that this fact is a check on the four-loop calculation as all non-conformal terms combine correctly in the end.

In order to achieve a conformally invariant series expansion in $\log|1-u_2|$ the relative weight of the translation coefficients has to be

$$\frac{\alpha_{\text{l.}}}{\alpha_{\text{sub-l.}}} = \frac{B}{(2l-1)A}\,. \quad (6.82)$$

Thus, the relative weight of the translation factors for the leading and next-leading poles for the hexagon at four loops using eq. (6.68) has to be

$$\frac{\alpha_{\text{l.}}}{\alpha_{\text{sub-l.}}} = \frac{4}{7} \ . \tag{6.83}$$

This is compatible with relative weight predicted by the heuristic translation rule in appendix 8.11 which suggests $\alpha_{\text{l.}} = 32/105$, $\alpha_{\text{sub-l.}} = 8/15$ and consequently $\alpha_{\text{l.}}/\alpha_{\text{sub-l.}} = 4/7$.

6.5 Discussion and comparison to previous results

In this section we have discussed the leading and next-leading divergences of a remainder function of a self-crossing Wilson loop with a crossing between two edges. The leading and next-leading divergences only depend on one-loop information of the anomalous dimension matrix (see. eq. (6.1)). In [23] the authors give the explicit form of the two loop hexagon remainder function

$$\begin{aligned}\mathcal{R}_6^{(2)}(u_1,u_2,u_3) = &\sum_{i=1}^{3}\left(L_4(x_i^+,x_i^-) - \frac{1}{2}\text{Li}_4(1-1/u_i)\right) \\ &- \frac{1}{8}\left(\sum_{i=1}^{3}\text{Li}_2(1-1/u_i)\right)^2 + \frac{1}{24}J^4 + \frac{\pi^2}{12}J^2 + \frac{\pi^4}{72} \ .\end{aligned} \tag{6.84}$$

Here,

$$\begin{aligned}x_i^{\pm} = u_i x^{\pm} \ , \quad x^{\pm} = \frac{u_1+u_2+u_3-1 \pm \sqrt{\Lambda}}{2u_1u_2u_3} \ , \\ \Lambda = (u_1+u_2+u_3-1)^2 - 4u_1u_2u_3 \ .\end{aligned} \tag{6.85}$$

Furthermore,

$$L_4(x^+,x^-) = \frac{1}{8!!}\log^4 x^+x^- + \sum_{m=0}^{3}\frac{(-1)^m}{(2m)!!}\log^m x^+x^-\left(l_{4-m}(x^+) + l_{4-m}(x^-)\right) \ , \tag{6.86}$$

$$l_n(x) = \frac{1}{2}\left(\text{Li}_n(x) - (-1)^n\text{Li}_n(1/x)\right) \ , \tag{6.87}$$

$$J = \sum_{i=1}^{3}\left(l_1(x_i^+) - l_1(x_i^-)\right) \ . \tag{6.88}$$

The important part to compare with is the term

$$\mathcal{R}_6^{(2)} = \; -\frac{1}{2}\mathrm{Li}_4(1-1/u_2) - \frac{1}{8}\left(\mathrm{Li}_2(1-1/u_2)\right)^2 \; + \; \ldots \; . \tag{6.89}$$

Obviously, the analytic expression for the remainder function does not have any singular term in the self-crossing limit. However, the cross ratios do not uniquely fix the conformal class of a given light-like contour. The expressions above are valid in the Euclidean region, meaning that every distance between cusps is either light-like (if they are adjacent) or space-like. It is easy to show, that there are no self-crossing light-like *Euclidean* hexagons in $\mathbb{R}^{(1,3)}$. Now, the divergences arise in the discontinuity of the branch-cut that extends from 1 to $+\infty$ in the polylogarithms

$$\lim_{\varepsilon\to 0}\left(\mathrm{Li}_n(x+i\varepsilon) - \mathrm{Li}_n(x-i\varepsilon)\right) = \frac{2\pi i}{(n-1)!}\log^{n-1} x \; , \tag{6.90}$$

for $x \in (1, +\infty)$. In order to understand how the discontinuity is picked up during the continuation from the Euclidean Wilson loop to the self-crossing one may consider the following family of Wilson loops.

$$\begin{aligned} &x_2 = (2,1,1,0), \quad x_3 \; = \; (2-\sqrt{b^2-2b+2},0,b,0), \quad x_4 \; = \; (2,-1,1,0) \\ &x_1 = (x_{10},\cos\psi,-1,\sin\psi), \quad x_5 = (x_{50},-\cos\psi,-1,-\sin\psi), \\ &x_6 = (x_{60},0,-b,0), \end{aligned} \tag{6.91}$$

with

$$x_{10} \; = \; x_{50} \; = \; 2-\sqrt{6-2\cos\psi}, \quad x_{60} \; = \; 2-\sqrt{6-2\cos\psi}+\sqrt{2+b^2-2b} \; . \tag{6.92}$$

This Wilson-loop has a crossing with $pq < 0$. The related cross-ratios are

$$\begin{aligned} u_2 &= \frac{1}{\cos^2\psi} \; , \\ u &= -\frac{(\; 3-\cos\psi-2b-\sqrt{6-2\cos\psi}\sqrt{b^2-2b+2}\;)^2}{\cos\psi\;(14-8b-2\cos\psi-4\sqrt{6-2\cos\psi}\sqrt{b^2-2b+2})} \; . \end{aligned} \tag{6.93}$$

Then, ψ parametrises the homotopy between the Euclidean non-self-crossing and the self-crossing Wilson loop. If ψ goes from 0 to π, the argument of the polylogarithms, which is $1-1/u_2$, goes from 0 to 1 and back to zero. If we take the $i\varepsilon$- prescription from the gluon propagator also inside the cross ratios and substitute $(x_k-x_l)^2 \to (x_k-x_l)^2 \mp i\varepsilon$, the argument of the polylogarithms encircles the branch cut in a counter-clockwise manner for the

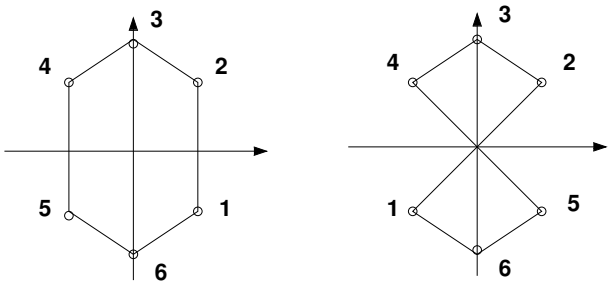

Figure 17: *Projection to the (1,2)-plane of a null hexagon without self-crossing, but with $u_2 = 1$ (left) and after rotating x_1 and x_5 with angle π in the (1,3)-plane (right).*

standard $i\varepsilon$-prescription and clockwise for a switched $i\varepsilon$-prescription. All four options in the eqns. (6.74) and (6.76) can now be obtained by analytic continuation from eq. (6.89). It is clear that $u_2 > 0$ in the Euclidean case, as all Mandelstam variables inside the cross ratios have the same sign and so $1 - \frac{1}{u_2} < 1$. Encircling $1 - \frac{1}{u_2} = 1$ in eq. (6.89) counter-clockwise (clockwise) results in eq. (6.74) with the standard (switched) $i\varepsilon$ prescription. Likewise, one can obtain eq. (6.76) in the standard (switched) $i\varepsilon$ prescription by encircling $1 - \frac{1}{u_2} = 1$ in clockwise (counter-clockwise) orientation, then going to $1 - \frac{1}{u_2} < 0$ encircling 0 with the same orientation and finally approaching 0 from below.

At three loops we also expect that the divergent terms can be connected via analytic continuation to the finite remainder function in the Euclidean regime. In [38] the authors present the complete Symbol of the three-loop remainder function. The result has independently been confirmed in [40]. The leading singularity at three loops can be read off from [38] and is $\pm\frac{i\pi}{40}\log^5(1-u_2)$. This mismatches our result (6.80) by a factor of 6/7. A short definition of the symbol and a comparison with $\mathcal{S}(\mathcal{R}_6^{(3)})$ from [38]can be found in the appendix 8.10. From this mismatch one may conclude that the heuristic translation rule that we motivate in the appendix is wrong starting at three loops. At three loops it still gives the correct relative weight to make (6.80) conformally invariant, however, the overall pre-factor turns out to be incorrect. Also at four loops the relative weight generated by the heuristic translation rule turns out to be correctly 4/7 in order to give a conformally invariant result. The series $\alpha_{\text{l.}}/\alpha_{\text{sub-l.}}$ of relative weights of the translation coefficients that are necessary to give a conformally invariant result starting

at two loops up to four loops is

$$\frac{2}{3}\,,\quad \frac{3}{5}\,,\quad \frac{4}{7}\,\cdots\,, \tag{6.94}$$

which is compatible with the heuristic translation rule that suggests that this series should be $\alpha_{\text{l.}}/\alpha_{\text{sub-l.}} = l/(2l-1)$.

Forgetting about any explicit translation rule the procedure that we have presented will in general result in a expression (6.81) with the three parameters A, B and C given. The relative weight of the translation rule will be adjusted in a manner that the remainder function expressed in a series expansion in $\log(1-u_2)$ is conformally invariant. The remainder will then have the structure

$$\begin{aligned}\mathcal{R}_6^{(l)} \;\propto\; & \pi i\;\tilde{A}\log^{(2l-1)}(1-u_2) \;+\; \pi^2\tilde{C}\log^{(2l-2)}(1-u_2) \\ & +\; \mathcal{O}(\log^{(2l-3)}(1-u_2))\;. \end{aligned} \tag{6.95}$$

Even without an explicit translation rule, the method is predictive and predicts the relative weight $\tilde{A}/\tilde{C}$ of the leading and sub-leading divergence. There are no obstacles that prevent us from carrying out the method recursively to obtain results at higher loop orders. Also, the results are more general. If one is interested in self-crossing Wilson loops with more than six edges, all results from this section can be reused. One merely needs a kinematical calculation to find an expression that relates logarithms of the distance between the legs to cross ratios.

7 Crossing at two vertices

In this section we will use a renormalisation group equation to determine the leading divergences of remainder functions of self-crossing Wilson loops with a crossing at two vertices. The polygon with the least number of cusps necessary for this configuration is the octagon. The two-loop calculations presented here originate from our work in [27], although we use a slightly different notation here. The three and four loop results have not been published so far. In four dimensions the vertices adjacent to the crossing ($x_{\hat{l}-1}, x_{\hat{l}+1}, x_{\hat{k}-1}, x_{\hat{k}+1}$in fig. 15) form two independent cross ratios that are, in general, not constrained. We expect that the divergent terms of the remainder function are a function of those two cross ratios. The two cross ratios are

$$C_1 = \frac{s_{\hat{k}-1,\hat{k}+1}\ s_{\hat{l}-1,\hat{l}+1}}{s_{\hat{k}+1,\hat{l}+1}\ s_{\hat{k}-1,\hat{l}-1}}\ , \quad \exp\left(\Gamma^{(1)}_{12}\right) = C_2 = \frac{s_{\hat{k}-1,\hat{l}+1}s_{\hat{k}+1,\hat{l}-1}}{s_{\hat{k}-1,\hat{l}-1}s_{\hat{k}+1,\hat{l}+1}}\ . \tag{7.1}$$

We use a similar attempt as before. Again, the renormalisation group equation to evaluate is

$$\mu\frac{\mathrm{d}}{\mathrm{d}\mu}\ \log\mathcal{W}_1^{\mathrm{ren}}\ =\ -\ \Gamma_{12}\ \frac{\mathcal{W}_2^{\mathrm{ren}}}{\mathcal{W}_1^{\mathrm{ren}}}\ -\ \Gamma_{11}\ . \tag{7.2}$$

Contrary to the last section, we are only interested in the leading divergences of the remainder here. Of course, we have to calculate the crossing anomalous dimensions and the corresponding $\mathcal{Z}$ matrix in a similar manner as we did for the crossing between two edges.

7.1 $\mathcal{Z}$ factors

We start by spelling out the anomalous dimension matrix for the self-crossing Wilson loop with a crossing between two vertices

$$\Gamma = \begin{pmatrix}1 & 0\\ 0 & 1\end{pmatrix}\frac{\Gamma_{\mathrm{cusp}}(a)}{2}\sum_{k\in\mathrm{cusps}}\log(-s_k\mu^2) + \begin{pmatrix}A & \Gamma_{12}(a)\\ 0 & B\end{pmatrix}\ . \tag{7.3}$$

Here, (contrary to the crossing of two edges) the sum runs over all cusps that are away from the crossing point. This difference comes from the fact that a crossing at two vertices does not cut any momenta into two pieces. Thus the other functions are given by

$$A = \gamma_{11}(a)\ \left(\log\left(-s_{\hat{k}-1,\hat{k}+1}\mu^2\right) + \log\left(-s_{\hat{l}-1,\hat{l}+1}\mu^2\right)\right) \tag{7.4}$$

$$B = \gamma_{22}(a)\ \left(\log\left(-s_{\hat{k}-1,\hat{l}+1}\mu^2\right) + \log\left(-s_{\hat{l}-1,\hat{k}+1}\mu^2\right)\right)\ . \tag{7.5}$$

Additionally, we know

$$\gamma_{11}^{(1)} = \gamma_{22}^{(1)} = \frac{\Gamma_{\text{cusp}}^{(1)}}{2} = 1 \ , \quad \Gamma_{12}^{(1)} = \log C_2 \ . \tag{7.6}$$

In appendix 8.9 we explicitly perform the one-loop calculation for this crossing anomalous dimension matrix. We now solve the differential equation (5.19). For convenience, we copy

$$\begin{aligned} \mu\frac{\mathrm{d}}{\mathrm{d}\mu}\log \mathcal{Z}_{11} \ &= \Gamma_{11} \ , \qquad \mu\frac{\mathrm{d}}{\mathrm{d}\mu}\mathcal{Z}_{12} = \mathcal{Z}_{11}\Gamma_{12} + \mathcal{Z}_{12}\Gamma_{22} \ , \\ \mu\frac{\mathrm{d}}{\mathrm{d}\mu}\log \mathcal{Z}_{22} \ &= \Gamma_{22} \ . \end{aligned} \tag{7.7}$$

Solving these differential equations we find

$$\mathcal{Z}_{11}^{(0)} = 1 \ , \quad \mathcal{Z}_{11}^{(1)} = -\frac{n\ \Gamma_{\text{cusp}}^{(1)}}{4\epsilon^2} - \frac{\Gamma_{11}^{(1)}}{2\epsilon} \tag{7.8}$$

$$\mathcal{Z}_{11}^{(2)} = \frac{n^2\left(\Gamma_{\text{cusp}}^{(1)}\right)^2}{32\epsilon^4} + \frac{n\Gamma_{\text{cusp}}^{(1)}\Gamma_{11}^{(1)}}{8\epsilon^3} - \frac{4\gamma_{11}^{(2)} + (n-2)\Gamma_{\text{cusp}}^{(2)} - 2\left(\Gamma_{11}^{(1)}\right)^2}{16\epsilon^2} + \frac{\Gamma_{11}^{(2)}}{4\epsilon}$$

$$\mathcal{Z}_{22}^{(0)} = 1 \ , \quad \mathcal{Z}_{22}^{(1)} = -\frac{n\ \Gamma_{\text{cusp}}^{(1)}}{4\epsilon^2} - \frac{\Gamma_{22}^{(1)}}{2\epsilon} \ . \tag{7.9}$$

For $\mathcal{Z}_{12}$ we find

$$\mathcal{Z}_{12}^{(0)} = 0 \ , \quad \mathcal{Z}_{12}^{(1)} = -\frac{\Gamma_{12}^{(1)}}{2\epsilon} \tag{7.10}$$

$$\mathcal{Z}_{12}^{(2)} = \frac{\Gamma_{12}^{(1)}\left(3\gamma_{11}^{(1)} + \gamma_{22}^{(1)} + (n-2)\,\Gamma_{\text{cusp}}^{(1)}\right)}{8\epsilon^3} + \frac{\Gamma_{12}^{(1)}\left(\Gamma_{11}^{(1)} + \Gamma_{22}^{(1)}\right)}{8\epsilon^2} - \frac{\Gamma_{12}^{(2)}}{4\epsilon} \tag{7.11}$$

For the four-loop calculation we will also need to calculate $\mathcal{Z}_{12}^{(3)}$, which is an extremely lengthy expression. It can be computed straightforwardly by calculating

$$a^3\ \mathcal{Z}_{12}^{(3)} = \int \frac{\mathrm{d}\mu}{\mu} a(\mu)^3 \left(\Gamma_{12}^{(3)} + \mathcal{Z}_{11}^{(1)}\Gamma_{12}^{(2)} + \mathcal{Z}_{11}^{(2)}\Gamma_{12}^{(1)} + \mathcal{Z}_{12}^{(1)}\Gamma_{22}^{(2)} + \mathcal{Z}_{12}^{(2)}\Gamma_{22}^{(1)}\right) \ . \tag{7.12}$$

7.2 On 2-loop divergences

Expanding eq. (7.2) at order $\mathcal{O}(a^2)$ we find

$$\begin{aligned} \mathrm{MS}\Big[[\mathrm{BDS}]^{(2)} + \mathcal{R}^{(2)} + \mathcal{Z}_{12}^{(1)}\left(\mathcal{W}_1^{\mathrm{ren}(1)} - \mathcal{W}_2^{\mathrm{ren}(1)}\right)\Big] = \\ - \int \left(\left(\Gamma_{12}\ \frac{\mathcal{W}_2^{\mathrm{ren}}}{\mathcal{W}_1^{\mathrm{ren}}}\right)^{(2)} + \Gamma_{11}^{(2)}\right)\frac{\mathrm{d}\mu}{\mu} \ . \end{aligned} \tag{7.13}$$

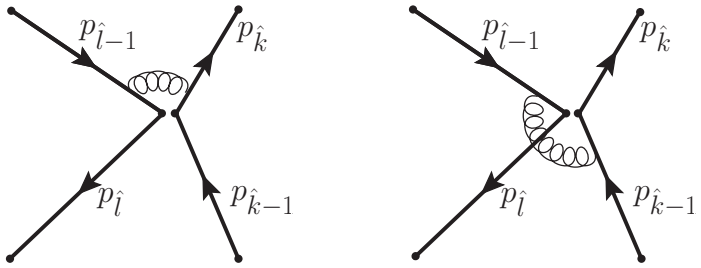

Figure 18: These are two of four diagrams that are responsible for the new divergences in F_n.

Anticipating that the result will be $\mathcal{O}(\log^2\mu^2)$ we are only interested in terms of $\mathcal{O}(\log^2\mu^2)$ or higher, although the $\mathcal{O}(\log^3\mu^2)$ will cancel in the end. We start by examining the two-loop BDS terms at the relevant orders of $\log\mu^2$. The expression of the BDS Ansatz up to two loops is

$$\begin{aligned}\log\mathcal{W} = -\frac{1}{4}\sum_{l=1,2} a^l \left(\frac{\Gamma^{(l)}_{\text{cusp}}}{(l\epsilon)^2}+\frac{\Gamma^{(l)}}{l\epsilon}\right)\sum_k(-\mu^2 s_{k-1,k+1})^{l\epsilon} \; + a\; F_n(\mu^2,\epsilon,s) - \frac{a^2 n}{8} f_2^{(2)} \\ + a^2\Big(\frac{\Gamma^{(2)}_{\text{cusp}}}{2}F_n(\mu^2,2\epsilon,s) + \epsilon\Gamma^{(2)}F_n(\mu^2,2\epsilon,s) + C^{(2)} + \mathcal{R}_n^{(2)}(\mu^2,\epsilon,s)\Big) + \mathcal{O}(\epsilon).\end{aligned} \tag{7.14}$$

It is important to notice that the one-loop finite part $F_n(\mu^2,\epsilon,s)$ now becomes divergent as a consequence of the diagrams in fig. 18 becoming divergent in the self-crossing case. However, they are finite in the generic case. The expression for the one-loop finite part $F_n(\mu^2,\epsilon,s)$ in the self-crossing case reads

$$\begin{aligned}F_n(\mu^2,\epsilon,s) =& \frac{1}{2\epsilon}\;\log\frac{s_{\hat{k}-1,\hat{l}-1}\;s_{\hat{k}+1,\hat{l}+1}}{s_{\hat{k}+1,\hat{l}-1}\;s_{\hat{k}-1,\hat{l}+1}} \\ &+\frac{1}{4}\big(\log^2(-s_{\hat{k}-1,\hat{l}-1}\mu^2\pm i\varepsilon)+\log^2(-s_{\hat{k}+1,\hat{l}+1}\mu^2\pm i\varepsilon) \\ &-\log^2(-s_{\hat{k}+1,\hat{l}-1}\mu^2\pm i\varepsilon)-\log^2(-s_{\hat{k}-1,\hat{l}+1}\mu^2\pm i\varepsilon)\big) \;+\; \tilde{F}_n(s) \;+\; \mathcal{O}(\epsilon)\;,\end{aligned} \tag{7.15}$$

where $\tilde{F}_n(s)$ is now independent of μ^2. Using the considerations above we find at leading order in $\mathcal{O}(\log\mu^2)$

$$\begin{aligned}\text{MS}\Big[[\text{BDS}]_1^{(2)}\Big] &= \frac{n\;\Gamma^{(2)}_{\text{cusp}}\left(1+2\epsilon\log\left(\mu^2\right)-\left(\mu^2\right)^{2\epsilon}\right)}{16\epsilon^2} \\ &= -\frac{1}{8}\left(n\;\Gamma^{(2)}_{\text{cusp}}\log^2\left(\mu^2\right)\right)+\mathcal{O}(\epsilon)\;,\end{aligned} \tag{7.16}$$

for all orders in ϵ, as we will need this expression in a later section. The next ingredient is $\mathcal{Z}_{12}^{(1)}\left(\mathcal{W}_1^{\text{ren}(1)}-\mathcal{W}_2^{\text{ren}(1)}\right)$. We remember that $\mathcal{Z}_{12}^{(1)}=-\frac{\Gamma_{12}^{(1)}}{2\epsilon}$.

$$\text{MS}\Big[\left(\mathcal{W}_1^{\text{ren}(1)}-\mathcal{W}_2^{\text{ren}(1)}\right)\Big]=-\frac{\log C_1\left(\left(\mu^2\right)^\epsilon-1\right)}{2\epsilon}\ . \tag{7.17}$$

And thus

$$\begin{aligned}\text{MS}\Big[\mathcal{Z}_{12}^{(1)}\left(\mathcal{W}_1^{\text{ren}(1)}-\mathcal{W}_2^{\text{ren}(1)}\right)\Big]&=\frac{\log C_1\log C_2\left(\left(\mu^2\right)^\epsilon-\epsilon\log\left(\mu^2\right)-1\right)}{4\epsilon^2}\\&=\frac{\log C_1\log C_2}{8}\log^2\left(\mu^2\right)+\mathcal{O}(\epsilon)\ .\end{aligned} \tag{7.18}$$

The last part to evaluate is $\left(\Gamma_{12}\,\frac{\mathcal{W}_2^{\text{ren}}}{\mathcal{W}_1^{\text{ren}}}\right)^{(2)}$. We know that $\Gamma_{12}^{(0)}=0$ and thus

$$\left(\Gamma_{12}\,\frac{\mathcal{W}_2^{\text{ren}}}{\mathcal{W}_1^{\text{ren}}}\right)^{(2)}=\Gamma_{12}^{(1)}\ \left(\frac{\mathcal{W}_2^{\text{ren}}}{\mathcal{W}_1^{\text{ren}}}\right)^{(1)}+\Gamma_{12}^{(2)}\ . \tag{7.19}$$

As $\Gamma_{12}^{(2)}$ is μ-independent we are interested in

$$\Gamma_{12}^{(1)}\ \left(\frac{\mathcal{W}_2^{\text{ren}}}{\mathcal{W}_1^{\text{ren}}}\right)=\Gamma_{12}^{(1)}\ \left(\mathcal{W}_2^{\text{ren}(1)}-\mathcal{W}_1^{\text{ren}(1)}\right)=\frac{\log C_1\log C_2\left(\left(\mu^2\right)^\epsilon-1\right)}{2\epsilon}\ . \tag{7.20}$$

Remembering that at leading order $\log\mu^2$

$$\Gamma_{11}^{(2)}\approx\left(2\ \gamma_{11}^{(2)}+(n-2)\frac{\Gamma_{\text{cusp}}^{(2)}}{2}\right)\log\mu^2 \tag{7.21}$$

Performing the integration, we find that

$$\begin{aligned}&-\int\left(\left(\Gamma_{12}\,\frac{\mathcal{W}_2^{\text{ren}}}{\mathcal{W}_1^{\text{ren}}}\right)^{(2)}+\Gamma_{11}^{(2)}\right)\frac{\text{d}\mu}{\mu}\\&=\left(-\frac{1}{8}\log C_1\log C_2-\frac{\gamma_{11}^{(2)}}{2}-(n-2)\frac{\Gamma_{\text{cusp}}^{(2)}}{8}\right)\log^2\left(\mu^2\right)\ .\end{aligned} \tag{7.22}$$

Putting everything together, we find

$$\text{MS}\Big[\mathcal{R}^{(2)}\Big]=\left(-\frac{\log C_1\log C_2}{4}-\frac{\gamma_{11}^{(2)}}{2}+\frac{\Gamma_{\text{cusp}}^{(2)}}{4}\right)\log^2\left(\mu^2\right)\ . \tag{7.23}$$

Here we see that the dependence on the total number of cusps is cancelled out as it should be. The divergences of the remainder function are only

caused by the crossing divergences and thus only depend on "local" data at the crossing. We know that the μ-dependence in $\mathrm{MS}\big[\mathcal{R}^{(2)}\big]$ is introduced only by the rescaling of $a = a_{\mathrm{bare}}\mu^{-2\epsilon}$. Expanding $\frac{a_{\mathrm{bare}}^2\mu^{-4\epsilon}}{\epsilon^2}$ we deduce that $\log^2\mu^2$ terms originate from $\frac{1}{2\epsilon^2}$ poles. Thus, we find for the "remainder function" of a self-crossing polygon in dimensional regularisation at leading order divergences in ϵ [8]

$$\mathcal{R}^{(2)} = \frac{1}{8\epsilon^2}\left(-\log C_1 \log C_2 - 2\gamma_{11}^{(2)} + \Gamma_{\mathrm{cusp}}^{(2)}\right) . \tag{7.24}$$

7.3 On 3-loop divergences

The following analysis extends our work in [27]. We start to evaluate (5.18) at three loops with the abbreviations (5.13) and (5.14) and copy eq. (6.23)

$$\mathrm{MS}\Big[[\mathrm{BDS}]^{(3)} + \mathcal{R}^{(3)}(\mu,\epsilon,p_i) - T_1 - T_2\Big] = \int\Big(-T_3 - \Gamma_{11}^{(3)}\Big)\,\frac{\mathrm{d}\mu}{\mu}\,, \tag{7.25}$$

and again

$$T_3 := \left(\Gamma_{12}\,\frac{\mathcal{W}_2^{\mathrm{ren}}}{\mathcal{W}_1^{\mathrm{ren}}}\right)^{(3)} . \tag{7.26}$$

As the BDS structure only contributes at most at $\mathcal{O}(\log^2\mu^2)$ at all loop orders we have

$$\mathrm{MS}\Big[[\mathrm{BDS}]^{(3)}\Big] \approx 0\,. \tag{7.27}$$

We start evaluating the T-terms term by term.

Evaluating T_1

Copying from eq. (5.13), we have

$$T_1 = \mathcal{Z}_{12}^{(1)}\left(\frac{1}{2}\left(\mathcal{W}_1^{\mathrm{ren}(1)} - \mathcal{W}_2^{\mathrm{ren}(1)}\right)^2 - \log\mathcal{W}_1^{\mathrm{ren}(2)} + \log\mathcal{W}_2^{\mathrm{ren}(2)}\right) . \tag{7.28}$$

It will prove useful to calculate $\mathrm{MS}\Big[\,\Big(\log\mathcal{W}_1^{\mathrm{ren}(2)} - \log\mathcal{W}_2^{\mathrm{ren}(2)}\Big)\,\Big]$ at leading order in $\log\mu^2$ for all orders in ϵ. Spelling this out explicitly, we have

$$\begin{aligned}&\mathrm{MS}\Big[\,\Big(\log\mathcal{W}_1^{\mathrm{ren}(2)} - \log\mathcal{W}_2^{\mathrm{ren}(2)}\Big)\,\Big] = \\ &\mathrm{MS}\Big[\,\Big([\mathrm{BDS}]_1^{(2)} + \mathcal{R}^{(2)} + \mathcal{Z}_{12}^{(1)}\Big(\log\mathcal{W}_1^{\mathrm{ren}(1)} - \log\mathcal{W}_2^{\mathrm{ren}(1)}\Big) - [\mathrm{BDS}]_2^{(2)}\Big)\,\Big]\,.\end{aligned} \tag{7.29}$$

[8] In [27] we used the cross ratio $1/C_1$ for the result. This results in a different sign for the product of the logarithms of cross ratios.

We can copy $\mathcal{Z}_{12}^{(1)}\left(\log\mathcal{W}_1^{\text{ren}(1)}-\log\mathcal{W}_2^{\text{ren}(1)}\right)$ from eq.(7.18) from the previous section. The remainder function can be taken from the previous section, as well.

$$\text{MS}\Big[\mathcal{R}^{(2)}\Big]=\frac{\left(1-(\mu^2)^{2\epsilon}+2\epsilon\log(\mu^2)\right)}{8\epsilon^2}\left(\log C_1\log C_2+2\gamma_{11}^{(2)}-\Gamma_{\text{cusp}}^{(2)}\right) \tag{7.30}$$

The difference of the BDS terms only contributes sub-leading

$$\text{MS}\Big[\left([\text{BDS}]_1^{(2)}-[\text{BDS}]_2^{(2)}\right)\Big]\propto\log C_1\log\mu^2\approx 0\ . \tag{7.31}$$

Putting everything together, we find for $\epsilon\to 0$

$$\text{MS}\Big[T_1\Big]=-\frac{1}{48}\log C_2\left(3\log C_1\log C_2+3\log^2 C_1+8\gamma_{11}^{(2)}-4\Gamma_{\text{cusp}}^{(2)}\right)\log^3\mu^2\ . \tag{7.32}$$

Evaluating T_2

Copying from eq. (5.14), we have

$$T_2=\left(\left(\mathcal{Z}_{12}^{(1)}\right)^2+\mathcal{Z}_{12}^{(1)}\mathcal{Z}_{11}^{(1)}-\mathcal{Z}_{12}^{(2)}\right)\left(\mathcal{W}_1^{\text{ren}(1)}-\mathcal{W}_2^{\text{ren}(1)}\right)\ . \tag{7.33}$$

The combination of $\mathcal{Z}$-factors can be computed

$$\begin{aligned}&\left(\left(\mathcal{Z}_{12}^{(1)}\right)^2+\mathcal{Z}_{12}^{(1)}\mathcal{Z}_{11}^{(1)}-\mathcal{Z}_{12}^{(2)}\right)\\&\qquad=\frac{\Gamma_{12}^{(1)}\left(\gamma_{11}^{(1)}-\gamma_{22}^{(1)}\right)}{8\epsilon^3}+\frac{\Gamma_{12}^{(1)}\left(2\Gamma_{12}^{(1)}+\Gamma_{11}^{(1)}-\Gamma_{22}^{(1)}\right)}{8\epsilon^2}+\frac{\Gamma_{12}^{(2)}}{4\epsilon}\\&\qquad=\frac{\log C_2\left(\log C_2+\log C_1\right)}{8\epsilon^2}+\frac{\Gamma_{12}^{(2)}}{4\epsilon}\ .\end{aligned} \tag{7.34}$$

The second term can be discarded here. Recalling eq. (7.17), we find

$$\text{MS}\Big[T_2\Big]=-\frac{\log C_1\log C_2\left(\log C_2+\log C_1\right)}{96}\log^3\mu^2\ . \tag{7.35}$$

Evaluating T_3

We have to calculate

$$T_3\ =\ \Gamma_{12}^{(1)}\left(\frac{\mathcal{W}_2^{\text{ren}}}{\mathcal{W}_1^{\text{ren}}}\right)^{(2)}+\Gamma_{12}^{(2)}\left(\frac{\mathcal{W}_2^{\text{ren}}}{\mathcal{W}_1^{\text{ren}}}\right)^{(1)}+\ \Gamma_{12}^{(3)}\ . \tag{7.36}$$

From previous sections we know that $\Gamma^{(2)}_{12}\left(\frac{\mathcal{W}_2^{\text{ren}}}{\mathcal{W}_1^{\text{ren}}}\right)^{(1)}$ contributes at $\mathcal{O}(\log\mu^2)$. Although we have to perform a $\mathrm{d}\log\mu$ integration, these terms will be subleading (as well as terms coming from $\Gamma^{(3)}_{12}$). Thus, we have

$$\left(\frac{\mathcal{W}_2^{\text{ren}}}{\mathcal{W}_1^{\text{ren}}}\right)^{(2)} = \log\mathcal{W}_2^{\text{ren}(2)} - \log\mathcal{W}_1^{\text{ren}(2)} + \frac{1}{2}\left(\mathcal{W}_1^{\text{ren}(1)} - \mathcal{W}_1^{\text{ren}(1)}\right)^2 \ . \quad (7.37)$$

Using the expressions and taking $\epsilon \to 0$, we find

$$\text{MS}\Big[T_3\Big] = \frac{1}{8}\log C_2\left(\log C_1(\log C_1 + \log C_2) + 4\gamma^{(2)}_{11} - 2\Gamma^{(2)}_{\text{cusp}}\right)\log^2\mu^2 \quad (7.38)$$

Calculating the Integral

$$-\int\frac{\mathrm{d}\mu}{\mu}T_3 = -\frac{1}{48}\log C_2\left(\log C_1(\log C_1 + \log C_2) + 4\gamma^{(2)}_{11} - 2\Gamma^{(2)}_{\text{cusp}}\right)\log^3\mu^2 \quad (7.39)$$

we find for the three loop remainder

$$\begin{aligned}\mathcal{R}^{(3)} &= T_1 + T_2 - \int\frac{\mathrm{d}\mu}{\mu}T_3 \quad (7.40)\\ &= -\frac{1}{32}\log C_2\left(3\log C_1(\log C_1 + \log C_2) + 8\gamma^{(2)}_{11} - 4\Gamma^{(2)}_{\text{cusp}}\right)\log^3\mu^2 \ .\end{aligned}$$

The "bare" remainder function then has the leading divergence

$$\mathcal{R}^{(3)} = -\frac{\log C_2}{144\epsilon^3}\left(3\log C_1(\log C_1 + \log C_2) + 8\gamma^{(2)}_{11} - 4\Gamma^{(2)}_{\text{cusp}}\right) \ . \quad (7.41)$$

7.4 On 4-loop divergences

At order $\mathcal{O}(a^4)$ the renormalisation group equation to examine reads

$$\log \mathcal{W}_1^{\mathrm{ren}(4)} = -\int \frac{\mathrm{d}\mu}{\mu} \left(\Gamma_{12} \frac{\mathcal{W}_2^{\mathrm{ren}}}{\mathcal{W}_1^{\mathrm{ren}}} \right)^{(4)} \quad . \tag{7.42}$$

The expansion of $\log \mathcal{W}_1^{\mathrm{ren}}$ at order $\mathcal{O}(a^4)$ yields

$$\begin{aligned}
&\log \mathcal{W}_1^{\mathrm{ren}(4)} \\
&= \mathrm{MS}\Big[\log \mathcal{W}_1^{(4)} - \left(\mathcal{W}_1^{\mathrm{ren}(1)} - \mathcal{W}_2^{\mathrm{ren}(1)} \right) \left((\mathcal{Z}_{11}^{(1)})^2 \mathcal{Z}_{12}^{(1)} - \mathcal{Z}_{11}^{(2)} \mathcal{Z}_{12}^{(1)} + 2\mathcal{Z}_{11}^{(1)} (\mathcal{Z}_{12}^{(1)})^2 \right. \\
&\left. + (\mathcal{Z}_{12}^{(1)})^3 - \mathcal{Z}_{11}^{(1)} \mathcal{Z}_{12}^{(2)} - 2\mathcal{Z}_{12}^{(1)} \mathcal{Z}_{12}^{(2)} + \mathcal{Z}_{12}^{(3)} \right) \\
&- \left(\log \mathcal{W}_1^{\mathrm{ren}(3)} - \log \mathcal{W}_2^{\mathrm{ren}(3)} \right) \mathcal{Z}_{12}^{(1)} \\
&+ \left(\mathcal{Z}_{11}^{(1)} \mathcal{Z}_{12}^{(1)} + (\mathcal{Z}_{12}^{(1)})^2 - \mathcal{Z}_{12}^{(2)} \right) \left(\log \mathcal{W}_1^{\mathrm{ren}(2)} - \log \mathcal{W}_2^{\mathrm{ren}(2)} \right) \\
&+ \left(\mathcal{W}_1^{\mathrm{ren}(1)} - \mathcal{W}_2^{\mathrm{ren}(1)} \right) \left(\log \mathcal{W}_1^{\mathrm{ren}(2)} - \log \mathcal{W}_2^{\mathrm{ren}(2)} \right) \mathcal{Z}_{12}^{(1)} \\
&- \frac{1}{2} \left(\mathcal{W}_1^{\mathrm{ren}(1)} - \mathcal{W}_2^{\mathrm{ren}(1)} \right)^2 \left(\mathcal{Z}_{11}^{(1)} \mathcal{Z}_{12}^{(1)} + 2(\mathcal{Z}_{12}^{(1)})^2 - \mathcal{Z}_{12}^{(2)} \right) - \frac{1}{6} \left(\mathcal{W}_1^{\mathrm{ren}(1)} - \mathcal{W}_2^{\mathrm{ren}(1)} \right)^3 \mathcal{Z}_{12}^{(1)} \Big] \, .
\end{aligned} \tag{7.43}$$

We will neglect all terms that do not contribute to $\mathcal{O}(\log^4 \mu^2)$. We will calculate this expression term by term.

2nd-3rd line of eq. (7.43)

The first term to evaluate is the large combination of $\mathcal{Z}$-factors

$$\begin{aligned}
&\left((\mathcal{Z}_{11}^{(1)})^2 \mathcal{Z}_{12}^{(1)} - \mathcal{Z}_{11}^{(2)} \mathcal{Z}_{12}^{(1)} + 2\mathcal{Z}_{11}^{(1)} (\mathcal{Z}_{12}^{(1)})^2 + (\mathcal{Z}_{12}^{(1)})^3 - \mathcal{Z}_{11}^{(1)} \mathcal{Z}_{12}^{(2)} - 2\mathcal{Z}_{12}^{(1)} \mathcal{Z}_{12}^{(2)} + \mathcal{Z}_{12}^{(3)} \right) \\
&= -\frac{\log C_2 \left(3 \left(4 \log C_1 \log C_2 + \log^2 C_1 + \log^2 C_2 \right) + 8(\gamma_{11}^{(2)} - \gamma_{22}^{(2)}) \right)}{144\epsilon^3} \\
&+ \frac{\left(\log(-s_{\hat{k}-1,\hat{l}+1}\mu^2) + \log(-s_{\hat{l}-1,\hat{k}+1}\mu^2) \right) \left(2 \log C_2 \gamma_{22}^{(2)} + \Gamma_{12}^{(2)} \right) - 6 \log C_2 \Gamma_{12}^{(2)}}{24\epsilon^2} \\
&- \frac{\left(\log(-s_{\hat{k}-1,\hat{k}+1}\mu^2) + \log(-s_{\hat{l}-1,\hat{l}+1}\mu^2) \right) \left(2 \log C_2 \gamma_{11}^{(2)} + \Gamma_{12}^{(2)} \right)}{24\epsilon^2} - \frac{\Gamma_{12}^{(3)}}{6\epsilon} \, .
\end{aligned} \tag{7.44}$$

This is a remarkable simplification for this long combination of $\mathcal{Z}$-factors. Naively, the long combination also has terms contributing to $\frac{1}{\epsilon^5}$ and also to $\frac{1}{\epsilon^4}$. Those divergent parts cancel out exactly. Again, all dependence on the total number of cusps as well as the dependence on Mandelstam variables

associated to cusps away from the crossing cancels out, also. The term $\mathcal{Z}_{12}^{(3)}$ can be calculated using eq. (7.12). However, we do not spell out this large term explicitly. The part that is responsible for leading order divergences in $\mathcal{R}^{(4)}$ reads

$$(\mathcal{Z}\text{-factors}) = -\frac{\log C_2 \left(3\left(4\log C_1 \log C_2 + \log^2 C_1 + \log^2 C_2\right) + 8(\gamma_{11}^{(2)} - \gamma_{22}^{(2)})\right)}{144\epsilon^3} - \frac{\log C_2 \left(\gamma_{11}^{(2)} - \gamma_{22}^{(2)}\right)\log\mu^2}{6\epsilon^2} \ . \tag{7.45}$$

Together with the expression eq. (7.17) we find for $\epsilon \to 0$

$$-\left(\mathcal{W}_1^{\text{ren}(1)} - \mathcal{W}_2^{\text{ren}(1)}\right)(\mathcal{Z}\text{-factors}) = \tag{7.46}$$
$$-\frac{\log C_1 \log C_2 \left(3\left(4\log C_1 \log C_2 + \log^2 C_1 + \log^2 C_2\right) + 104\left(\gamma_{11}^{(2)} - \gamma_{22}^{(2)}\right)\right)}{6912}\log^4\mu^2 \ .$$

4th line of eq. (7.43)

We analyse $\left(\log \mathcal{W}_1^{\text{ren}(3)} - \log \mathcal{W}_2^{\text{ren}(3)}\right)\mathcal{Z}_{12}^{(1)}$ now.

$$\left(\log \mathcal{W}_1^{\text{ren}(3)} - \log \mathcal{W}_2^{\text{ren}(3)}\right) = \text{MS}\Big[\left([\text{BDS}]_1^{(3)} - [\text{BDS}]_2^{(3)}\right) + \mathcal{R}^{(3)} \tag{7.47}$$
$$-\mathcal{Z}_{12}^{(1)}\left(\frac{1}{2}\left(\mathcal{W}_1^{\text{ren}(1)} - \mathcal{W}_2^{\text{ren}(1)}\right)^2 - \log \mathcal{W}_1^{\text{ren}(2)} + \log \mathcal{W}_2^{\text{ren}(2)}\right)$$
$$-\left(\left(\mathcal{Z}_{12}^{(1)}\right)^2 + \mathcal{Z}_{12}^{(1)}\mathcal{Z}_{11}^{(1)} - \mathcal{Z}_{12}^{(2)}\right)\left(\mathcal{W}_1^{\text{ren}(1)} - \mathcal{W}_2^{\text{ren}(1)}\right)\Big]$$

The difference of the BDS terms does not contribute to the order in $\mathcal{O}(\log^4\mu^2)$ that we are calculating. The three loop remainder contributes at $\mathcal{O}(\epsilon)$ with

$$\mathcal{R}^{(3)} = -\frac{3}{128}\epsilon \log C_2 \left(3\log C_1 \log C_2 + 3\log^2 C_1 + 8\gamma_{11}^{(2)} - 4\Gamma_{\text{cusp}}^{(2)}\right)\log^4\mu^2 \ . \tag{7.48}$$

The other terms have already been calculated earlier. Altogether we find for this contribution

$$-\left(\log \mathcal{W}_1^{\text{ren}(3)} - \log \mathcal{W}_2^{\text{ren}(3)}\right)\mathcal{Z}_{12}^{(1)} = \tag{7.49}$$
$$-\frac{1}{192}\log^2 C_2 \left(3\log C_1 \log C_2 + 3\log^2 C_1 + 10\gamma_{11}^{(2)} - 5\Gamma_{\text{cusp}}^{(2)}\right)\log^4\mu^2 \ .$$

5th line of eq. (7.43)

Up to now, we have calculated everything in order to evaluate

$$\mathrm{MS}\Big[\left(\mathcal{Z}_{11}^{(1)}\mathcal{Z}_{12}^{(1)}+(\mathcal{Z}_{12}^{(1)})^2-\mathcal{Z}_{12}^{(2)}\right)\left(\log\mathcal{W}_1^{\mathrm{ren}(2)}-\log\mathcal{W}_2^{\mathrm{ren}(2)}\right)\Big]$$

and consequently find for $\epsilon\to 0$

$$\begin{aligned}&\mathrm{MS}\Big[\left(\mathcal{Z}_{11}^{(1)}\mathcal{Z}_{12}^{(1)}+(\mathcal{Z}_{12}^{(1)})^2-\mathcal{Z}_{12}^{(2)}\right)\left(\log\mathcal{W}_1^{\mathrm{ren}(2)}-\log\mathcal{W}_2^{\mathrm{ren}(2)}\right)\Big]= \qquad (7.50)\\ &-\frac{1}{768}\log C_2\left(\log C_1+\log C_2\right)\left(7\log C_1\log C_2+16\gamma_{11}^{(2)}-8\Gamma_{\mathrm{cusp}}^{(2)}\right)\log^4\mu^2\ .\end{aligned}$$

6th line of eq. (7.43)

In the limit $\epsilon\to 0$ we find for the sixth line

$$\begin{aligned}&\mathrm{MS}\Big[\left(\mathcal{W}_1^{\mathrm{ren}(1)}-\mathcal{W}_2^{\mathrm{ren}(1)}\right)\left(\log\mathcal{W}_1^{\mathrm{ren}(2)}-\log\mathcal{W}_2^{\mathrm{ren}(2)}\right)\mathcal{Z}_{12}^{(1)}\Big]= \qquad (7.51)\\ &-\frac{1}{192}\log C_1\log C_2\left(9\log C_1\log C_2+28\gamma_{11}^{(2)}-14\Gamma_{\mathrm{cusp}}^{(2)}\right)\log^4\mu^2\ .\end{aligned}$$

7th line of eq. (7.43)

Here we encounter a new combination of $\mathcal{Z}$-factors. this combination reads

$$\left(\mathcal{Z}_{11}^{(1)}\mathcal{Z}_{12}^{(1)}+2(\mathcal{Z}_{12}^{(1)})^2-\mathcal{Z}_{12}^{(2)}\right)=\frac{\log C_2\left(3\log C_2+\log C_1\right)}{8\epsilon^2}+\frac{\Gamma_{12}^{(2)}}{4\epsilon} \qquad (7.52)$$

Then, in the limit $\epsilon\to 0$, the last line becomes

$$\begin{aligned}&\mathrm{MS}\Big[-\frac{1}{2}\left(\mathcal{W}_1^{\mathrm{ren}(1)}-\mathcal{W}_2^{\mathrm{ren}(1)}\right)^2\left(\mathcal{Z}_{11}^{(1)}\mathcal{Z}_{12}^{(1)}+2(\mathcal{Z}_{12}^{(1)})^2-\mathcal{Z}_{12}^{(2)}\right)\\ &\quad-\frac{1}{6}\left(\mathcal{W}_1^{\mathrm{ren}(1)}-\mathcal{W}_2^{\mathrm{ren}(1)}\right)^3\mathcal{Z}_{12}^{(1)}\Big]=\\ &\quad-\frac{1}{768}\log^2 C_1\log C_2\left(19\log C_1+21\log C_2\right)\log^4\mu^2\ . \qquad (7.53)\end{aligned}$$

Putting it together, the equation (7.43) reads

$$\begin{aligned}\log\mathcal{W}_1^{\mathrm{ren}(4)}&=\mathrm{MS}\Big[\mathcal{R}^{(4)}\Big] \qquad (7.54)\\ &-\frac{\log C_2\log^4\mu^2}{3456}\Big(87\log C_1\left(4\log C_1\log C_2+\log^2 C_1+\log^2 C_2\right)\\ &+52\log C_1(\gamma_{11}^{(2)}-\gamma_{22}^{(2)})+(288\log C_1+126\log C_2)(2\gamma_{11}^{(2)}-\Gamma_{\mathrm{cusp}}^{(2)})\Big)\ .\end{aligned}$$

r.h.s.. of eq. (7.42)

By expansion we find that

$$\begin{aligned}\left(\frac{\mathcal{W}_2^{\text{ren}}}{\mathcal{W}_1^{\text{ren}}}\right)^{(3)} &= \left(\log \mathcal{W}_2^{\text{ren}(3)} - \log \mathcal{W}_1^{\text{ren}(3)}\right) \\ &- \left(\log \mathcal{W}_2^{\text{ren}(2)} - \log \mathcal{W}_1^{\text{ren}(2)}\right)\left(\mathcal{W}_1^{\text{ren}(1)} - \mathcal{W}_2^{\text{ren}(1)}\right) \\ &- \frac{1}{6}\left(\mathcal{W}_1^{\text{ren}(1)} - \mathcal{W}_2^{\text{ren}(1)}\right)^3 \ .\end{aligned} \tag{7.55}$$

We need this expression up to $\mathcal{O}(\log^3 \mu^2)$. Thus the relevant terms are

$$\begin{aligned}-\Gamma_{12}^{(1)}\left(\frac{\mathcal{W}_2^{\text{ren}}}{\mathcal{W}_1^{\text{ren}}}\right)^{(3)} = -\frac{1}{48}\log C_2\Big(&\log C_1\left(12\gamma_{11}^{(2)} + \log^2 C_2 - 6\Gamma_{\text{cusp}}^{(2)}\right) \\ &+ 4\log^2 C_1 \log C_2 + \log^3 C_1 + 2(2\gamma_{11}^{(2)} - \Gamma_{\text{cusp}}^{(2)})\log C_2\Big)\log^3 \mu^2 \ .\end{aligned} \tag{7.56}$$

Performing the $\mathrm{d}\log\mu$ integration and putting everything together, we find for the remainder function

$$\begin{aligned}\text{MS}[\mathcal{R}^{(4)}] =& \frac{\log C_2}{1726}\Big(26\log C_1(\gamma_{11}^{(2)} - \gamma_{22}^{(2)}) + (2\gamma_{11}^{(2)} - \Gamma_{\text{cusp}}^{(2)})\,(117\log C_1 + 54\log C_2) \\ &+ 39\log C_1\left(4\log C_1\log C_2 + \log^2 C_1 + \log^2 C_2\right)\Big)\log^4 \mu^2\end{aligned} \tag{7.57}$$

7.5 implications for $\mathcal{R}_8$

As an example, we now focus on the octagon and chose $\hat{k} = 1$ and $\hat{l} = 5$, see fig. 15. Following the logic of the section 6.4 , we introduce a geometrical regularisation. The configuration of an octagon (in every dimension) can be described using at most 12 conformally invariant cross ratios. In four dimensions there are only 9 independent cross ratios due to Gram constraints. So far it has not been possible to disentangle these relations for four dimensions. So we use the usual choice for the 12 conformal cross ratios

$$u_{ij} = \frac{(x_i - x_{j+1})^2(x_{i+1} - x_j)^2}{(x_i - x_j)^2(x_{i+1} - x_{j+1})^2} \ . \tag{7.58}$$

Let us look at these cross ratios in the limit $x_1 = x_5 + \delta\ v, \quad \delta \to 0$, when the loop becomes self-intersecting. We want to express a divergence in δ as a divergence in terms of conformal invariants. This relation will also

contain Mandelstam variables (which are not conformally invariant) because distances are also not conformally invariant.

In the aforementioned limit we encounter three classes of cross ratios. The ratios $u_{26}, u_{27}, u_{36}, u_{37}$ are not affected by this limit and remain untouched. Four cross ratios $u_{14}, u_{15}, u_{48}, u_{58}$ remain finite (in the general case) but depend on the direction v. For example, we find

$$u_{14} \;=\; \frac{v^2(x_2-x_4)^2}{4vp_4 \;\; vp_1} \;. \tag{7.59}$$

The last class diverges as we approach the crossing situation $u_{16}, u_{25}, u_{38}, u_{47}$, e.g.

$$u_{16} \;=\; -\frac{1}{\delta}\,\frac{(x_2-x_6)^2(x_1-x_7)^2}{2vp_5 \;\; (x_2-x_7)^2} \;. \tag{7.60}$$

We can eliminate the dependence on the direction of v by considering combinations of various u_{kl} and find the relation

$$2\log\delta^2 = -\log\left(u_{47}u_{38}u_{25}u_{16}\right) + \log\left(\frac{s_{48}s_{57}s_{13}s_{26}s_{35}s_{17}}{s_{47}s_{38}s_{36}s_{27}\;\; v^4}\right) - \log(u_{15}u_{48}) \tag{7.61}$$

for the crossing limit. The first term on the r.h.s. of (7.61) is conformally invariant and becomes divergent in the limit. The other two terms stay finite and balance the conformal non-invariance of the l.h.s..

7.5.1 Implications for $\mathcal{R}_8^{(2)}$

We use the abbreviation

$$u := u_{47}u_{38}u_{25}u_{16} \;. \tag{7.62}$$

From eq. (7.24) together with the translation factor of $\alpha = 1$ (i.e. $1/\epsilon^2 \Leftrightarrow \log^2\delta^2$) from the appendix 8.11

$$\mathcal{R}_8^{(2)} = \frac{1}{32}\log^2 u\,\Big(-\log C_1\log C_2 - 2\gamma_{11}^{(2)} + \Gamma_{\text{cusp}}^{(2)}\Big) \;+\; \mathcal{O}(\log u) \tag{7.63}$$

for $x_1 \to x_5$. This is valid as long as the vector v defining the direction of the approach is not light-like and has a non-zero scalar product with p_1, p_4, p_5, p_8.

7.5.2 Implications for $\mathcal{R}_8^{(3)}$

As we do not rely on the translation rule from appendix 8.11 beyond two loops, we give no overall pre-factor. Together with eq. (7.41) the three-loop result is expected to have the structure

$$\mathcal{R}_8^{(3)} \propto \log C_2\left(3\log C_1(\log C_1 + \log C_2) + 8\gamma_{11}^{(2)} - 4\Gamma_{\text{cusp}}^{(2)}\right)\log^3 u \;. \tag{7.64}$$

7.5.3 Implications for $\mathcal{R}_8^{(4)}$

Using eq. (7.57), we find for the four-loop octagon remainder function

$$\begin{aligned}\mathcal{R}_8^{(4)} \propto \log C_2 \Big(& 26 \log C_1 (\gamma_{11}^{(2)} - \gamma_{22}^{(2)}) + (2\gamma_{11}^{(2)} - \Gamma_{\text{cusp}}^{(2)}) (117 \log C_1 + 54 \log C_2) \\ & + 39 \log C_1 \left(4 \log C_1 \log C_2 + \log^2 C_1 + \log^2 C_2\right) \Big) \log^4 u \ . \end{aligned} \tag{7.65}$$

7.6 Conclusions and discussion

In the last section we have discussed the self-crossing polygonal light-like Wilson loop in $\mathcal{N} = 4$ sYM with a crossing at two vertices in order to extract the divergent terms in the self-crossing case. We have restricted ourselves to the leading singularities. Up to four loops the results have the general structure

$$\mathcal{R}_8^{(l)} = \log C_2 \mathrm{Pol}^{(l-1)} \left(\log C_1, \log C_2, (\gamma_{11}^{(2)} - \gamma_{22}^{(2)}), (2\gamma_{11}^{(2)} - \Gamma_{\mathrm{cusp}}^{(2)}) \right) \log^{(l)}(u) \ . \tag{7.66}$$

C_1 and C_2 are two conformal invariants that characterise the crossing, see eq. (7.1). By $\mathrm{Pol}^{(l-1)}(.)$ we denote a polynomial of degree $(l-1)$ in the given variables. $\gamma_{11}^{(2)}$ and $\gamma_{22}^{(2)}$ are numbers that appear in our Ansatz for the crossing anomalous dimension matrix, see eq. (7.3). The combinations $(\gamma_{11}^{(2)} - \gamma_{22}^{(2)})$ and $(2\gamma_{11}^{(2)} - \Gamma_{\mathrm{cusp}}^{(2)})$ have to be determined in a two-loop calculation. The analogous one-loop terms $(\gamma_{11}^{(1)} - \gamma_{22}^{(1)})$ and $(2\gamma_{11}^{(1)} - \Gamma_{\mathrm{cusp}}^{(1)})$ vanish.

The $\log^{(l)} u$ terms are responsible for the divergences when approaching the self-crossing configuration. If one is interested in Wilson loops with more cusps $n > 8$, the results can be reused. $\log^{(l)} u$ will then be replaced by $\log^{(l)} f(\{u\})$ with a different function of the cross ratios, which has to be determined in a kinematic calculation.

The results are also compatible with divergences of the remainder of the self-crossing hexagon. Looking at the collinear limit

$$p_l \cdot p_{l-1} \ , \quad p_k \cdot p_{k-1} \to 0 \tag{7.67}$$

the term $\log C_1$ will become divergent. These additional divergences add up to give the correct degree of the leading divergence for the remainder of a self-crossing hexagon.

Contrary to the crossing between two vertices, the leading divergences are *not* determined just by one-loop information. We expect that at higher loops also three-loop coefficients of the crossing anomalous dimension matrix (7.3) will become important. Naively, the large combination of $\mathcal{Z}$-factors in eq. (7.44) contains poles up to $\frac{1}{\epsilon^5}$. For the leading divergence of the remainder, the $\frac{1}{\epsilon^3}$ term is important and higher terms have to cancel. It can be expected that calculating at higher loops more and more terms in these combinations of $\mathcal{Z}$-factors have to cancel. This cancellation does not appear for a crossing between two edges. Therefore, we expect that at some point also higher loop information of the crossing matrix will enter the relevant terms in the $\mathcal{Z}$-combinations.

Another important difference is, that the arising divergences are not related to a discontinuity of the remainder in the Euclidean regime. The results are real and already have the correct weight $2l$.

The remainder function of the self-crossing octagon is known for the special kinematical case, in which the Wilson loop can be embedded in a two dimensional Minkowski space, [25]. In this case there are only two independent cross ratios that characterise the polygon. The authors use the parameters χ^- and χ^+ to characterise the cross ratios. In these special kinematics the complete octagon remainder reads

$$\mathcal{R}_8^{(2),\mathbb{R}^{1,1}}(\chi^-,\chi^+) = \tag{7.68}$$
$$-\frac{\pi^4}{18} - \frac{1}{2}\log\left(1+\chi^+\right)\log\left(1+\frac{1}{\chi^+}\right)\log\left(1+\chi^-\right)\log\left(1+\frac{1}{\chi^-}\right) \ .$$

However, the kinematical region does not involve self-crossing octagons. Equivalently, this kinematic region leads to $\log u = 0$.

Part III
Appendices

8 Appendix

8.1 Conformal symmetry and conformal invariants

Conformal symmetry is an extension of Poincaré symmetry. Let (M, g) be a Lorentzian Manifold (usually $M = \mathbb{R}^{1,3}$ and g =diag$(1, -1, -1, -1)$). A map $h : M \to M$ is a conformal map iff $h^*g = e^\alpha g$, where α is a real scalar function on M. Thus, conformal maps "preserve angles" as $g(V,W)/\sqrt{g(V,V)g(W,W)}$ remains untouched. Those conformal maps form a group, where the group product is given as the composition of maps.

Suppose M is the $d > 2$ dimensional conformally compactified Minkowski space, this group is finite dimensional and isomorphic to $\mathrm{SO}(2, d)$. It is generated by d translations P^μ, d special conformal transformations K^μ, $(d-1)$ Lorentz boosts and $(d-1)(d-2)/2$ rotations $M^{\mu\nu}$ and one dilatation D. The generators P^μ and $M^{\mu\nu}$ form a Poincaré algebra and thus

$$\begin{aligned}
&[P^\mu, P^\nu] = 0 \quad , \quad [M^{\mu\nu}, P^\rho] = i(\eta^{\nu\rho}P^\mu - \eta^{\mu\rho}P^\nu) \\
&[M^{\mu\nu}, M^{\rho\sigma}] = i(\eta^{\mu\rho}M^{\nu\sigma} + \eta^{\nu\sigma}M^{\mu\rho} - \eta^{\nu\rho}M^{\mu\sigma} - \eta^{\mu\sigma}M^{\nu\rho}) \quad .
\end{aligned}$$

Additionally to the Poincaré algebra the other generators obey

$$\begin{aligned}
&[D, P^\mu] = iP^\mu \quad , \quad [M^{\mu\nu}, K^\rho] = i(\eta^{\rho\nu}K^\mu - \eta^{\rho\mu}K^\nu) \quad , \\
&[K^\mu, D] = iK^\mu \quad , \quad [K^\mu, P^\nu] = 2i(\eta^{\mu\nu}D - M^{\mu\nu}) \; .
\end{aligned}$$

In the case of $d = 4$ the algebra is $\mathfrak{so}(2,4) \simeq \mathfrak{su}(2,2)$ which has 15 generators. Finite transformations act as

$$\begin{aligned}
\text{translations} &: x'^\mu = x^\mu - a^\mu \quad , \\
\text{Lorentz} &: x'^\mu = L^\mu{}_\nu x^\nu \quad , \quad L^\mu{}_\nu \in \mathrm{SO}_\uparrow(1,3) \quad , \\
\text{dilatation} &: x'^\mu = ax^\mu \quad , \quad a > 0 \quad , \\
\text{special conformal transformation} &: x'^\mu = \frac{x^\mu - b^\mu x^2}{1 - 2bx + b^2x^2} \quad ,
\end{aligned} \tag{8.1}$$

where $x^2 = x^\mu x_\mu$ and $bx = b^\mu x_\mu$. Using the inversion at the unit sphere

$$Ix^\mu := \frac{x^\mu}{x^2} \tag{8.2}$$

it is easy to verify that one can write the special conformal transformations as a composition of an inversion, a translation and another inversion.

Finally we show that the cross ratio

$$\frac{x_{12}^2 x_{34}^2}{x_{13}^2 x_{24}^2} = \frac{(x_1 - x_2)^2 (x_3 - x_4)^2}{(x_1 - x_3)^2 (x_2 - x_4)^2} \tag{8.3}$$

formed out of four arbitrary points is invariant under conformal transformations. The only non-trivial check has to be done for the special conformal transformations. Under inversion at the unit sphere

$$x_{ij}^2 \xrightarrow{I} \frac{x_{ij}^2}{x_i^2 x_j^2} \ , \tag{8.4}$$

which shows that the cross ratios are conformally invariant.

8.2 Dirac construction

Here follow [36, 37] and show how the finite transformations (8.1) in Minkowski space can be related to the fundamental representation of the conformal group $\mathrm{SO}_\uparrow(2,4)$. $\mathrm{SO}_\uparrow(2,4)$ acts on $\mathbb{R}^{(2,4)}$. We consider the cone in $\mathbb{R}^{(2,4)}$ which is defined via

$$W^i W_i = W_{0'}^2 + W_0^2 - W_1^2 - W_2^2 - W_3^2 - W_4^2 = 0 \ . \tag{8.5}$$

Now we consider the equivalence classes given by $W \sim \lambda W \ , \ \ \lambda \in \mathbb{R}$. Then the map between $[W]$ and four dimensional Minkowski space x^μ is

$$\begin{aligned} W^\mu &= \lambda \ x^\mu, \quad \mu = 0,1,2,3 \ , \\ W^{0'} &= \frac{1}{2}\lambda \ (1 - x^\mu x_\mu), \qquad W^4 \ = \ \frac{1}{2}\lambda \ (1 + x^\mu x_\mu) \end{aligned} \tag{8.6}$$

and the inverse

$$x^\mu \ = \ \frac{W^\mu}{W^{0'} + W^4} \ . \tag{8.7}$$

It is obvious that points on the cone that obey $W^{0'} + W^4 = 0$ correspond to conformal infinity. In [37] the authors decompose the fundamental representations of $\mathrm{SO}_\uparrow(2,4)$ relate it to the usual representation in Minkowski space using the map (8.6) and (8.7). Using a map from Minkowski space to $\mathbb{R}^{(2,4)}$ with (8.6), performing a $\Lambda \in \mathrm{SO}_\uparrow(2,4)$ transformation in $\mathbb{R}^{2,4}$ and then going back to Minkowski via (8.7) they find

$$x'^\mu = \frac{\Lambda^\mu{}_\nu x^\nu + \frac{1}{2}(\Lambda^\mu{}_{0'} + \Lambda^\mu{}_4) - \frac{1}{2}(\Lambda^\mu{}_{0'} - \Lambda^\mu{}_4)x^2}{(\Lambda^{0'}{}_\nu + \Lambda^4{}_\nu)x^\nu + \frac{1}{2}(\Lambda^{0'}{}_{0'} + \Lambda^4{}_{0'} + \Lambda^{0'}{}_4 + \Lambda^4{}_4) - \frac{1}{2}(\Lambda^{0'}{}_{0'} + \Lambda^4{}_{0'} - \Lambda^{0'}{}_4 - \Lambda^4{}_4)x^2} \ . \tag{8.8}$$

Comparing this equation with (8.1) they find the following expressions. Together with $x'^\mu = x^\mu + a^\mu$ it follows

$$\underline{\text{translation}}: \ \Lambda^M{}_N \ = \ \begin{pmatrix} \mathbb{1} & a^\mu & a^\mu \\ -a_\nu & 1 - \frac{a^2}{2} & -\frac{a^2}{2} \\ a_\nu & \frac{a^2}{2} & 1 + \frac{a^2}{2} \end{pmatrix} \ , \tag{8.9}$$

where capital indices have the ordering $0, 1, 2, 3, 0', 4$ here. In a similar manner, they get $x'^\mu = \frac{x^\mu + c^\mu x^2}{1 + 2cx + c^2 x^2}$ via

$$\underline{\text{special conformal}}: \ \Lambda^M{}_N \ = \ \begin{pmatrix} \mathbb{1} & -c^\mu & c^\mu \\ c_\nu & 1 - \frac{c^2}{2} & \frac{c^2}{2} \\ c_\nu & -\frac{c^2}{2} & 1 + \frac{c^2}{2} \end{pmatrix} \ . \tag{8.10}$$

Lorentz transformations in Minkowski space correspond to

$$\underline{\text{Lorentz}}: \ \Lambda^M_{\ N} \ = \ \begin{pmatrix} \Lambda^\mu_{\ \nu} & 0 & 0 \\ 0 & 1 & 0 \\ 0 & 0 & 1 \end{pmatrix} \ , \qquad \Lambda^\mu_{\ \nu} \ \in \ \mathrm{SO}_\uparrow(1,3). \tag{8.11}$$

And finally, the dilatation $x'^\mu = e^{-\rho} x^\mu$ is realised via

$$\underline{\text{dilatation}}: \ \Lambda^M_{\ N} \ = \ \begin{pmatrix} \mathbb{1} & 0 & 0 \\ 0 & \cosh\rho & \sinh\rho \\ 0 & \sinh\rho & \cosh\rho \end{pmatrix} \ . \tag{8.12}$$

8.3 Minimal surfaces

Let $(M, g^{(M)})$ be a metric manifold with the Levi Civita connection $\nabla^{(M)}$ which is completely determined by the metric $g^{(M)}$. Now consider $N \subset M$ to be a lower dimensional sub-manifold. Then we define the induced metric on N by

$$g^{(N)}(X,Y) = g^{(M)}(X,Y) \ , \quad \forall X, Y \in \mathrm{T}N \ , \tag{8.13}$$

with $\mathrm{T}N \subset \mathrm{T}M$ being the tangent bundle of N. Then we can also define a connection (which is the Levi Civita connection) on N by setting

$$\nabla^{(N)}_Y X := \mathrm{pr}_{\mathrm{T}N}\left(\nabla^{(M)}_Y X\right) \ , \quad \forall X, Y \in \mathrm{T}N \ , \tag{8.14}$$

because generically $\nabla^{(M)}_Y X$ will not be a vector field in the tangent bundle of N. $\mathrm{pr}_{\mathrm{T}N}$ denotes the projection onto the tangent bundle of N. Using the metric on M and the embedding $N \subset M$ we also have a normal bundle of N, that we call $\mathrm{N}N$. Then we can define

$$\mathrm{II}(X,Y) := \nabla^{(M)}_X Y - \nabla^{(N)}_X Y = \mathrm{pr}_{\mathrm{N}N}\left(\nabla^{(M)}_X Y\right) \ , \quad \forall X, Y \in \mathrm{T}N \tag{8.15}$$

to be the second fundamental form of the embedding $N \subset M$. A sub-manifold N is said to be embedded minimally in M iff all second fundamental forms (for every vector field in the normal bundle) are traceless. If N is two dimensional we call N a minimal surface.

In the context of Pohlmeyer reduction of strings in $\mathrm{AdS}_3 \times \mathrm{S}^3$, we have the following chain of embeddings

$$N^2 \subset \mathrm{AdS}_3 \times \mathrm{S}^3 \subset \mathbb{R}^{(2,2)} \times \mathbb{R}^4 \ . \tag{8.16}$$

Consequently the surface N^2 has six normal vectors and thus six second fundamental forms if we are talking about $N^2 \subset \mathbb{R}^{(2,2)} \times \mathbb{R}^4$. The metrics and connections on N^2 and $\mathrm{AdS}_3 \times \mathrm{S}^3$ are induced by the flat metric and flat connection of $\mathbb{R}^{(2,2)} \times \mathbb{R}^4$. If N^2 is a minimal surface in $\mathrm{AdS}_3 \times \mathrm{S}^3$ the four second fundamental forms corresponding to this embedding are traceless. The fundamental forms for the normal directions of $\mathrm{AdS}_3 \times \mathrm{S}^3 \subset \mathbb{R}^{(2,2)} \times \mathbb{R}^4$ are not traceless.

8.4 Conformal boundary of AdS × S

Here we will give some remarks on AdS space and on the conformal boundary of $\mathrm{AdS}_5 \times \mathrm{S}^5$. AdS_n can be embedded into $\mathbb{R}^{(2,n-1)}$. If $\eta_{AB} = \mathrm{diag}\,(-1,-1,1,\ldots,1)$ is the metric we have

$$\mathrm{AdS}_n = \left\{ X^A \in \mathbb{R}^{(2,n-1)} \mid \eta_{AB} X^A X^B = -1 \right\} . \tag{8.17}$$

8.4.1 Global AdS coordinates

One can introduce global coordinates by setting

$$\begin{aligned} X^{-1} &= \cosh\tau \ \cos\alpha \ , \quad \tau \in (0,\infty) \quad , \alpha \in [0, 2\pi) \\ X^0 &= \cosh\tau \ \sin\alpha \ , \\ X^i &= \sinh\tau \ \Omega^i \ , \quad i \in \{1,\ldots,n-1\} \ , \end{aligned} \tag{8.18}$$

with Ω^i being a parametrisation of the $(n-2)$-dimensional unit sphere in $\mathbb{R}^{n-1}$. Here we observe that topologically AdS_2 and AdS_3 are special. Starting with AdS_4 the sphere parametrised by Ω^i has a trivial first fundamental group π_1. We see that AdS_n is a non-compact manifold. Assigning a conformal boundary to AdS_n involves introducing a suitable compactification. The metric will then diverge as one approaches the boundary. The compactification is said to be a conformal boundary if there exists a metric within the conformal class of the usual metric of AdS such that the new metric is non-degenerated and finite on the whole compactification. The metric of AdS_n expressed in the coordinates from eq. (8.18) reads

$$\mathrm{d}s^2 = -\cosh^2\tau \ \mathrm{d}\alpha^2 + \mathrm{d}\tau^2 + \sinh^2\tau \ \mathrm{d}\Omega^2 \ . \tag{8.19}$$

In order to map AdS_n onto an open sub-manifold of a compact space we choose

$$\sinh\tau = \tan\theta \ , \quad \cosh^2\tau = \frac{1}{\cos^2\theta} \ , \quad \mathrm{d}\tau = \frac{1}{\cos\theta}\mathrm{d}\theta \ ,$$

with $\theta \in [0, \frac{\pi}{2})$. Then the metric becomes

$$\mathrm{d}s^2 = \frac{1}{\cos^2\theta}\left(-\ \mathrm{d}\alpha^2 + \mathrm{d}\theta^2 + \sin^2\theta \ \mathrm{d}\Omega^2\right) \ . \tag{8.20}$$

We approach infinity ($\tau \to \infty$) for $\theta \to \frac{\pi}{2}$. Thus we see that changing the metric within the conformal class simply by erasing the divergent prefactor $\frac{1}{\cos^2\theta}$ leads to a well defined metric on the boundary

$$\mathrm{d}\tilde{s}^2 \ |_{\partial\mathrm{AdS}} = -\ \mathrm{d}\alpha^2 + \ \mathrm{d}\Omega^2 \ . \tag{8.21}$$

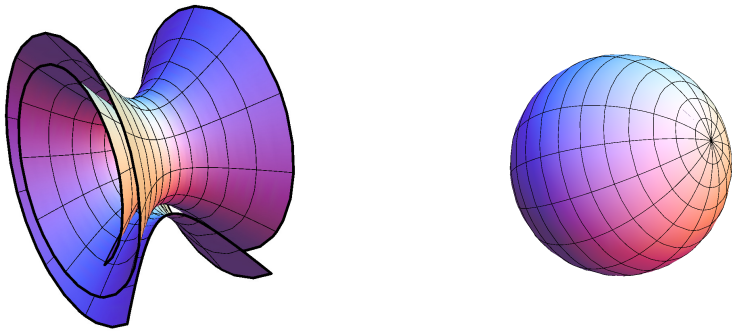

Figure 19: The $\widetilde{\mathrm{AdS}} \times \mathrm{S}$ background.

We also can read off that the conformal boundary of AdS_n is $\partial\mathrm{AdS}_n = \mathrm{S}^1 \times \mathrm{S}^{n-2}$ and for the lower dimensional case $\partial\mathrm{AdS}_2 = \mathrm{S}^1 \times \{1, -1\}$. In our notation the time coordinate is α as we can see from eq. (8.20). However, this coordinate is cyclic. As this is unphysical one can use the universal covering space of AdS_n and allow $\alpha \in \mathbb{R}$. Then also the conformal boundary will be $\partial\widetilde{\mathrm{AdS}_n} = \mathbb{R} \times \mathrm{S}^{n-2}$. If we consider $\mathrm{AdS}_5 \times \mathrm{S}^5$ the metric will be the sum

$$\mathrm{d}s^2 = \frac{1}{\cos^2\theta}\left(-\,\mathrm{d}\alpha^2 + \mathrm{d}\theta^2 + \sin^2\theta\;\mathrm{d}\Omega^2\right) \;+\; \mathrm{d}s^2_{\text{5-sphere}}\;. \tag{8.22}$$

This means that erasing the $\frac{1}{\cos^2\theta}$-factor will create a $\cos^2\theta$-factor in front of the metric of the sphere. This means that the radius of the sphere becomes $r = \cos\theta$ and shrinks to zero if we approach infinity. Thus, we still have

$$\partial\left(\widetilde{\mathrm{AdS}_5} \times \mathrm{S}^5\right) = \mathbb{R} \times \mathrm{S}^3\;.$$

8.4.2 Poincaré coordinates

For use in the AdS/CFT duality it is useful to note that one half of the AdS space can be covered with Poincaré coordinates. Using these coordinates it becomes apparent that one half of the conformal boundary is equivalent to a Minkowski space. The mapping to Poincaré coordinates is realised by

$$\begin{aligned} X^\mu &= \frac{x^\mu}{r}\;, \quad \mu \in \{0, 1, \ldots, n-2\} \\ X^{-1} + X^{n-1} &= \frac{1}{r} \\ X^{-1} - X^{n-1} &= \frac{r^2 - (x^0)^2 + (x^1)^2 + \cdots + (x^{n-2})^2}{r}\;. \end{aligned} \tag{8.23}$$

Thus, the induced metric reads

$$\mathrm{d}s^2 = \frac{1}{r^2}\left(-(\mathrm{d}x^0)^2 + (\mathrm{d}x^1)^2 + \cdots + (\mathrm{d}x^{n-1})^2 + \mathrm{d}r^2\right) \ . \tag{8.24}$$

The conformal boundary is reached by $r \to 0$ and is the standard Minkowski space. However, these Poincaré coordinates include for $r > 0$ only the upper half of the $X^{-1} + X^{n-1} = 0$ hypersurface. The other half of AdS space is realised with negative r. Those two patches are glued together at $r = \pm\infty$.

8.4.3 Minimal surfaces in lower dimensional AdS × S

As we are considering space-like minimal surfaces in $\mathrm{AdS}_3 \times \mathrm{S}^3$ in the first part of this thesis we want to comment why these surfaces are also minimal in $\mathrm{AdS}_5 \times \mathrm{S}^5$. We have the chain of embeddings

$$\mathrm{AdS}_3 \times \mathrm{S}^3 \subset \mathrm{AdS}_5 \times \mathrm{S}^5 \subset \mathbb{R}^{(2,4)} \times \mathbb{R}^6 \ . \tag{8.25}$$

One can choose four constant vector fields in the normal space of $\mathrm{AdS}_3 \times \mathrm{S}^3 \subset \mathrm{AdS}_5 \times \mathrm{S}^5$. These vector fields are then constant in $\mathbb{R}^{(2,4)} \times \mathbb{R}^6$. To calculate the corresponding second fundamental forms, we have to calculate the (ordinary) derivative of these four vector fields in $\mathbb{R}^{(2,4)} \times \mathbb{R}^6$, see eq. (8.15). If N is such a constant normal vector field, V, W are two tangential fields on $\mathrm{AdS}_3 \times \mathrm{S}^3$ and g is the metric of $\mathbb{R}^{(2,4)} \times \mathbb{R}^6$ the second fundamental form reads

$$\mathrm{II}(V, W) = g(\nabla_V W, N) = V(g(W, N)) - g(W, \nabla_V N) \ . \tag{8.26}$$

This step uses the property of the Levi Civita connection to be a metric connection. $V(g(W, N))$ means the derivative of the scalar function $g(W, N)$ along the vector field V. However, by definition $g(W, N) = 0$. The second term involves a derivative of a constant vector field and therefore also vanishes. We conclude that all these second fundamental forms are zero and thus traceless. So all minimal sub-manifolds of $\mathrm{AdS}_3 \times \mathrm{S}^3$ will automatically be minimal in $\mathrm{AdS}_5 \times \mathrm{S}^5$. This statement is only true because of the special form of the embedding. Such an embedding is called *totally geodesic*.

8.5 Isometries and conformal transformations

Isometries of a (pseudo-) Riemannian manifold are the set of transformations such that the pullback of the metric remains unchanged, i.e.

$$Iso(M, g) = \{h : M \to M \mid h^* g = g\} \ . \tag{8.27}$$

By a theorem of Stenrood and Myers all isometries form a differentiable Lie-group. The group product is the composition of maps. By definition it is clear that isometries are conformal, too. The isometry group of an n-dimensional sphere is $\mathrm{O}(n+1)$ and accordingly the isometry group for AdS_n is $\mathrm{O}(2, n-1)$.

8.5.1 Homogeneous space structure of AdS

The term *homogeneous space* can be used in two equivalent ways. A smooth manifold M is called homogeneous space if there is a Lie-group $\mathcal{G}$ with a continuous and transitive group action on M. Equivalently, M is a homogeneous space if there exists a Lie-group $\mathcal{G}$ together with a Lie-subgroup $\mathcal{H} \subset \mathcal{G}$ such that

$$M = \mathcal{G} \diagup \mathcal{H} \ .$$

If $\mathcal{G}$ acts continuously and transitively on M one can prove that

$$\mathcal{H} = \mathrm{stab}(x_0) = \{g \in \mathcal{G} \mid g \triangleright x_0 = x_0\}$$

where $\mathrm{stab}(x_0)$ is the stabiliser of the point x_0. As the action is transitive, the choice of x_0 is irrelevant. However, one should note that in general simply factoring a Lie-group by a Lie-subgroup will not lead to a homogeneous space (not even a topological space).

It is straightforward to see that $\mathrm{SO}(2, n-1)$ acts transitively and continuously on AdS_n and thus AdS_n is a homogeneous space with the representation

$$\mathrm{AdS}_n = \mathrm{SO}(2, n-1) \diagup \mathrm{SO}(1, n-2) \tag{8.28}$$

and similarly

$$\mathrm{S}^n = \mathrm{SO}(n+1) \diagup \mathrm{SO}(n) \ . \tag{8.29}$$

8.6 Boundary behaviour

In order to analyse the boundary of the minimal surfaces we use the following global coordinates of AdS_3 that realise the embedding of $AdS_3 \in \mathbb{R}^{2,2}$

$$Y = \left(\frac{1}{\cos\vartheta} \cos t \ , \quad \frac{1}{\cos\vartheta} \sin t \ , \quad \tan\vartheta \ \cos\gamma \ , \quad \tan\vartheta \ \sin\gamma \right) \ , \tag{8.30}$$

where $\vartheta \in [0,\ \frac{\pi}{2})$, $\gamma \in [0,\ 2\pi)$ and $t \in [-\pi,\ \pi)$. Approaching the conformal boundary is equivalent to $\vartheta \to \frac{\pi}{2}$. In order to demonstrate how to obtain the boundary behaviour, we start with the quadratic relation defining a minimal surface with a space-like AdS projection

$$(Y^{0'})^2 - (Y^1)^2 = \sin^2\theta \ . \tag{8.31}$$

Using global coordinates this is equivalent to

$$\cos t = \pm\sqrt{\sin^2\theta\cos^2\vartheta + \cos^2\gamma\sin^2\vartheta} \ . \tag{8.32}$$

Taking the limit $\vartheta \to \frac{\pi}{2}$ eq. (8.32) reads

$$\cos t = \pm \mid \cos\gamma \mid \ . \tag{8.33}$$

Thus, the boundary that is generated by the quadratic relation with $\gamma \in [0,\ 2\pi)$ and $t \in [-\pi,\ \pi)$ consists of the lines

$$t = \pm\gamma \ , \quad t = \pi - \gamma \ , \quad t = \gamma - \pi \ , \quad t = 2\pi - \gamma \ , \quad t = \gamma - 2\pi \ . \tag{8.34}$$

These lines are depicted green in fig. 12. For $\vartheta < \frac{\pi}{2}$ each pair (θ, γ) generates four values of t, taking into account the periodicity of cos and $t \in [-\pi,\ \pi)$. Thus, the quadratic relation generates four disconnected parts that are glued together on the conformal boundary. The boundary of an individual surface is a zig-zag line in the lines that are generated by (8.34). This individual boundary is depicted blue in fig 12.

The boundaries of the remaining surfaces have been analysed in a similar way in order to obtain the boundary plots.

8.7 Regularised area of the time-like tetragon

We repeat the calculations from [35]. The idea is to embed the surface into $\mathrm{AdS}_4 \subset \mathrm{AdS}_5$. Considering the solution of section 4.2.2, the embedding in AdS_4 is realised via

$$Y = (\cosh\theta\cosh\xi_-,\ \ \sinh\theta\sinh\xi_+,\ \ \sinh\theta\cosh\xi_+,\ \ \cosh\theta\sinh\xi_-,\ 0)\ . \tag{8.35}$$

Let us consider the two $\mathrm{SO}(2,3)$ matrices

$$A = \begin{pmatrix} 1 & 0 & 0 & 0 & 0 \\ 0 & \frac{1+a^2}{2a} & 0 & 0 & \frac{1-a^2}{2a} \\ 0 & 0 & 1 & 0 & 0 \\ 0 & 0 & 0 & 1 & 0 \\ 0 & \frac{1-a^2}{2a} & 0 & 0 & \frac{1+a^2}{2a} \end{pmatrix}\ ,\ B = \begin{pmatrix} 1 & 0 & 0 & 0 & 0 \\ 0 & 1 & 0 & 0 & 0 \\ 0 & 0 & 1 & 0 & 0 \\ 0 & 0 & 0 & \frac{1}{\sqrt{1+b^2}} & \frac{-b}{\sqrt{1+b^2}} \\ 0 & 0 & 0 & \frac{b}{\sqrt{1+b^2}} & \frac{1}{\sqrt{1+b^2}} \end{pmatrix}\ . \tag{8.36}$$

Calculating $A^I{}_J \cdot B^J{}_K \cdot Y^K$ and then introducing Poincaré coordinates $(r,\ y^\mu),\ \mu \in \{0', 1, 2\}$ via

$$Y^\mu = \frac{y^\mu}{r}, \qquad Y^0 + Y^3 = \frac{1}{r}\ , \qquad Y^0 - Y^3 = \frac{r^2 + y_\mu y^\mu}{r}\ , \tag{8.37}$$

we find that

$$\begin{aligned} r &= \frac{a\sqrt{b^2+1}}{\sqrt{b^2+1}\sinh\theta\sinh\xi_+ + b\cosh\theta\sinh\xi_-}\ , \\ y^{0'} &= \frac{a\sqrt{b^2+1}\cosh\theta\cosh\xi_+}{\sqrt{b^2+1}\sinh\theta\sinh\xi_+ + b\cosh\theta\sinh\xi_-}\ , \\ y^1 &= \frac{a\sqrt{b^2+1}\sinh\theta\cosh\xi_+}{\sqrt{b^2+1}\sinh\theta\sinh\xi_+ + b\cosh\theta\sinh\xi_-}\ , \\ y^2 &= \frac{a\cosh\theta\sinh\xi_-}{\sqrt{b^2+1}\sinh\theta\sinh\xi_+ + b\cosh\theta\sinh\xi_-}\ . \end{aligned} \tag{8.38}$$

The conformal boundary of AdS is reached with $r \to 0$ which is realised by $\xi_\pm \to \pm\infty$. By inspection of eq. (8.35), we see that the cusps are reached with the same limits. Thus the coordinates of the cusps in Minkowski space are

$$\begin{aligned} \vec{c}_1 &= \left(-\frac{a\sqrt{1+b^2}}{b}, 0, \frac{a}{b}\right)\ ,\ \vec{c}_2 = (0, +a, 0)\ , \\ \vec{c}_3 &= \left(+\frac{a\sqrt{1+b^2}}{b}, 0, \frac{a}{b}\right)\ ,\ \vec{c}_4 = (0, -a, 0)\ , \end{aligned} \tag{8.39}$$

with $\vec{c} = (y^{0'}, y^1, y^2)$. The cusps are θ-independent. It can easily be checked that the edges of the tetragon are light-like. The momenta associated with the edges of the tetragon are defined by $2\pi\, k^\mu = \Delta c^\mu$. In this way we get

$$k_1 = \frac{1}{2}\left(\sqrt{s},\, \sqrt{-t},\, -\sqrt{-u}\right),\ k_2 = \frac{1}{2}\left(\sqrt{s},\, -\sqrt{-t},\, \sqrt{-u}\right), \tag{8.40}$$

$$k_3 = \frac{1}{2}\left(-\sqrt{s},\, -\sqrt{-t},\, -\sqrt{-u}\right),\ k_4 = \frac{1}{2}\left(-\sqrt{s},\, \sqrt{-t},\, \sqrt{-u}\right)\ . \tag{8.41}$$

Here $(s,\, t,\, u)$ are the Mandelstam variables, which are related to the parameters $(a,\, b)$ by

$$s = -2k_1\cdot k_2 = \frac{a^2(1+b^2)}{\pi^2 b^2}\ , \qquad -t = 2k_1\cdot k_4 = \frac{a^2}{\pi^2}\ , \qquad -u = 2k_1\cdot k_3 = \frac{a^2}{\pi^2\, b^2}\ . \tag{8.42}$$

To calculate the regularised action, we introduce a constant cut-off at $r = r_c$ in Poincaré coordinates. Terms that vanish for $r_c \to 0$ will be discarded. The metric tensor on the surface (including by both AdS_3 and S^3 parts) reads

$$g_{ab}(\sigma,\tau) = f_{a\,b} + (f_s)_{a\,b} = (\rho^2 + \rho_s^2)\,\delta_{ab}\ . \tag{8.43}$$

Then the regularised action (4.4) is given by

$$S_{reg} = \frac{\sqrt{\lambda}}{2\pi}(\rho^2+\rho_s^2)\int_{r\geq r_c} \mathrm{d}\tau\mathrm{d}\sigma\ . \tag{8.44}$$

The integral runs over that part of the $(\sigma,\, \tau)$- plane where $r \geq r_c$. In the $(\xi,\, \eta)$- plane this area is bound by the contour

$$\epsilon\, \cosh\eta + \epsilon'\, \sinh\xi = 1, \tag{8.45}$$

with

$$\epsilon = \frac{\sinh\theta}{\pi\,\sqrt{s}}\ , \qquad \epsilon' = \frac{\cosh\theta}{\pi\,\sqrt{-t}}\ , \tag{8.46}$$

and we can rewrite (8.44) as

$$S_{reg} = \frac{\sqrt{\lambda}}{2\pi}(\rho^2+\rho_s^2)\, 2\,\mathcal{J}\ \cdot I(r_c)\ . \tag{8.47}$$

Here $\mathcal{J}$ is the Jacobian of the linear map between the $(\xi,\, \eta)$ and $(\sigma,\, \tau)$ coordinates

$$\begin{aligned}\xi &= \frac{1}{\sqrt{2}}\sqrt{-1+2\rho^2+\cos^2\phi}(\cos\phi\sigma + \sin\phi\tau)\ ,\\ \eta &= \frac{1}{\sqrt{2}}\sqrt{-1+2\rho^2-\cos^2\phi}(\sin\phi\sigma - \cos\phi\tau)\ ,\end{aligned} \tag{8.48}$$

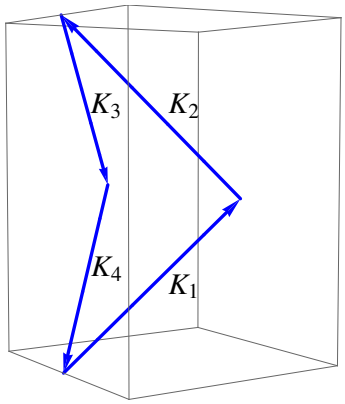

Figure 20: The time-like tetragon configuration in Minkowski space corresponding to s-channel scattering.

and

$$I(r_c) = \frac{1}{2}\int_{r\geq r_c} \mathrm{d}\eta \mathrm{d}\xi \ . \tag{8.49}$$

The dependence of $I(r_c)$ on ϵ and ϵ' can be taken from [34]. Inserting the new definitions from (8.46) we find

$$I(r_c) = \frac{1}{4}\left(\log\frac{r_c^2\sinh^2\theta}{4\pi^2\, s}\right)^2 + \frac{1}{4}\left(\log\frac{r_c^2\cosh^2\theta}{-4\pi^2\, t}\right)^2 - \frac{1}{4}\left(\log\frac{s\,\coth^2\theta}{-t}\right)^2 - \frac{\pi^2}{3}\ . \tag{8.50}$$

Then the regularised action reads

$$S_{reg} = \frac{\sqrt{\lambda}}{2\pi}\frac{(\rho^2+\rho_s^2)\sinh 2\theta}{\rho\sqrt{1-\rho^2}}\ \ I(r_c)\ . \tag{8.51}$$

8.8 The cusped Wilson-line at one loop

Let us consider the time-like cusped Wilson line. The cusp is spanned between the vectors p and q with $pq < 0$, $p^2 > 0$ and $q^2 > 0$. The one-loop contribution is given by

$$\begin{aligned}\mathcal{W}^{(1)}_{\text{cusp}} &= -\frac{g^2 C_f}{2}\int_{-1}^{1}\int_{-1}^{1} \mathrm{d}x^\mu \mathrm{d}y^\nu D_{\mu\nu}(x-y) + \\ &= I_{pq} + J_p + J_q \ , \end{aligned} \tag{8.52}$$

with

$$I_{pq} = \frac{g^2 C_f pq}{4\pi^2}\int_{-1}^{0}\mathrm{d}t\int_{0}^{1}\mathrm{d}s \frac{1}{(-s^2q^2 - t^2p^2 - 2stpq \pm i\varepsilon)^{1-\epsilon}} \tag{8.53}$$

and

$$\begin{aligned} J_q &= \frac{g^2 C_f q^2}{8\pi^2}\int_0^1 \mathrm{d}s\int_0^1 \mathrm{d}t \frac{1}{(-(s-t)^2q^2 \pm i\varepsilon)^{1-\epsilon}} \\ &= \frac{g^2}{4\pi^2}\frac{1}{4\epsilon} + \text{finite} \ . \end{aligned} \tag{8.54}$$

Introducing a change of variables, we arrive at

$$I_{pq} = -\frac{g^2 C_f \cosh\gamma}{4\pi^2}\int_0^{\sqrt{q^2}}\mathrm{d}\tau\int_0^{\sqrt{p^2}}\mathrm{d}\sigma \frac{1}{(\sigma^2+\tau^2 - 2\sigma\tau\cosh\gamma \mp i\varepsilon)^{1-\epsilon}} \ , \tag{8.55}$$

where $\cosh(\gamma) = -\frac{pq}{\sqrt{p^2q^2}}$. Introducing polar coordinates in the (τ,σ) plane we find

$$I_{pq} = -\frac{g^2 C_f \cosh(\gamma)}{4\pi^2}\int_0 \mathrm{d}r\ r^{2\epsilon-1}\int_0^{\pi/2}\mathrm{d}\phi \frac{1}{(1+\sin 2\phi\cosh\gamma \mp i\varepsilon)^{1-\epsilon}} \tag{8.56}$$

$$= -\gamma\coth\gamma\frac{g^2}{4\pi^2}\frac{1}{2\epsilon} + \text{finite} \ , \tag{8.57}$$

So the one loop result for a cusp is given by

$$\mathcal{W}^{(1)}_{\text{cusp}} = \frac{g^2 C_f}{4\pi^2}\frac{1}{2\epsilon}(1-\gamma\coth\gamma) + \text{finite} \ . \tag{8.58}$$

8.9 The cross anomalous dimension at one loop

We will discuss a self-crossing at the vertices $x_{\hat{l}} = x_{\hat{k}}$ here (i.e. we consider the configuration from fig. 15). In order to calculate the cross anomalous dimension at one loop, we have to calculate the divergent one-loop contributions at the crossing. Furthermore, we have to keep track of the colour structure. When we calculate a loop correction for the Wilson loop $\mathcal{W}_1$ the result will have a mixed colour structure. One part will have the colour structure of the Wilson loop $\mathcal{W}_1$ (i.e. a single colour trace) while another part will have the characteristic colour structure of $\mathcal{W}_2$, which has two colour traces. Accordingly, we will put the first term into $\mathcal{Z}_{11}$ while the second term will be assigned to $\mathcal{Z}_{12}$. To clarify this we consider for example

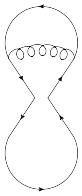

$$= -\tfrac{g^2}{4\pi^2}\tfrac{1}{2\epsilon}\gamma_{\hat{l}-1,\hat{k}}\coth\gamma_{\hat{l}-1,\hat{k}} \times \text{colour-term}$$

This contribution has to be split into parts that belong to $\mathcal{Z}_{11}$ and $\mathcal{Z}_{12}$. Keeping in mind that $\mathcal{W}_2$ is defined with an additional $1/N$ (see eq. (5.8)) the contributions are

$$\mathcal{Z}_{11}^{(1)} = \frac{g^2}{4\pi^2}\frac{1}{2\epsilon N}\gamma_{\hat{l}-1,\hat{k}}\coth\gamma_{\hat{l}-1,\hat{k}}+\dots\ ,\ \ \mathcal{Z}_{12}^{(1)} = -\frac{g^2}{4\pi^2}\frac{N}{2\epsilon}\gamma_{\hat{l}-1,\hat{k}}\coth\gamma_{\hat{l}-1,\hat{k}}+\dots\ . \tag{8.59}$$

The other diagrams are treated in the same way. Examining the colour structure for the gluon exchange over the crossing point, we find the contributions depicted in fig. 21.

Additionally, there are divergences when a gluon approaches the crossing point. These terms are depicted in fig. 22. At order $\mathcal{O}(a)$, the definitions of the cross anomalous dimension matrix in eq. (5.17) reads

$$\Gamma^{(1)} = \mu\frac{\mathrm{d}}{\mathrm{d}\mu}\mathcal{Z}^{(1)}\ . \tag{8.60}$$

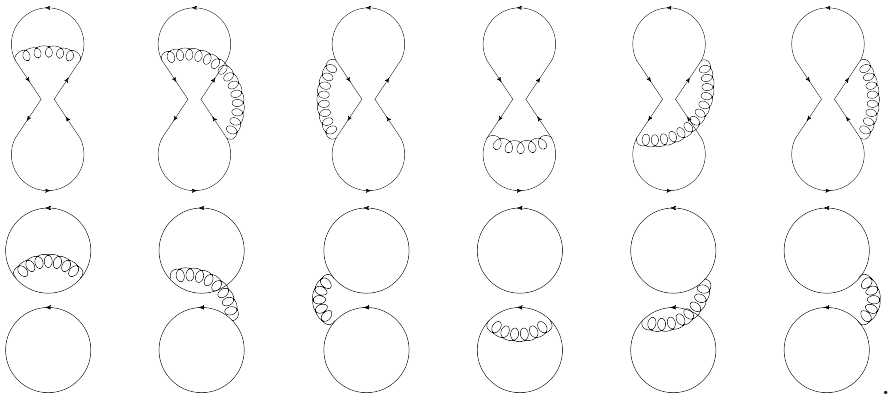

Figure 21: These gluon exchanges over the crossing contribute to the crossing anomalous dimension at one loop.

Now we can read off the crossing matrix

$$\begin{aligned}
\Gamma_{ij} =& \begin{pmatrix} \Gamma_{11} & \Gamma_{12} \\ \Gamma_{21} & \Gamma_{22} \end{pmatrix} \\
\Gamma_{11} =& \frac{g^2}{8\pi^2}\left(\frac{N^2-1}{N}\big(f_{\hat{l}-1,l}+f_{\hat{k}-1,\hat{k}}-2\big)-\frac{1}{N}\big(B_2 \;+\; i\pi\; h_{\hat{k},\hat{l}}\big)\right) \\
\Gamma_{22} =& \frac{g^2}{8\pi^2}\left(\frac{N^2-1}{N}\big(f_{\hat{k},\hat{l}-1}+f_{\hat{k}-1,\hat{l}}-2\big)-\frac{1}{N}\big(B_1 \;+\; i\pi\; h_{\hat{k},\hat{l}}\big)\right) \\
\Gamma_{12} =& \frac{g^2}{8\pi^2} N\big(B_2 \;+\; i\pi h_{\hat{k},\hat{l}}\big) \\
\Gamma_{21} =& \frac{g^2}{8\pi^2}\frac{1}{N}\big(B_1 \;+\; i\pi h_{\hat{k},\hat{l}}\big)\;,
\end{aligned}$$

with the abbreviations

$$\begin{aligned}
&f_{k,l} := \gamma_{k,l}\coth\gamma_{k,l}\;, \qquad h_{\hat{k},\hat{l}} \;:=\; \coth\gamma_{\hat{k}-1,\hat{l}-1}+\coth\gamma_{\hat{k},\hat{l}}\;, \\
&B_1 := f_{\hat{k}-1,\hat{k}}+f_{\hat{l}-1,\hat{l}}-f_{\hat{k},\hat{l}}-f_{\hat{k}-1,\hat{l}-1}\;, \\
&B_2 := f_{\hat{k},\hat{l}-1}+f_{\hat{k}-1,\hat{l}}-f_{\hat{k},\hat{l}}-f_{\hat{k}-1,\hat{l}-1}\;.
\end{aligned} \tag{8.61}$$

The angles γ_{ij} are defined in the obvious way

$$\cosh\gamma_{ij} = \frac{(p_i p_j - i\varepsilon)}{\sqrt{(p_i^2-i\varepsilon)(p_j^2-i\varepsilon)}}\;. \tag{8.62}$$

However, there is a little subtlety with $\gamma_{\hat{k},\hat{l}}$ and $\gamma_{\hat{k}-1,\hat{l}-1}$. For the calculation of the one-loop cusp result, we assumed that one of p or q is ingoing while

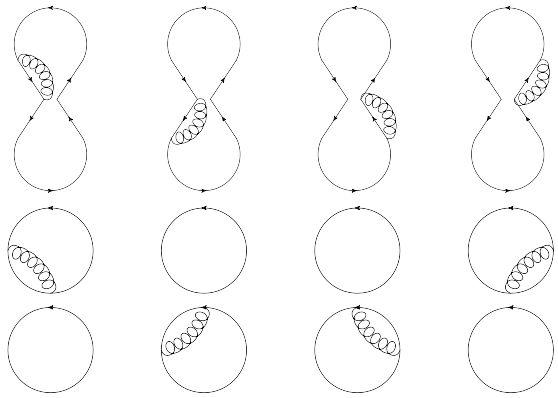

Figure 22: Approaching the crossing with a gluon vertex gives further contributions.

the other one is outgoing. But in our convention we have $p_{\hat{k}-1}$ and $p_{\hat{l}-1}$ ingoing and $p_{\hat{k}}$ and $p_{\hat{l}}$ outgoing. To fix this we have defined $\cosh\tilde{\gamma}_{ij} = -p_i p_j/\sqrt{p_i^2 p_j^2}$. Then $\tilde{\gamma}_{ij}\coth\tilde{\gamma}_{ij} = (\gamma_{ij} - i\pi)\coth\gamma_{ij}$. This is the source for the imaginary parts in the above formula. Now we consider the light-like limit $\gamma \to \infty$ of the above equations. This means $\coth\gamma \to 1$. Furthermore $\gamma_{ij} = \text{arcosh}\,\left(p_i p_j/\sqrt{p_i^2 p_j^2}\right) \approx \log\left(2p_i p_j/\sqrt{p_i^2 p_j^2}\right)$.

In this limit we find

$$\begin{aligned} B_1 \;+\; 2\pi i \;&=\; \log\frac{s_{\hat{k}-1,\hat{k}+1}\; s_{\hat{l}-1,\hat{l}+1}}{s_{\hat{k}+1,\hat{l}+1}\; s_{\hat{k}-1,\hat{l}-1}} = \log C_1 \;, \\ B_2 \;+\; 2\pi i \;&=\; \log\frac{s_{\hat{k}+1,\hat{l}-1}\; s_{\hat{k}-1,\hat{l}+1}}{s_{\hat{k}+1,\hat{l}+1}\; s_{\hat{k}-1,\hat{l}-1}} = \log C_2 \;. \end{aligned} \tag{8.63}$$

These cross ratios are the same that we use in eq. (7.1). Additionally we find

$$f_{ij} \to \gamma_{ij} \;. \tag{8.64}$$

Performing t'Hooft limit $N \to \infty$ with $a = \frac{g^2 N}{8\pi^2}$ kept fixed, we arrive at

$$\Gamma_{ij} = a\begin{pmatrix} \gamma_{\hat{l}-1,\hat{l}} + \gamma_{\hat{k}-1,\hat{k}} - 2 & \log C_2 \\ 0 & \gamma_{\hat{l}-1,\hat{k}} + \gamma_{\hat{l},\hat{k}-1} - 2 \end{pmatrix} + \mathcal{O}(a^2) \;. \tag{8.65}$$

Then for self-crossing light-like Wilson loops, we expect the expression

$$\begin{aligned}
\Gamma^{(1)}_{11,\text{light-like}} &= \Big(\log(-s_{\hat{l}-1,\hat{l}+1}\ \mu^2) + \log(-s_{\hat{k}-1,\hat{k}+1}\ \mu^2)\Big)\ , \\
\Gamma^{(1)}_{12,\text{light-like}} &= \log C_2\ , \\
\Gamma^{(1)}_{21,\text{light-like}} &= 0\ , \\
\Gamma^{(1)}_{22,\text{light-like}} &= \Big(\log(-s_{\hat{l}-1,\hat{k}+1}\ \mu^2) + \log(-s_{\hat{l}+1,\hat{k}-1}\ \mu^2)\Big)\ .
\end{aligned} \tag{8.66}$$

Here, the Mandelstam variables are defined as usual $s_{ij} = (x_i - x_j)^2$. The usual cusp anomalous has the aforementioned property

$$\lim_{\text{light-like}} \frac{2\Gamma_{\text{cusp}}(a,\gamma)}{\gamma} = \Gamma_{\text{cusp}}(a) \tag{8.67}$$

at all loops. Therefore, we also expect that the μ dependence of the crossing matrix can be probed at one-loop level.

8.10 On the symbol $\mathcal{S}(\mathcal{R}_6^{(3)})$

As much progress concerning the hexagon remainder function has been made using symbols, we review the relevant definition and show how to extract the piece of information out of the symbol of the hexagon remainder at three loops from [38] that is by a factor of 6/7 in disagreement with the heuristic translation rule. A pure function of degree k is defined by the relation

$$\mathrm{d}f^{(k)} = \sum_r f_r^{(k-1)} \, \mathrm{d}\log\phi_r \ , \tag{8.68}$$

where the sum is finite. The ϕ_r are rational functions. This definition is recursive and for positive k and the only pure functions of degree $k = 0$ are constants. Then, the symbol of a pure function is also defined recursively

$$\mathcal{S}(f^{(k)}) = \sum_r \mathcal{S}(f_r^{(k-1)}) \otimes \phi_r \ . \tag{8.69}$$

By this definition the symbol of a pure function of degree k is then an element of the space of k-fold tensor products of algebraic functions. Let us give an example. We know that for polylogarithms

$$\mathrm{d}\ \mathrm{Li}_n(z) = \mathrm{Li}_{n-1}(z) \, \mathrm{d}\log z \ , \quad \forall\ n > 2 \ , \tag{8.70}$$

and additionally

$$\mathrm{d}\ \mathrm{Li}_2(z) = -\log(1-z) \, \mathrm{d}\log z \ . \tag{8.71}$$

Thus the polylogarithms Li_n are pure functions of degree n. Their symbols can be read off from the relation (8.70)

$$\mathcal{S}(\mathrm{Li}_n(z)) = -(1-z) \otimes \underbrace{z \otimes z \otimes \cdots \otimes z}_{\text{n-1 times}} \ . \tag{8.72}$$

It is also easy to verify that

$$\mathcal{S}(\log^n z) = \underbrace{z \otimes z \otimes \cdots \otimes z}_{\text{n- times}} \ . \tag{8.73}$$

Another useful property that follows directly from the property $\log ab = \log a + \log b$ is that

$$\phi_1 \otimes ...\phi_l\psi_l... \otimes \phi_k = \phi_1 \otimes ...\phi_l... \otimes \phi_k + \phi_1 \otimes ...\psi_l... \otimes \phi_k \ . \tag{8.74}$$

The symbol also provides information about the location of discontinuities and the symbol of the branch cut. If

$$\mathcal{S}(f^{(k)}) = \phi_1 \otimes \cdots \otimes \phi_k \ , \tag{8.75}$$

$f^{(k)}$ has a branch cut starting at $\phi_1 = 0$ and the symbol of the discontinuity is obtained by removing the first entry in the symbol

$$\mathcal{S}(\Delta_{\phi_1} f^{(k)}) = \phi_2 \otimes \cdots \otimes \phi_k \ . \tag{8.76}$$

Thus we see that the symbol of the discontinuity of a polylogarithm is the symbol of a power of logarithms (with one degree less). In [38] the authors give the symbol of the hexagon remainder function at three loops in the Euclidean regime. We expect that there should appear

$$\begin{aligned} \mathcal{S}\left(\mathrm{Li}_6\left(\frac{u-1}{u}\right)\right) &= u \otimes \frac{1-u}{u} \otimes \frac{1-u}{u} \otimes \frac{1-u}{u} \otimes \frac{1-u}{u} \otimes \frac{1-u}{u} \\ &= u \otimes 1-u \otimes 1-u \otimes 1-u \otimes 1-u \otimes 1-u + \dots \ . \end{aligned} \tag{8.77}$$

Extracting the part that is proportional to the above tensor product from the result given in [38]

$$\mathcal{S}(\mathcal{R}_6^{(3)}) = \frac{3}{2}\, u \otimes 1-u \otimes 1-u \otimes 1-u \otimes 1-u \otimes 1-u + \dots \tag{8.78}$$

Thus the prefactor of a potential $\mathrm{Li}_6(1-1/u)$ is $3/2$. This reasoning is valid under the assumption that the remainder function can be expressed using logarithms and polylogarithms only. The discontinuity of the remainder then becomes

$$\frac{3}{2}\Delta\mathrm{Li}_6\left(1-\frac{1}{u}\right) = \frac{1}{40}\pi i \log^5\left(1-\frac{1}{u}\right) \tag{8.79}$$

which disagrees by a factor of $6/7$ with (6.80).

8.11 Translation between geometric and dimensional regularisation

Here we give the motivation for a "translation rule" for the pole terms of the remainder functions in the limit of self-crossing, see [28]. Renormalisation $\mathcal{Z}$-factors are given as a formal series in the regulator and the coupling. The regulators that are interesting here is $\frac{1}{\epsilon}$ in dimensional regularisation and $\log(\frac{1}{-z_\perp^2\mu^2})$, where $z_\perp$ is the distance between the nearly crossing legs or vertices. In the non-self-crossing case the remainder function is finite. Thus, in the self-crossing configuration it can be regularised using this version of "point-splitting" regularisation. By m we denote the pole order and by l the loop order. In the case of correlation functions of local operators only terms with $m \leq l$ contribute. The complete all loop information on β-functions and anomalous dimensions is contained in the coefficients of the $m = 1$ terms. On the other side, the coefficients of the terms with $m = l$ are fixed by one loop information and are independent of the renormalisation scheme.

In contrast to this situation, for polygonal Wilson loops with light-like edges also terms with $m > l$ appear. In dimensional regularisation the RG-scale enters exclusively in the combination $g^2\mu^{2\epsilon}$ and we have to deal with (s some squared distance of polygon vertices)

$$g^{2l}\ \frac{1}{\epsilon^m}(-\mu^2 s)^{l\epsilon}\ =\ g^{2l}\ \frac{1}{\epsilon^m}\left(1+\cdots+\frac{(l\epsilon)^{m-l}}{(m-l)!}\ \log^{m-l}(-\mu^2 s)+\cdots\right)\ . \tag{8.80}$$

The analogous term in cut-off regularisation looks like

$$\begin{aligned} g^{2l}\ \log^m(\frac{s}{z_\perp^2}) &= g^{2l}\ \left(\log(-\mu^2 s)+\log(\frac{1}{-\mu^2 z_\perp^2})\right)^m \\ &= \cdots + g^{2l}\ \binom{m}{l}\log^{m-l}(-\mu^2 s)\ \log^l\left(\frac{1}{-\mu^2 z_\perp^2}\right)\ +\ \cdots \end{aligned} \tag{8.81}$$

In both cases a term with $m > l$ generates descendants with lower powers of $\frac{1}{\epsilon}$ or $\log\frac{1}{-\mu^2 z_\perp^2}$, respectively.
Now we assume the existence of a translation factor α

$$g^{2l}\ \frac{1}{\epsilon^m}(-\mu^2 s)^{l\epsilon}\ \Leftrightarrow\ \alpha\ g^{2l}\ \log^m(\frac{s}{z_\perp^2})\ . \tag{8.82}$$

Inserting in this correspondence (8.80) and (8.81) one finds, by comparison of the coefficients of $\log^{m-l}(-\mu^2 s)$

$$g^{2l}\frac{1}{\epsilon^l}\ \frac{l^{m-l}}{(m-l)!}\ \Leftrightarrow\ \alpha\ g^{2l}\log^l\left(\frac{1}{-\mu^2 z_\perp^2}\right)\binom{m}{l}\ . \tag{8.83}$$

Motivated by the scheme independence (for local operators) of factors in front of terms with equal powers of g^2 and $1/\epsilon$ or $\log(\frac{1}{-\mu^2 z_\perp^2})$, we further *assume* that the translation factor α has to be chosen in such a manner that (8.83) becomes $g^{2l}/\epsilon^l \Leftrightarrow g^{2l}\log^l$. This fixes

$$\alpha \;=\; \frac{l^{m-l}\; l!}{m!}\;. \tag{8.84}$$

Then, looking at the coefficients of $(\log(-\mu^2 s))^0$ we get

$$g^{2l}\;\frac{1}{\epsilon^m} \;\Leftrightarrow\; \alpha\; g^{2l}\;\log^m\left(\frac{1}{-\mu^2 z_\perp^2}\right)\;, \tag{8.85}$$

with α from (8.84).

In particular this means

- at one loop : $1/\epsilon^2 \;\Leftrightarrow\; 1/2\;\log^2\;,\;\; 1/\epsilon \;\Leftrightarrow\; \log$
- at two loops : $1/\epsilon^3 \;\Leftrightarrow\; 2/3\;\log^3\;,\;\; 1/\epsilon^2 \;\Leftrightarrow\; \log^2$
- at three loops : $1/\epsilon^5 \;\Leftrightarrow\; 9/20\;\log^5\;,\;\; 1/\epsilon^4 \;\Leftrightarrow\; 3/4\;\log^4$
- at four loops : $1/\epsilon^7 \;\Leftrightarrow\; 32/105\;\log^7\;,\;\; 1/\epsilon^6 \;\Leftrightarrow\; 8/15\;\log^6$

References

[1] J. M. Maldacena, "The Large N limit of superconformal field theories and supergravity," Adv. Theor. Math. Phys. **2** (1998) 231 [hep-th/9711200].

[2] J. M. Maldacena, "Wilson loops in large N field theories," Phys. Rev. Lett. **80** (1998) 4859 [hep-th/9803002].

[3] D. J. Gross and P. F. Mende, "String Theory Beyond the Planck Scale," Nucl. Phys. B **303** (1988) 407.

[4] L. F. Alday and J. M. Maldacena, "Gluon scattering amplitudes at strong coupling," JHEP **0706** (2007) 064 [arXiv:0705.0303 [hep-th]].

[5] M. Kruczenski, "A Note on twist two operators in N=4 sYM and Wilson loops in Minkowski signature," JHEP **0212** (2002) 024 [hep-th/0210115].

[6] L. F. Alday and J. Maldacena, "Comments on gluon scattering amplitudes via AdS/CFT," JHEP **0711** (2007) 068 [arXiv:0710.1060 [hep-th]].

[7] L. F. Alday, "Review of AdS/CFT Integrability, Chapter V.3: Scattering Amplitudes at Strong Coupling," Lett. Math. Phys. **99** (2012) 507 [arXiv:1012.4003 [hep-th]].

[8] L. F. Alday, "Lectures on Scattering Amplitudes via AdS/CFT," Fortsch. Phys. **56** (2008) 816 [arXiv:0804.0951 [hep-th]].

[9] L. F. Alday and J. Maldacena, "Null polygonal Wilson loops and minimal surfaces in Anti-de-Sitter space," JHEP **0911** (2009) 082 [arXiv:0904.0663 [hep-th]].

[10] L. F. Alday, D. Gaiotto and J. Maldacena, "Thermodynamic Bubble Ansatz," arXiv:0911.4708 [hep-th].

[11] L. F. Alday, J. Maldacena, A. Sever and P. Vieira, "Y-system for Scattering Amplitudes," J. Phys. A **43** (2010) 485401 [arXiv:1002.2459 [hep-th]].

[12] C. Anastasiou, Z. Bern, L. J. Dixon and D. A. Kosower, "Planar amplitudes in maximally supersymmetric Yang-Mills theory," Phys. Rev. Lett. **91** (2003) 251602 [arXiv:hep-th/0309040].

[13] Z. Bern, L. J. Dixon and V. A. Smirnov, "Iteration of planar amplitudes in maximally supersymmetric Yang-Mills theory at three loops and beyond," Phys. Rev. D **72** (2005) 085001 [arXiv:hep-th/0505205].

[14] C. Anastasiou, A. Brandhuber, P. Heslop, V. V. Khoze, B. Spence and G. Travaglini, "Two-Loop Polygon Wilson Loops in N=4 sYM," JHEP **0905** (2009) 115 [arXiv:0902.2245 [hep-th]].

[15] J. M. Drummond, J. Henn, G. P. Korchemsky and E. Sokatchev, "Hexagon Wilson loop = six-gluon MHV amplitude," Nucl. Phys. B **815** (2009) 142 [arXiv:0803.1466 [hep-th]].

[16] A. Brandhuber, P. Heslop and G. Travaglini, "MHV amplitudes in N=4 super Yang-Mills and Wilson loops," Nucl. Phys. B **794** (2008) 231 [arXiv:0707.1153 [hep-th]].

[17] J. M. Drummond, J. Henn, G. P. Korchemsky and E. Sokatchev, "Conformal Ward identities for Wilson loops and a test of the duality with gluon amplitudes," Nucl. Phys. B **826** (2010) 337 [arXiv:0712.1223 [hep-th]].

[18] J. M. Drummond, G. P. Korchemsky and E. Sokatchev, "Conformal properties of four-gluon planar amplitudes and Wilson loops," Nucl. Phys. B **795** (2008) 385 [arXiv:0707.0243 [hep-th]].

[19] J. M. Drummond, J. Henn, G. P. Korchemsky and E. Sokatchev, "On planar gluon amplitudes/Wilson loops duality," Nucl. Phys. B **795** (2008) 52 [arXiv:0709.2368 [hep-th]].

[20] I. A. Korchemskaya and G. P. Korchemsky, "On light-like Wilson loops," Phys. Lett. B **287**, 169 (1992).

[21] G. P. Korchemsky and A. V. Radyushkin, "Renormalisation of the Wilson Loops Beyond the Leading Order," Nucl. Phys. B **283** (1987) 342.

[22] V. Del Duca, C. Duhr and V. A. Smirnov, "The Two-Loop Hexagon Wilson Loop in N = 4 sYM," JHEP **1005** (2010) 084 [arXiv:1003.1702 [hep-th]].

[23] A. B. Goncharov, M. Spradlin, C. Vergu and A. Volovich, "Classical Polylogarithms for Amplitudes and Wilson Loops," Phys. Rev. Lett. **105** (2010) 151605 [arXiv:1006.5703 [hep-th]].

[24] L. J. Dixon, J. M. Drummond, M. von Hippel and J. Pennington, "Hexagon functions and the three-loop remainder function," arXiv:1308.2276 [hep-th].

[25] V. Del Duca, C. Duhr and V. A. Smirnov, "A Two-Loop Octagon Wilson Loop in N = 4 sYM," JHEP **1009** (2010) 015 [arXiv:1006.4127 [hep-th]].

[26] G. Georgiou, "Null Wilson loops with a self-crossing and the Wilson loop/amplitude conjecture," JHEP **0909** (2009) 021 [arXiv:0904.4675 [hep-th]].

[27] H. Dorn and S. Wuttke, "Wilson loop remainder function for null polygons in the limit of self-crossing," JHEP **1105** (2011) 114 [arXiv:1104.2469 [hep-th]].

[28] H. Dorn and S. Wuttke, "Hexagon Remainder Function in the Limit of Self-Crossing up to three Loops," JHEP **1204** (2012) 023 [arXiv:1111.6815 [hep-th]].

[29] L. Brink, J. H. Schwarz and J. Scherk, "Supersymmetric Yang-Mills Theories," Nucl. Phys. B **121** (1977) 77.

[30] S. J. Parke and T. R. Taylor, "An Amplitude for n Gluon Scattering," Phys. Rev. Lett. **56** (1986) 2459.

[31] R. Britto, F. Cachazo and B. Feng, "New recursion relations for tree amplitudes of gluons," Nucl. Phys. B **715** (2005) 499 [hep-th/0412308].

[32] R. Britto, F. Cachazo, B. Feng and E. Witten, "Direct proof of tree-level recursion relation in Yang-Mills theory," Phys. Rev. Lett. **94** (2005) 181602 [hep-th/0501052].

[33] H. Dorn, G. Jorjadze and S. Wuttke, "On space-like and time-like minimal surfaces in AdS(n)," JHEP **0905** (2009) 048 [arXiv:0903.0977 [hep-th]].

[34] H. Dorn, N. Drukker, G. Jorjadze and C. Kalousios, JHEP **1004** (2010) 004 [arXiv:0912.3829 [hep-th]].

[35] H. Dorn, G. Jorjadze, C. Kalousios, L. Megrelidze and S. Wuttke, J. Phys. A **44** (2011) 025403 [arXiv:1007.1204 [hep-th]].

[36] P. A. M. Dirac, "Wave equations in conformal space," Annals Math. **37** (1936) 429.

[37] H. Dorn, H. Munkler and C. Spielvogel, amplitudes," arXiv:1211.5537 [hep-th].

[38] L. J. Dixon, J. M. Drummond and J. M. Henn, "Bootstrapping the three-loop hexagon," JHEP **1111** (2011) 023 [arXiv:1108.4461 [hep-th]].

[39] S. Caron-Huot, "Superconformal symmetry and two-loop amplitudes in planar N=4 super Yang-Mills," JHEP **1112** (2011) 066 [arXiv:1105.5606 [hep-th]].

[40] S. Caron-Huot and S. He, "Jumpstarting the all-loop S-matrix of planar N=4 super Yang-Mills," arXiv:1112.1060 [hep-th].

[41] A. M. Polyakov, "Gauge Fields As Rings Of Glue," Nucl. Phys. B **164** (1980) 171.

[42] R. A. Brandt, F. Neri and M. A. Sato, "Renormalisation Of Loop Functions For All Loops," Phys. Rev. D **24** (1981) 879.

[43] R. A. Brandt, A. Gocksch, M. A. Sato and F. Neri, "Loop Space," Phys. Rev. D **26** (1982) 3611.

[44] H. Dorn, "RENORMALIZATION OF PATH ORDERED PHASE FACTORS AND RELATED HADRON OPERATORS IN GAUGE FIELD THEORIES," Fortsch. Phys. **34** (1986) 11.

[45] I. A. Korchemskaya and G. P. Korchemsky, "High-energy scattering in QCD and cross singularities of Wilson loops," Nucl. Phys. B **437** (1995) 127 [arXiv:hep-ph/9409446].

[46] A. Brandhuber, P. Heslop, P. Katsaroumpas, D. Nguyen, B. Spence, M. Spradlin and G. Travaglini, "A Surprise in the Amplitude/Wilson Loop Duality," JHEP **1007** (2010) 080 [arXiv:1004.2855 [hep-th]].

Hilfsmittel

- Diese Arbeit wurde in LaTeX 2_ε verfasst.
- Die Rechnungen wurden unter Zuhilfenahme von Wolfram Mathematica 9.0 durchgeführt.
- Graphiken wurden mit JaxoDraw und Wolfram Mathematica 9.0 erstellt.

Selbstständigkeitserklärung

Hiermit erkläre ich, daß ich die vorliegende Arbeit selbständig, ohne fremde Hilfe und nur unter Verwendung der angegeben Literatur und Hilfsmittel angefertigt habe.

Sebastian Wuttke
Berlin, 13. Januar 2014